Simulation of Hydro-Ecological Indices in a Long-Term Hydrologic Model using Downscaled Climate Data

by

© **Diana Lakshmi Sankar**

A thesis submitted to the School of Graduate Studies in partial fulfillment of the requirements for the degree of Master of Engineering.

Department of Civil Engineering

Memorial University

May 2020

St. John's, Newfoundland and Labrador, Canada

Abstract

The effects of climate change are likely to have a significant impact on environmental flows, which are often represented by alterations in hydrologic and ecological indices. Changes in flow regimes caused by climate change have implications for river ecology, and projections of future flow regimes must be reliable. In this study, the performance of hydrological models was evaluated with hydro-ecological indices to determine if stream flow characteristics could be reasonably modelled with RCM (Regional Climate Model) driven data. In general, it was found that RCM driven hydrological models could well simulate ecological stream flow characteristics with seasonal or monthly bias correction. However, characteristics that represented the frequency and rate of change of stream flow were not well simulated even with bias correction. RCM data driven models resulted in comparable error to the simulation of ERSS in a regional analysis. This gave confidence to the use of RCM driven data to simulate stream flow characteristics.

Acknowledgements

First, I would like to thank my supervisors Dr. Joe Daraio and Dr. Bing Chen without whose support I would not have been able to come to Memorial University. I am grateful for their knowledge and support to help me develop my thesis project. I would like to thank Dr. Jonathan Kennen who helped with the development of my research topic and who provided invaluable insight into this research and field of study. I would like to thank my parents (Vijay and Sharon) and sister (Eve) for supporting my decision to pursue my Master's far from home on the East Coast of Canada and congratulate my sister for starting her Bachelor's of Engineering at UBC. I would also like to acknowledge my friends Cristiana Gheorghe and Su Jin Kim without whose support I would not have been able to finish this thesis.

Table of contents

List of tables

List of figures

Chapter 1

Introduction

The natural flow regime and the ecological health of a river are inextricably linked. The natural flow regime is the characteristic pattern of a river's flow and varies between long and short time scales [1]. When the natural flow regime is changed spawning cues for fish can be eliminated and microorganism disturbance can take place [2]–[4]. These changes to the natural flow regime affect the environmental flows necessary to maintain human and ecological health in a waterway according to the Brisbane Declaration [5]. It is well established that human modification, by way of land use changes, large construction works or anthropogenic climate change alters the stream flow regime and therefore the ecology of a waterway and riparian area[1], [6], [7]. Hydro-ecological indices have to be consistently used as a way to to evaluate the effects or impact of changes to the natural flow regime. Hydro-ecological indices are described in this thesis as Ecologically Relevant Stream flow Statistics (ERSS).

The natural flow regime is described by the magnitude, duration, timing, frequency and rate of change of a waterway. Statistics that characterize these five components of stream flow are known as ERSS [8]. Changes in ERSS values represent

changes to the waterway which may have ecological significance and impact. One useful approach is to create a set of future stream flows using a sensitivity model or climate ensemble model and future ERSS are calculated from these stream flow predictions [9]–[11]. However, there is concern over the accuracy and uncertainty of climate projections and their application to ecological concerns. Climate extremes are of particular interest as they are ecologically relevant [12]. For example, continuous low flows can reduce dissolved oxygen levels and lead to drought conditions.

Dynamical downscaling is one method to bring global climate processes (affected by climate change) to the local scale to be used in hydrological modelling and determine environmental impacts. Dynamical downscaling is an intensive technique to predict climate change impacts but has been found to better represent regional climate [13]. However, current methods of dynamical downscaling do not well estimate hydrologic variables [14]. Downscaled data input into a hydrological model results in the poor estimation of hydrological variables due to the spatial mismatch between the data and model.

This study tests the ability of a hydrological model to simulate ERSS and dynamically downscaled data to simulate ERSS. Daily data simulated from GCMs (General Circulation Model) should not be compared, only statistics that describe the long term flow regime should be used [15]. The hypothesis of this research is that bias correcting stream flows will improve hydrologic simulations ability to capture flow indices and improve the performance of GCM driven models to represent these indices. Research was needed to test bias correction of stream flows using seasonally based methods [15]. This study focused on two watersheds of ecological significance located on the Coastal Plain in New Jersey, USA.

The objectives of this study were to:

1. **Identify parsimonious sets of ERSS that define the watersheds and region of interest**

2. **Compare ERSS simulated through hydrological modelling driven by observed historical data (1955–2005) and dynamically downscaled GCM simulations of the historical period (1955–2005) to observed ERSS**

3. **Compare ERSS derived from bias corrected stream flow from simulations in objective 2 to observed ERSS**

The intent of this research is to support the development of accurate climate change predictions and predictions of hydro-ecological indices to determine appropriate mitigation measures. To use a model for climate change predictions with confidence the model must perform well over a long time period [15]. More detailed analysis of the flow regime and ecological characteristics of this data were necessary as there are projected changes in stream flow [15].

This thesis is separated into 7 chapters. Chapter 2 discusses the pertaining literature to this topic: downscaling, ecology and hydrological modelling. Chapter 3 outlines the data used in this research. Chapters 4, 5 and 6 present methodology and results obtained in three phases of this analysis along with discussions of each phase. Chapter 7 is the conclusion of the study.

Chapter 2

Literature Review

Throughout history humans have altered stream flow patterns and these changes have had ecological consequences. Large water infrastructure works, such as dams, have altered stream flow regimes and biota [1]. Human-caused land use changes have altered the ecology of river systems by changing evapotranspiration, runoff and groundwater recharge [16]. In the 1970's new environmental regulations in the United States paved the way for developments in ecological rehabilitation and watershed modelling, leading to reduced impact on the stream flow regime due to human development. However, climate change is now impacting riparian systems and attenuating human alterations of the landscape, such as increasing the frequency of flooding, droughts and other extreme events. New methods must be created to understand the impact of climate change on stream flow regimes as there are ecological consequences to climate change on freshwater resources [17].

Changes to the flow regime have ecological consequences and this has been known for a long time. For example, the flood-pulse concept states that a long or short flood pulse impacts the type of biota in a river-floodplain system [2]. However, changes

to stream flow characteristics due to climate change are being increasingly studied as climate change may impact ecological processes and economic activities such as fisheries and urban planning [18]–[20].

Hydrological models are often a foundational step of analysis to better understand alteration of a waterway or to create environmental flows [11]. Environmental flows are the flows necessary to maintain human and ecological health in a waterway [5]. The five fundamental components of stream flow are magnitude, duration, timing, frequency and rate of change [1]. Various hydrological models have been used to determine environmental impacts and ecological aspects of flow [21]. However, no one hydrological model has been found that is superior for ecological modelling and environmental purposes [8].

Land use and land cover change impact the stream flow regime [22]. The effect of such changes have been studied recently in various climates around the world and can exacerbate drought conditions, increase nutrient concentrations and change flow regimes which have ecological consequences [23], [24]. While land use changes can have a significant change on flow regimes, climate change can have just as large or a greater impact on stream flow [25].

2.1 Ecologically Relevant Stream flow Statistics

Environmental flows can be represented by statistics that describe the flow of a waterway or stream flow regime. These statistics are known as Ecologically Relevant Stream flow Statistics (ERSS) [26]. ERSS can be used to create management targets, they are useful as a measure of how the ecology of a riparian area is changing [27]. ERSS can also be used to classify flows to determine changes in a waterway and imply

changes to the ecology of an area. There are a large number of hydro-ecological indices and there are many different ways to pick a parsimonious set of indices that represents the stream flow signal [27].

Olden and Poff (2003) took long term flow records from across the continental United States and used Principal Component analysis (PCA) to determine a parsimonious set of ERSS while still representing the stream flow regime [27]. An ERSS for each aspect of the regime (magnitude, frequency, duration, timing, rate of change) was chosen for each flow condition (high flow, low flow, average flow). This analysis was performed for each stream type in the 420 sites.

There are also pre-determined sets of ERSS. Relevant indices should be chosen based on some consultation with biologists and ecologists and popular methods to subset indices are discussed below.

2.1.1 Indicators of Hydrologic Alteration

One common method of determining relevant streamflow statistics is to use the Indicators of Hydrologic Alteration (IHA) a program designed to determine human impacts on flow [28]. The IHA method consists of thirty three hydrologic parameters that can be correlated to ecological conditions. However, the primary purpose is to determine human alteration on a system through activities such as construction where there are known years where the stream flow regime was expected to change (e.g. the creation of a dam in the year 2000). Determination of IHA requires one year to divide pre- and postconditions which may not be appropriate for all types of analysis. Some research has been done using this method to assess impacted waterways due to climate change [29]. There are some disadvantages of this system. No indicators

directly quantify the magnitude of high flow conditions, this system is mainly set out to only look at extreme low flow conditions [27]. The IHA system is an extremely common tool for hydroecological impact assessment [29], [30].

2.1.2 Range of Variability Approach

A similar method to the IHA system is the Range of Variability Approach (RVA). Thirty three IHA parameters are analyzed that represent the five flow components: frequency, magnitude, timing, duration and rate of change. This method looks at the variation of the pre-impact indices, this determines the amount of alteration of a waterway [31]. A range of variation of each of these parameters is selected as initial flow management targets [32]. This method has the additional benefit of capturing variation, however, the set of IHA parameters may not be ideal to the specific area of interest. A minimum period of record is required to analyze the baseline or natural range of variation, although estimation and modelling techniques can be used to expand or create a flow record [32].

2.1.3 Hydroecological Integrity Assessment Process

The USGS has processes put in place for determining stream flow alteration that would impact aquatic species. It is known as the Hydrolecological Integrity Assessment Process (HIP) [33]. There are four main steps in the process: 1) perform hydrological classification, 2) identify ERSS of interest, 3) develop area-specific stream classification, and 4) develop an area specific Hydrologic Assessment Tool which can be used to determine hydrological modification and flow standards [34]. Step 2 - determining ERSS of interest can be completed using the pre-determined indices

noted above or other methods.

One tool that can be used to determine ERSS is HIT (Hydrologic Index Tool) that was developed for the Hydroecological Integrity Assessment Process. The program calculates 171 indices from daily flow data [34]. These ERSS represent the five fundamental aspects of flow [1]. An ERSS should be selected that represents each aspect of flow at each condition (high flow, low flow and average flow) to give an adequate representation of the flow regime. In 2013, HIT was moved from a software interface to a package called EflowStats [35] in the programming language R [36]. This increased the functionality of the program by allowing data to be input that was not connected to the USGS site, such as hydrological model simulations.

2.1.4 Importance of Accurate ERSS Simulation

Traditionally hydrological model calibration has been performed on a hydrograph; some calibration has been done using flow duration curves. However, the ecological relationship between the flow and the accuracy of how flow is predicted has not been a concern of most hydrological modelling projects to date. A focus on Ecologically Relevant Stream flow Statistics (ERSS) is needed.

ERSS are statistics that represent the ecological relationship between flow and local biota. Only in the past 15 years has the importance of the natural flow regime been noted, thanks to the landmark research by Olden and Poff [1]. In some projects the water quality statistic 7Q10 (the minimum seven day consecutive flow with a 10 year frequency), is used as the only environmental flow criteria [37]–[39]. The environmental aspects of waterways must be analyzed more deeply for there to be an adequate preservation of the ecological health of an area. These indices represent

a connection to the ecology of an area, even if they only appear to describe the hydrodynamics of a system.

The timing and intensity of flood events are crucial in maintaining riparian diversity through the influence of sediment dynamics [40]. Flood duration may also provide insight into the ability to restore abundance of a riparian area [41]. Certain indices are of interest to specific species, many examples were found that demonstrated this impact. Along the Missouri River peak flows heavily influenced cottonwood recruitment; cottonwood is a habitat for many wildlife species [42]. This is one example of many.

The establishment of an invasive species in an environment can have poor consequences for the existing ecology of an area. In a global study of Holoarctic regions the invasive success of rainbow trout could be explained by the timing of fry emergence and the timing of low monthly flows [43] . Low flow indices may also be of particular concern in areas where there is potential for drought. Changes in ERSS due to climate change predicted a minimum of 38 species to have declines in abundance in Missouri (USA) [44]. A select list of potential consequences to flow alteration are in Table 2.1 [1].

2.2 Hydrological Modelling and Environmental Effects

Hydrological modelling simulates observed natural processes so that engineering design and scientific analysis can be completed. There are multiple calibration and validation techniques. However, the question remains, has there been enough focus

Table 2.1: A sample of ecological responses to select alterations in the five fundamental components of the flow regime [1].

Flow Component	**Specific Alteration**	**Ecological Response**
Magnitude and Frequency	Increased Variation	Wash-out and/or stranding Lots of sensitive species Increased algal scour and wash-out of organic matter Life cycle disruption Altered energy flow
	Flow Stabilization	Invasion or establishment of exotic species leading to: Local Extinction and Threat to the native commercial species Reduced water and nutrients to the floodplain plant species, causing: Seedling desiccation Loss of secondary channels needed for plant establishment
Timing	Loss of Seasonal Flow Peaks	Disrupt Spawning cues for fish Loss of fish access to wetlands or backwaters Modification of aquatic web food structure Reduction or elimination of Riparian plant recruitment
Duration	Prolonged low flows	Reduction or elimination of plant cover Diminished plant species diversity Desertification of riparian species composition Concentration of aquatic organisms
	Prolonged baseflow ("spikes")	Downstream loss of floating eggs
	Altered inundation duration	Altered plant cover types
	Prolonged inundation	Change in vegetation functional type Tree mortality Loss of riffle habitat for aquatic species
Rate of Change	Rapid changes in river stage	Wash-out and stranding of aquatic species
	Accelerated Flood Recession	Failure of seedling establishment

on the calibration of models for ecological purposes, such as flow regimes? Often calibration is completed by comparing daily runoff versus simulated runoff for a hydrological model [45]. Calibration is also completed by using traditional error measures such as Nash-Sutcliffe Error (NSE) on a flow regime, but this does not take the natural flow regime into account [1]. Some hydrological models better account for magnitude than the other four aspects of flow [46].

Downscaling is a source of uncertainty, but the hydrological model is another source of uncertainty as well. There are three primary sources of uncertainty from the hydrological model: uncertainty in observations, parameter uncertainty and model structure uncertainty [47], [48]. These errors stem from both human error and limitations of our knowledge of the natural world. While no model is perfect, some hydrological models perform better than others. One model that has performed well in previous studies is the Precipitation-Runoff modelling system which has been used in various studies where hydro-ecological indices were of interest [8].

Caldwell (2015) tested six hydrological models at five study sites with varying levels of calibration: uncalibrated, calibrated to a downstream site, calibrated specifically for the site and calibrated for the site with adjusted precipitation and temperature inputs [8]. The authors found that the hydrological model's calibration had a greater impact on simulation of ERSS than model selection. It was additionally found that simple regional scale models had comparable performance to more complex models [8]. However, strong consideration should always be given to the type of hydrological model chosen for a given area or region based on applicability, parsimony and availability of input data. The strengths of a hydrological model should always be considered before moving forward with the calculation of ERSS.

The output of a hydrological model and the calculation of an ERSS can lead to

very different mitigation measures. Comparing a rainfall-runoff model to a regional regression model, it was found that both hydrological models underestimated observed variability but their calculation in some observed ERSS led to very different values in insectivore scores, important for the health of the area [49]. Murphy et al. (2013) found that the rainfall-runoff model had a 90% difference and the regional regression model had a 16% difference from the observed insectivore score [49]. Poor hydrological models and unexamined error can distort the perceived ecological health, risk and lead to the creation of poor mitigation measures.

How well a hydrological model simulates a type of flow is also a concern. Mitigation measures and preparedness for future environmental disasters can only be done when ERSS have been calculated and analyzed. To accurately and precisely simulate future conditions, present (baseline) conditions must be simulated well first. In one Australian study stream flow characteristics were simulated well at high and average flow but poorly at low flows, indicating an area for model improvement [9]. A similar result was found in a study of stream flow characteristics over Northeastern Canada [10]. A goal of this study is to determine if these stream flow characteristics can be improved with bias correction (BC).

Often in model calibration the average flows are reproduced the best, in part due to the selection of an error criterion that places less value on deviations at extreme high and low flows. In one study in Brazil, it was found that the flows with 90% and 95% exceedance were overestimated at 24% and 16% respectively [50]. The overestimation of extreme high and low flows in hydrological models needs to be continually researched since these types of flows are often ecologically significant [51].

2.3 Climate Downscaling

Changes in global climatic conditions are known to affect small scale regional weather patterns. Downscaling connects the global scale and the local scale; creating local details as well as bridging the gap between the large scale atmospheric processes and the small scale climatic conditions. Probability density functions of temperature, precipitation or other climatic characteristics of a region are found through the downscaling method [52]. The origins of downscaling are in the field of weather forecasting but it is also used in climate research with applications towards climate change.

Traditionally, extreme events are based on historical data and extreme events have set return periods based on the concept of stationarity [53]. Stationarity describes the idea that the variability in a watershed does not change [53]. For example, a 100 year flood has a 1% chance of occurrence in any given year and a construction project would be built to withstand a 100 year flood event. Climate change has eroded the classic methods of estimating future conditions as stationarity no longer holds true. Estimating future extreme events by analyzing the severity and frequency of past events is no longer reliable [53].

To estimate future scenarios that have variability in (extreme) events new methods must be created to model extreme future data. General circulation models (GCMs) contain climate information such as temperature, wind speeds, and precipitation for a large area [54]. GCMs are used in conjunction with estimated future land-use changes, and greenhouse gas emissions to determine future climate change projections [54]. However, GCM data cannot be used directly as there are two major impediments: 1) the spatial scale of the GCM may not be as fine as required in a hydrological model

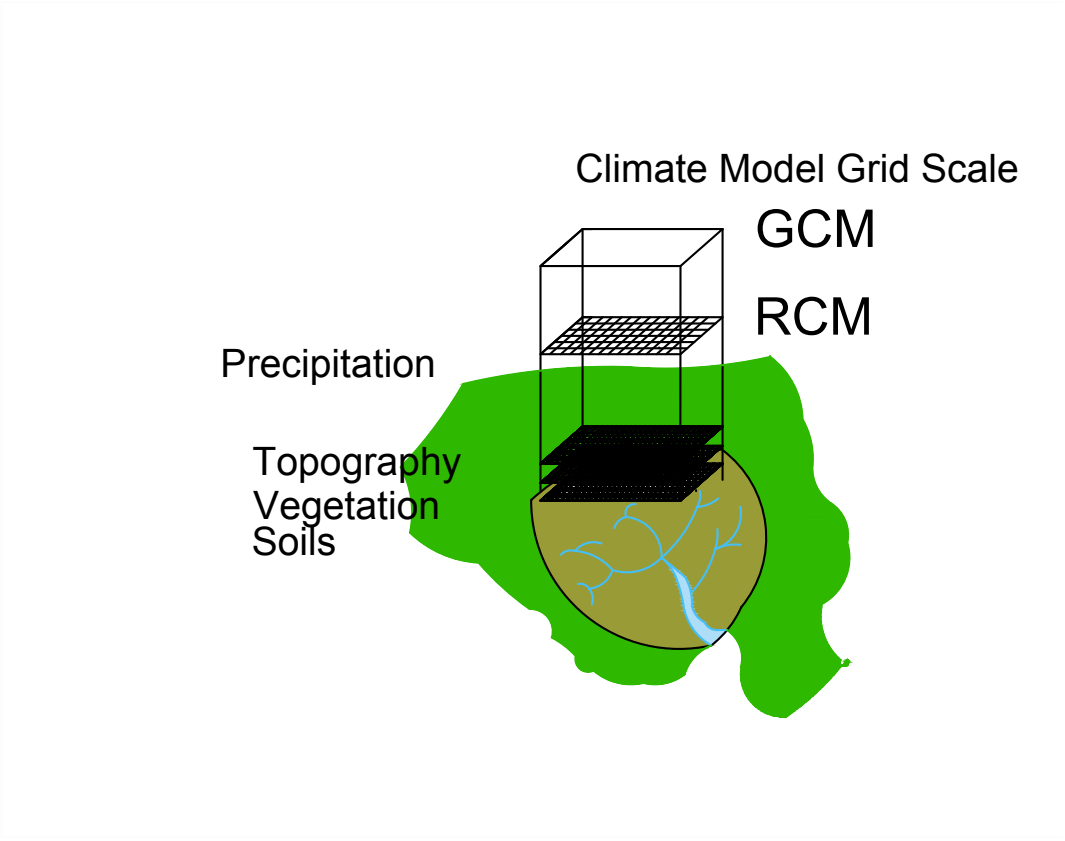

Figure 2.1: Data storage of climate information in GCM (General Circulation Model) and RCM (Regional Climate Model) grids and illustration of downscaling [56].

and 2) GCM output data contains biases relative to observed data [55].

Downscaling is the process of taking stored climate information in GCMs and transforming it to the appropriate size for use by those studying local impacts [56], [57], see Figure 2.1. There are two broad categories of downscaling - dynamical and statistical. The choice of downscaling technique and inputs is dependent upon the sites and variables of interest. Studies using downscaling have shown temperature is better simulated than precipitation, however, to determine ERSS the simulation of stream flow is necessary [58]. While there are benefits and detractions for each technique there is no universally superior downscaling technique [56].

2.3.1 Statistical Downscaling

Statistical downscaling is the older of the two downscaling techniques. In statistical downscaling, relationships are determined between observed climate data and large-scale climate patterns resolved by GCMs [55]. The statistical relationships are then applied to the GCM ouputs to give data more appropriate for local climate impact studies [55]. The first statistical downscaling techniques were regression models [59]. Statistical downscaling methods now include but are not limited to transfer functions, weather typing and weather generator methods [57]. The downscaling method has a large influence on the uncertainty of the predictions and the method should be chosen on a case-by-case basis [57], [58]. Statistical downscaling is limited by stationarity as it is based upon empirical relationships [45].

One of the simplest and most widely used forms of statistical downscaling is the change factor method (also known as the delta change factor method). This method takes the difference between the GCM output for the current time period and the GCM output from the future time period for a variable of interest [60]. The difference is then applied to the climate variable that has been directly downscaled to the observed resolution at the present time scale to get a present day observational data set [60]. However, this method only changes the average values of the climate variables, and not the variability [56]. The change factor method does not require any validation because it is based on the observed time series [57].

2.3.2 Dynamical Downscaling

Dynamical downscaling is a newer development in the field of climate research and downscaling techniques. PRUDENCE was the first international dynamical

downscaling project and it was used to create climate change predictions for Europe [61]. The PRUDENCE project started in 2001, making the field of dynamical downscaling quite new compared to statistical downscaling which has origins in weather forecasting techniques from the 1950's [52].

In dynamical downscaling the large GCM grids are restricted to smaller areas, creating regional climate models (RCMs). The boundary conditions are forced by the GCMs. The RCM is the model and the GCM is the driver. In dynamical downscaling both the large scale (atmospheric) and local conditions are calculated simultaneously [52]. Dynamical downscaling has been shown to better simulate the regional climate, however there are disadvantages to this method [13].

RCMs contain a better spatial resolution than GCMs, but are not necessarily more accurate to the desired degree [56]. Dynamical downscaling is sensitive to initial conditions and computationally intense. Additionally, this method does not allow for feedback into the global model. However, dynamical downscaling has been shown to better represent regional climate [13]. Dynamical downscaling is more physically based [45]. Bias correction is necessary (or another post-processing method), in dynamical downscaling as the physical and geographical characteristics of the basin are usually underrepresented and GCM errors propogate into RCM output [57], [62], [63]. Dynamically downscaled data is difficult to transfer to other regions as it is very specific to the local area. However, this may be viewed as a benefit or neutral in this research since only two basins are being considered.

Dynamical downscaling is a newer technique and is evolving quickly. Current research across all downscaling techniques involves increasing GCM resolutions and expanding ensemble projects. Data for climate research from dynamical downscaling comes from large national or international projects. The Intergovernmental Panel on

Climate Change (IPCC) has the goal to advance science related to climate change and assess the impact of climate change on the Earth's systems, both environmental and socio-economic [64]. To further understand climate change and predict future climate change impacts the CMIP (Coupled Model Intercomparison Project) was created, a collection of climate simulations [65]. The project is now in it's fifth phase (CMIP5). Progress needs to be made in terms of reducing uncertainty and creating more accurate climate simulations. One way that is being accomplished is by bias correction.

2.3.3 Uncertainty in Downscaling

Observed climate data does contain uncertainty stemming from measurement error and data management [46]. Uncertainty also propagates into hydrological models. This is particularly true regarding low flow and high flow events simulated by hydrological models which are important for ecological function [51] . However, downscaled data introduces additional uncertainty into hydrological models.

All downscaling methods introduce additional uncertainty to that already present from GCMs [51], [58], [66, among others]. The choice of downscaling method has been found to be a source of uncertainty [57]. Uncertainty propogates from emission scenario chosen, to GCM, RCM through to the downscaling method [15]. Using data with a finer resolution from information at a course resolution can lead to the the inability of the downscaling method to capture extreme events which are ecologically important [57]. RCMs best represent typical weather conditions and the complex relationships in a watershed may not necessessarily be kept when performing downscaling [67]. Chen et al.(2011) compared the uncertainty from six downscaling methods and the majority of the models resulted in hydrographs very similar to the

observed hydrograph but with poorly simulated timing and peak data [57]. Different downscaling methods can cause variation in results, and thus climate change impact studies using only one downscaling method should be interpreted with caution [57]. This uncertainty can propogate and can lead to simulation error in ERSS; Shrestha et al.(2014) found that certain ERSS were subject to considerable uncertainties with eight GCMs as data inputs in a hydrological model [68].

Aside from known uncertainties such as incomplete knowledge of climate systems and model simplification there are additional unknowns when projecting future climate using downscaling methods. These include, but are not limited to, unknown future climate policy which will affect carbon emissions and atmospheric processes [56]. Representative Concentration Pathways (RCPs) are emission scenarios based on different future scenarios of human population size, economic activity land use changes and climate policy [54]. There are four RCPs based on future emissions levels: RCP 2.6, RCP 4.5, RCP 6.0, and RCP 8.5 each representing a future with higher greenhouse gas emissions. However, only present conditions are considered in this study to remove the uncertainty of using future climate data. The process of creating downscaled climate data and comparing simulations using said data to observed conditions is the first step in creating future climate predictions.

Bias Correction

Due to the uncertainty from downscaling, bias correction is necessary to gain accurate predictions. Observed data often require modification due to poor estimation of local conditions [57]. Sometimes biases are small enough to be dealt with by a hydrological model, however that is not appropriate for every case [57]. Bias correction cannot compensate for a poor choice of a downscaling method [45].

Generally, bias correction first involves adjusting the long term differences between the variable of interest (i.e., precipitation, temperature) and then correcting the daily variability of the data to match that of the observed data, Equations 2.1 and 2.2 show a general approach of correcting monthly mean precipitation values [69].

$$c = \sum_{i=1}^{m=40} P_i^{FD} / \sum_{i=1}^{m=40} P_i^{GCM} \tag{2.1}$$

$$\bar{P}_{ij}^{GCM} = c * P_{ij}^{GCM} \tag{2.2}$$

where, P_i^{FD} is the monthly mean precipitation values of the forcing data and P_i^{GCM} is the monthly mean precipitation values of the GCM data. An offset value c is calculated from Equation 2.1. The daily mean values are then corrected in Equation 2.2 to create a new precipitation time series from the offset value. P_{ij}^{GCM} is the daily mean precipitation from the GCM and $\bar{P}_{ij}^{GCM}$ is the bias corrected daily mean precipitation. Bias correction can be done in many ways and Equations 2.1 and 2.2 are just one example. Another method is via flow duration curves (FDCs).

A flow duration curve (FDC) is a cumulative frequency curve that shows the relationship between flow magnitude and frequency [70] (Figure 2.2). It is an alternative validation technique to compare modelled flow duration curves to observed flow duration curves as opposed to comparing hydrographs [71]. Flow duration curves better highlight the highest and lowest flows, whose calibration is important when looking at ecological impacts. However, a hydrograph is a more complete picture of the flow signature [72]. Stream flows can be characterized by their FDCs just as they can be classified by hydro-ecological indices[73].

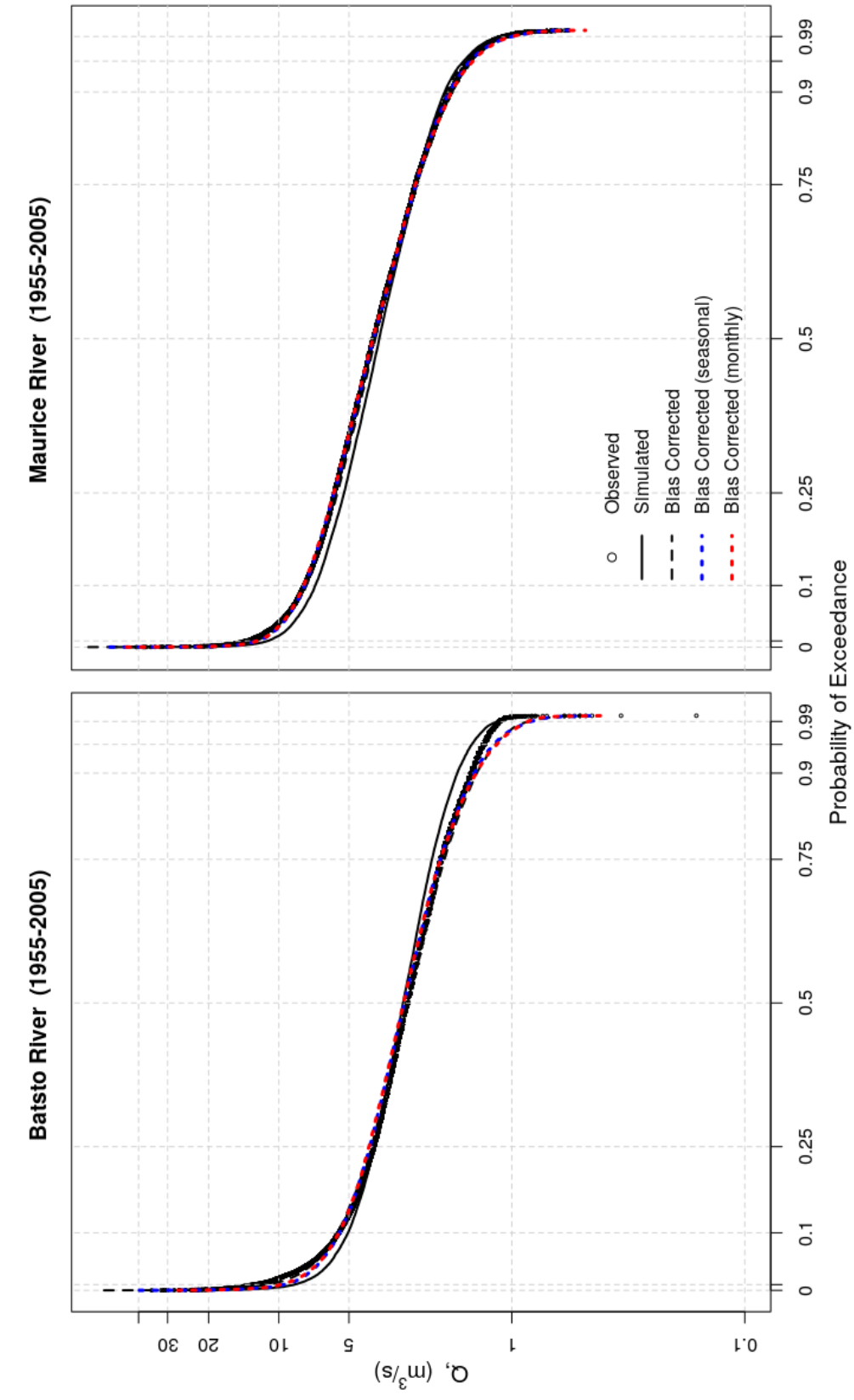

Figure 2.2: FDCs of the Batsto and Maurice River watersheds with bias correction across the full stream flow record [74].

The FDC represents physio-geographical characteristics that dynamical downscaling lacks without bias correction [63], [71]. The upper part of the FDC is controlled by the interaction between extreme rainfall and fast runoff, while baseflow recession determines the lower part of the FDC, the mid-range is controlled by within-year flow variations [71], [75], [76].

2.4 Summary

Climate change has been shown to impact the hydrograph and stream flow characteristics which in turn impacts ecological health of a waterway. Previous research has indicated that climate change alters hydro-ecological indices, but to my knowledge a comprehensive analysis of climate change prediction methods (i.e. downscaling) on the calculation of ERSS has not been researched to date [77]. Instead of analyzing multiple study sites this research focuses on downscaling, multiple GCMs and bias correction methods. In future, calibration criteria may include hydro-ecological indices in water resources modelling. The focus in this research is on the simulation of ecologically relevant stream flow characteristics (ERSS) and not on the calculation of ecological scores or metrics, which is beyond the scope of this research. However, it would be a continuation of this work and should be examined in future analysis. This research analyzes the ability of hydrological models and downscaled climate data to simulate ERSS. Previous work was done to obtain the stream flow projections used to calculate ERSS for two basins of interest.

Chapter 3

Data

This chapter describes previously completed work, mainly by Daraio (2017) that was used in this thesis. Familiarity with downscaling, hydrological modelling and bias correction processes is necessary to understand the research described in this chapter. This chapter is broken into three sections: observed data, simulated data and bias correction of stream flows. Hydro-ecological indices (ERSS) were calculated from these previously simulated stream flows.

ERSS were calculated from different sets of stream flow data. Details of how ERSS were calculated are in the following chapters. ERSS were calculated for each set of stream flows simulated using hydrologic models developed by Daraio (2017). The stream flows include observed conditions for each watershed, simulated stream flows calculated from inputting observed climate data into a hydrological model and simulated stream flows from inputting dynamically downscaled data into a hydrological model, Figure 3.1. Bias correction was also done on the stream flows. Green text in Figure 3.1 represents climate data, blue represents hydrological data and orange represents the statistical calculation of ecologically relevant stream flow

characteristics. This chapter deals with the precursory work done in the green and blue fields. The research and analysis done in this thesis belongs to the orange field which is described in the following chapters.

3.1 Observed Data

This study focused on the Pinelands Ecoregion (Pine Barrens), a unique ecosystem and home to 38 plant species and 43 animal species that are classified as threatened or endangered [78]. The Pinelands National Reserve (PNR) occupies 1.1 million acres of the Pinelands Ecoregion [78]. In addition to large land resources, the Pinelands Ecoregion contains a large river system. Observed daily mean flows (water years 1956-2005) from two United States Geological Survey (USGS) gauging stations were used: the Batsto River at Batsto, NJ (USGS Site 01409500) and the Maurice River at Norma, NJ (USGS Site 01411500), Figure 3.2. Flow data were used for the water years 1956 - 2005, as this research focused on long-term predictions of flow and ERSS. The water year begins October 1 and ends September 30 of any year. The upper Maurice River watershed has a basin area of 290 km^2 and the Batsto River watershed has a basin area of 180 km^2. The upper Maurice River watershed is more urbanized compared to the Batsto while the Batsto River watershed is completely within the PNR. Both rivers were classified by the USGS as class B, which represents a stable stream with a high base flow, typically located on the coastal plain [33]. There have been minimal changes to both the Batsto and Maurice stream flows over time [79]. Observed stream flows from these two watersheds were used for calibration and evaluation of the hydrological models.

To simulate stream flows for the historical period, hydrological models were driven

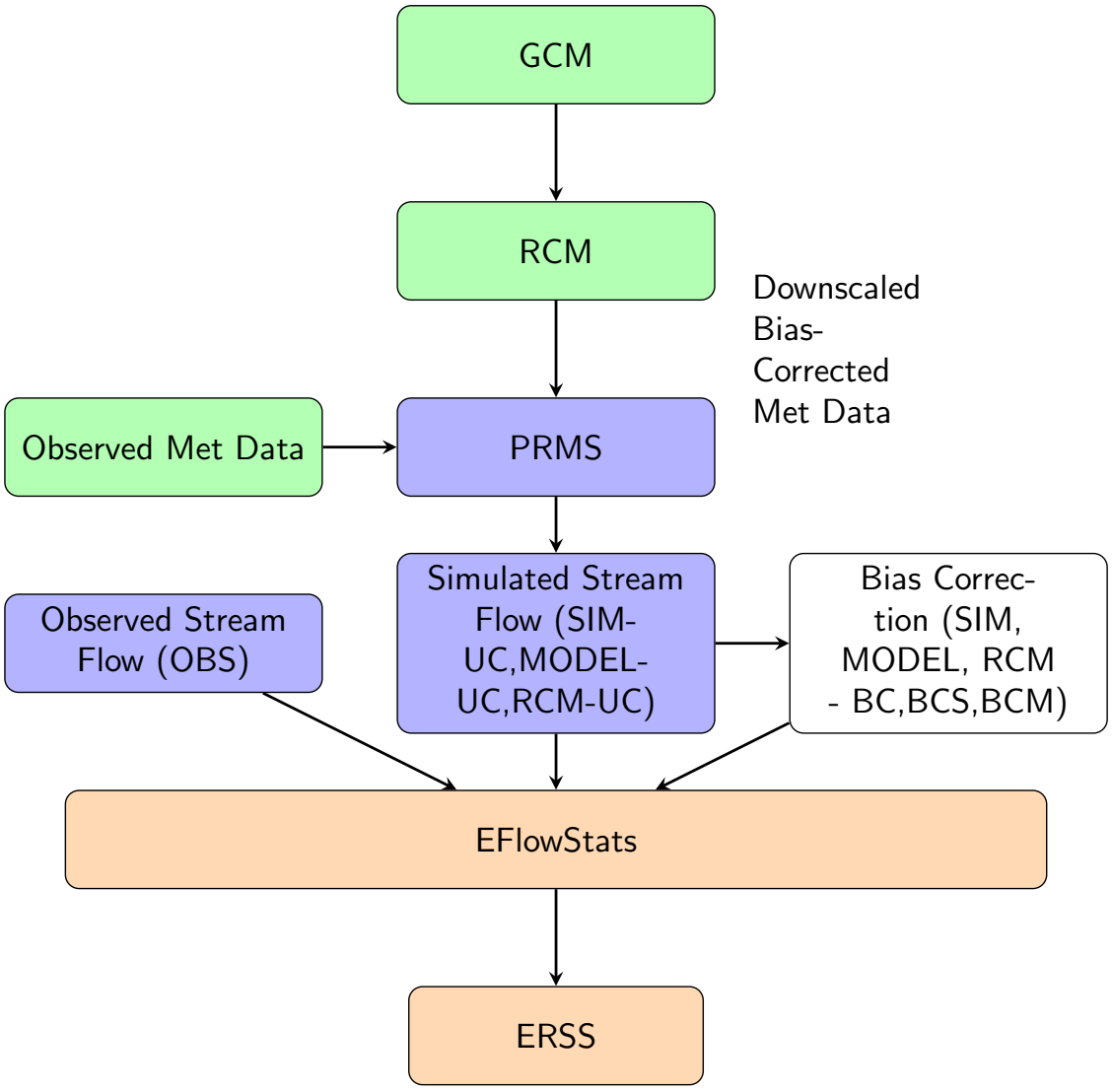

Figure 3.1: Connection between Climatic, Modelling and Statistical process to capture ERSS in this study.

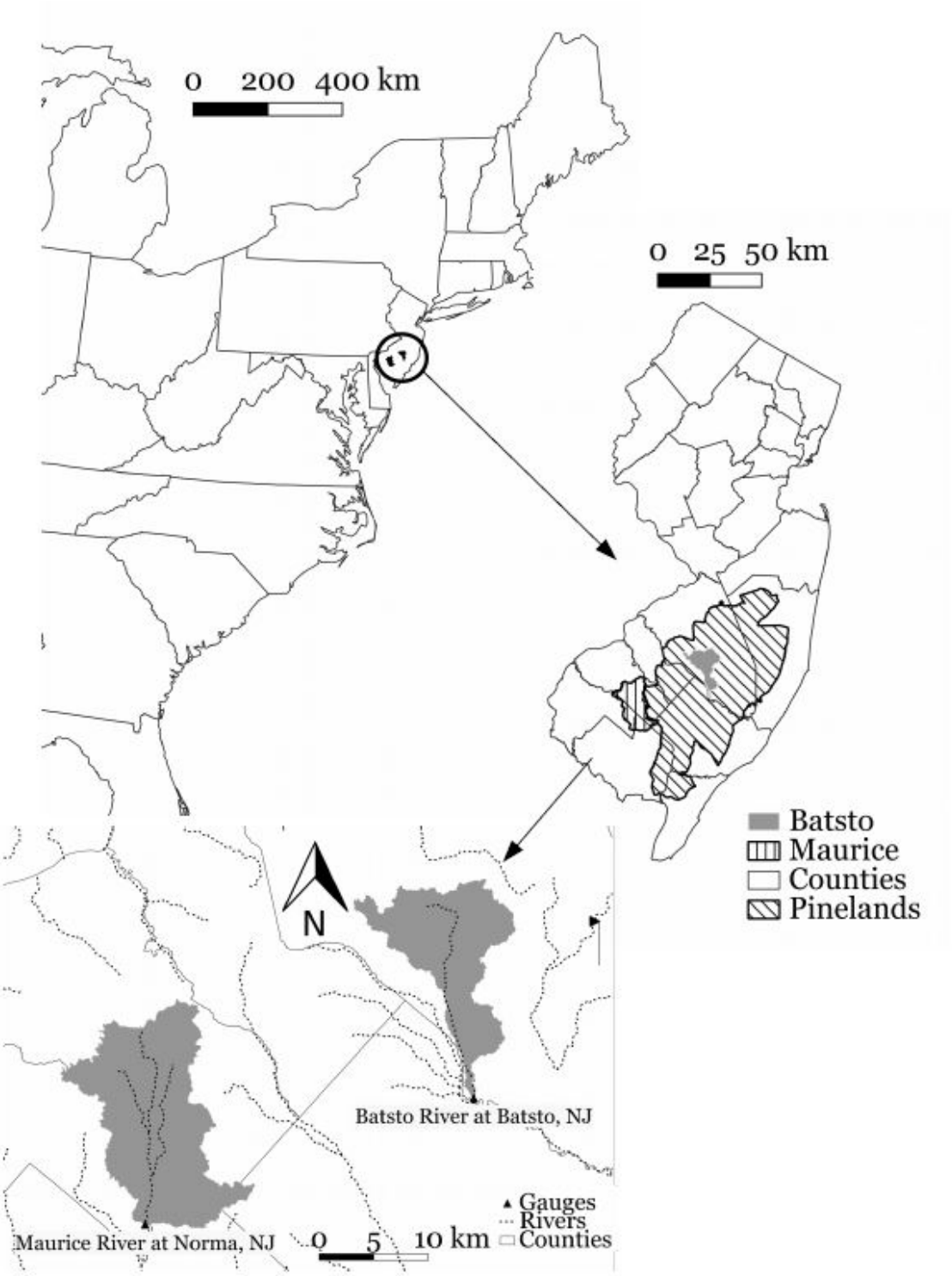

Figure 3.2: Site Map of the Study Areas, Batsto River watershed (USGS Site 01409500) and Maurice River watershed (USGS Site 01411500).

by observed and dynamically downscaled meteorological data, Figure 3.1. The sites of interest played a role in the decision to use downscaling. The New Jersey coastal plain is subject to hurricanes and tropical storms [74]. RCMs are known to have better predictions in mountainous areas and tropical areas where there are convective storms compared to GCMs [56]. Observed climate data in this study were input into the Precipitation Runoff Modelling System (PRMS), a hydrological model.PRMS is a deterministic (non-statistical) hydrological model which takes climate information and predicts hydrological outcomes, including stream flow [80]. PRMS has been used in many studies and has performed well in analyses with ERSS [8], [45]. The inputs of the model are precipitation, maximum and minimum air temperature, and solar radiation (from a daily time-scale) [45], [80]. Daily minimum and maximum air temperature and daily precipitation was taken from 12 km^2 gridded data found in the USGS Geo Data portal [81]. Observed Potential Evapotranspiration (PET) was estimated using USGS solar radiation data and the Priestly-Taylor equation [74].

3.2 Simulated Data

Flows were simulated using two different climate inputs, Figure 3.1, through 1) observed meteorological data and 2) dynamically downscaled meteorological (RCM) data. To evaluate model performance and to quantify the uncertainty the hydrological model was run with observed meteorological data and then separately run with RCM data to determine how much uncertainty was related to the model or the climate inputs. Climatic data was transformed into simulated flows in the Batsto and Maurice watersheds via the hydrological model PRMS.

In this study, the performance of PRMS was examined to more fully assess how

hydrological models simulate ERSS. Daraio (2017) used historical climate conditions along with RCM data to drive PRMS and the outputted stream flows were compared to the observed stream flow. It was found that when PRMS was simulated using dynamically downscaled climate data the high flows were significantly underpredicted in both basins [74].

3.2.1 Simulated Flows from Observed Climate Data

Daraio (2017) calibrated and evaluated the PRMS model using observed climate data in addition to using dynamically downscaled climate data from 13 GCMs, Table 3.1. Each basin's PRMS model was created using a calibrated amount of hydrologic response units (HRUs). Each HRU contained soil and land use information relevant to the respective watershed [82]. There were 116 HRUs and 236 HRUs created for the Maurice River watershed and the Batsto River watershed, respectively. Groundwater recharge was accounted for in the models using a three-reservoir system [80]. Stream flow was routed using the Muskingum method. Calibration was done stepwise using Let us calibrate (LUCA), a sensitivity and optimization tool [83]. Calibration was done in the following order: solar radiation, PET, stream flow volume and stream flow timing [74]. Stream flows were calibrated to mean daily flow and mean monthly flow, both were weighted equally. The calibration period for each model was the water years 1990-1996, the model was then validated for the water years 1997-2003. The model performance was evaluated using Goodness of Fit measures (GoF) [74]. The full historical period of record was 50 years (water years 1956-2005).

Both watersheds were calibrated for mean daily and mean monthly flows and performed well [74]. There were biases of -1.3% in both the mean daily and mean monthly flow calibration for the Batsto River watershed and there were biases of -0.7%

and -0.8% respectively for the mean daily and mean monthly stream flow calibrations in the Maurice River watershed. These mean daily and mean monthly stream flow calibrations for both watersheds had good fit to seasonal flows, showing well-simulated interannual variation [74]. In the evaluation of the Maurice River watershed the simulated stream flows had similar patterns to observed conditions. However, in the Batsto watershed model there was a bias of +45% and +35% in the summer and autumn respectively [74]. The calibration of Daraio's (2017) models found that simulated data had larger peaks than observed conditions, that indicates that there was too much runoff or a lack of surface storage [74]. This was particularly relevant in small storm events. Despite the limitations and biases of the PRMS modelling software and PRMS models of the two watersheds, these hydrological models of these New Jersey watersheds are considered optimized model simulations of this time period [84].

All hydrological models have strengths and weaknesses. The PRMS model has limitations in its ability to model groundwater and aquifers. In PRMS, the watershed boundaries for groundwater and surface water are often different [74]. Water flow in aquifers is simplified in PRMS and treated as a groundwater sink [74]. There were simplifications made when creating the Batsto and Maurice PRMS models. Daraio (Under Review-a) found through simulating the Batsto and Maurice River watersheds that a main limitation of PRMS is the simulation of peak high and low flows and groundwater-surface water interactions [15]. Another limitation of the PRMS models was the consideration of water withdrawals. While there was no explicit consideration of water withdrawal from the basins in the PRMS models, by using observed stream flows for calibration of the Batsto River and Maurice River watershed models water withdrawal was implicitly included [74].

Even when using observed climate inputs in a hydrological model uncertainty is still a concern and modelling limitation and may limit hydro-ecological assessments [46]. Uncertainty can arise from socio-economic changes, feedback loops from changes to the environment, observational error and parameter estimation [46], [85]. There is limited application of hydrological outputs due to the uncertainty in model outputs [84]. This uncertainty can propagate into the calculation of hydro-ecological indices, which this research is concerned with. Hydrological modelling can lead to large uncertainties in ERSS, particularly those that describe timing, duration, and rate of change [46]. The simulations of the ERSS from these hydrologically modelled stream flows is necessary to show whether ERSS are well estimated in hydrological modelling. Past research has shown that while magnitude ERSS are well simulated other stream flow aspects are not. However, creating hydrological models for the express purpose of modelling ERSS is time consuming and therefore expensive. This research tests whether specific simulations are necessary, or whether using hydrological models made for other purposes is a possibility.

3.2.2 GCM Driven Simulated Flows

The hydrological model for each watershed was first run with observed meteorological data listed in Section 3.1 and later run with RCM data to predict future water scenarios. As written in the Chapter 1 (Introduction) of this thesis, the goal of this research is to determine if dynamically downscaled climate data can predict ERSS. To attain this goal, GCMs must be dynamically downscaled. The process of dynamically downscaling and the uncertainty in downscaling is noted in Chpater 2 (Literature Review). Please refer to Chapter 2 for more information on the downscaling process and why downscaling is necessary to create climate model

predictions.

Dynamically downscaled climate data were used as meteorological inputs into the PRMS models of the Batsto and Maurice River watersheds to simulate stream flow. This was done to achieve the second objective (Chapter 1), comparing ERSS simulated through hydrological modelling, dynamically downscaled GCM simulations (RCM data) and observed historical data. The historical record (water years 1956-2005) was simulated using RCM data to compare records and determine whether the predictions were accurate or within reasonable error. This has applications to climate change impact assessments and mitigation measures. To create future plans stream flow and climate predictions must be within reasonable uncertainty. Using dynamically downscaled data to drive hydrological models involves a lot of uncertainty due to the top-down nature of the downscaling process, Figure 3.1 [86]. Uncertainty in the choice of emission scenario propagates into the GCM and the RCM through to the downscaling method until, in the worst case scenario, the future condition is very different and misleading from what was modelled [84].

Daraio (2017) selected 13 GCMs from the CMIP5 ensemble which were dynamically downscaled using a total of 40 RCM simulations for each watershed of interest, Table 3.1. Selection of these climate projections was based on data availability from the USGS Geo Data Portal [74]. The RCM data were input into PRMS and stream flows were output.

Comparisons were made between observed data and RCM driven stream flows. The RCM data driven PRMS model overestimated flows by 0.13 m^3/s for the Batsto River watershed and underestimated flows by 0.18 m^3/s for the Maurice River watershed. Daraio (2017) did not just simulate the PRMS model for the historical period (1970-2000), but additionally simulated two future periods for both

watersheds as comparisons, 2051-2065 and 2084-2099. Simulating these periods indicated an expected overall increase in stream flow in both basins. Simulation of future ERSS has not been included in this study as a main goal of this research was to determine uncertainty in the hydrological modelling and dynamically downscaling process. Uncertainty related to hydrological modelling versus dynamical downscaling is best analyzed by looking at the historical period where simulated records can be compared to observed records. Evaluation of the future periods is beyond the scope of this thesis.

The original objective of Daraio's (2017) study was to determine future water quantity concerns and stormwater infrastructure needs in the Batsto and Maurice River watersheds in New Jersey. However, by calculating the ERSS from the simulated stream flows used in the original 2017 research a new hydro-ecological component can be studied. By observing the changes in ERSS between observed and simulated stream flows mitigation measures can be produced not only for stormwater infrastructure but for the protection of ecological habitat and species. Future work will have to be done to create an environmental impact assessment of the area, however, this research is the first step in determining if the calculation of future ERSS via downscaling are appropriate for mitigation creation purposes.

Each of the RCM driven PRMS models created one set of stream flow data per basin, leading to a total of 40 stream flows per watershed. A set of ERSS was calculated for each simulated stream flow in this study. This section ends the description of what was done by Daraio (2017). However, further calculations were made on the stream flows more recently.

3.3 Bias Correction of Stream Flows

Flow Duration Curves

To improve the simulation of historical stream flows Daraio (Under Review-b) used Flow Duration Curves (FDCs) to bias correct the two watersheds at different time scales and compare GoF measures [84]. Using quantile mapping, Equation 3.1, Daraio (Under Review-a) improved the overall fit of of the FDC using BC [15]. Bias correction (BC) on the total record improved the overall fit of the FDC, but did not consistently improve GoF measures. Whereas, BC at smaller time scales, monthly and seasonal scales, improved the overall fit and consistently improved GoF measures [84]. The tails of the FDC, representing the extremes of the data, diverged between simulated and observed conditions (Figure 2.2). However, BC improved the fit of the tails to the FDC with smaller BC time steps [84]. Overall, BC of stream flows using either seasonal or monthly FDCs led to the greatest improvement of model performance in both basins [84].

Bias correction was done using the R package "qmap" [87] and Equation 3.1, creating a relationship between observed stream flow data (P_o) and simulated stream flow data (P_m):

$$P_o = F_o^{-1}[(F_m(P_m)] \tag{3.1}$$

where, F_o^{-1} is the inverse cumulative distribution function (CDF) for the observed stream flow and F_m is the CDF for the simulated stream flow. Limitations of bias correction are reviewed by Daraio (Under Review-b) [84].

While bias correction using the FDC did not consistently improve goodness of fit (GoF) measures, GoF measures were consistently improved when the timescales of

the bias correction were decreased [84]. Daraio (Under Review-a) used FDCs to bias correct the stream flow projections [15]. This resulted in two different sets of stream flows: 1) stream flows that were bias corrected directly to the observed data, hereafter known as MODEL results, and 2) stream flows that were bias correcting the RCM model driven results to the observed data, hereafter known as RCM results. Data was used that had bias correction done at varying time scales: 1) Bias correction of daily mean flows over the full period of record based on composite FDCs (BC), 2) based on seasonal FDCs (BCS), 3) and monthly FDCs (BCM) [84]. Data that were not bias corrected were designated as Uncorrected (UC). The sets of observed and simulated stream flows are in Table 3.2. In this thesis, these simulations were compared to observed conditions (OBS) through the evaluation of hydro-ecological indices (ERSS).

Table 3.1: List of models from the CMIP5 multi-model ensemble used in this paper [74].

Modeling Center (or Group)	**Institute ID**	**Model Name**
Commonwealth Scientific and Industrial Research Organization (CSIRO) and Bureau of Meteorology (BOM), Australia	CSIRO-BOM	ACCESS1.0
Beijing Climate Center, China Meteorological Administration	BCC	BCC-CSM1.1
College of Global Change and Earth System Science Beijing Normal University	GCESS	BNU-ESM
Canadian Centre for Climate Modelling and	CCCMA	CanESM2
National Center for Atmospheric Research	NCAR	CCSM4
Community Earth System Model Contributors	NSF-DOE-NCAR	CESM1(BGC)
Centre National de Recherches Météorologiques/Centre Européen de Recherche et Formation Avancée en Calcul Scientifique	CNRM-CERFACS	CNRM-CM5
Commonwealth Scientific and Industrial Research Organization in collaboration with Queensland Climate Change Centre of Excellence	CSIRO-QCCCE	CSIRO-Mk3.6.0
Institute for Numerical Mathematics	INM	INM-CM4
Institut Pierre-Simon Laplace	IPSL	IPSL-CM5A-LR IPSL-CM5A-MR
Japan Agency for Marine-Earth Science and Technology, Atmosphere and Ocean Research Institute (The University of Tokyo), and National Institute for Environmental Studies	MIROC	MIROC-ESM MIROC-ESM-CHEM
Atmosphere and Ocean Research Institute (The University of Tokyo), National Institute for Environmental Studies, and Japan Agency for Marine-Earth Science and Technology	MIROC	MIROC5
Max-Planck-Institut für Meteorologie (Max Planck Institute for Meteorology)	MPI-M	MPI-ESM-MR MPI-ESM-LR
Meteorological Research Institute	MRI	MRI-CGCM3
Norwegian Climate Centre	NCC	NorESM1-M

Table 3.2: Stream flow data used in this study per watershed.

Simulation	**Source and Description**	**Acronym**	**Number of predicted stream flows per basin**
Observed Stream flow Record	USGS	OBS	1
Simulated Stream flow record with historical climate inputs	PRMS and Historical Climate Data	SIM-UC SIM-BC SIM-BCS SIM-BCM	1 1 1 1
Simulated stream flow record with dynamically downscaled data	PRMS and Dynamically downscaled climate data	RCM-UC* MODEL-BC MODEL-BCS MODEL-BCM RCM-BC RCM-BCS MODEL-BCM	40 40 40 40 40 40 40

*Note that RCM-UC implies that there is no bias correction with the stream flows using dynamically downscaled data, the term RCM-UC is being used to distinguish between SIM-UC. This term could just be as easily called MODEL-UC.

Chapter 4

Phase 1: Preliminary Analysis of Ecologically Relevant Streamflow Statistics

4.1 Introduction

Hydro-ecological indices were chosen using three different methods to ensure that the selection of indices did not have an overly large systematic impact on this study's results. In the first phase a set of ERSS, the Seven Fundamental Daily Stream flow Statistics (7FDSS), was chosen for analysis. In the second phase of this research 171 ERSS were calculated and were reduced to minimally correlated indices using principal component analysis (PCA). In the third phase, hydro-ecological indices were chosen that were relevant to the Pinelands area. Phase 1 is discussed in this chapter while phase 2 and phase 3 are discussed later.

4.2 Method

The first objective of this research was to determine parsimonious sets of ERSS that defined the watersheds. The first phase of this research was a preliminary analysis and was conducted to evaluate the performance of simulated estimates of the 7FDSS from observed climate and RCM data driving the hydrological model [26]. These seven statistics were: mean (λ_1), coefficient of variation (τ_2), skewness (τ_3), kurtosis (τ_4), autoregressive lag-one correlation coefficient (r_1), amplitude (A) and phase (ω) of the seasonal signal, Table 4.1. The first four statistics captured the distribution of the stream flow, while the last three are correlated to the nature of the time series [26]. The first four of the 7FDSS were calculated using L-moments [88] [originally from 89]. The coefficient of variation (τ_2) and the mean daily flow (λ_1) are common statistical descriptors of stream flow, while the other five indices are less common. The symmetry of the probability distribution of stream flow is represented by τ_3. Skewness represents how large the disparity is between extreme high flows and average conditions [90]. Kurtosis (τ_4) is the peakedness of the probability distribution of stream flow compared to the normal distribution and described how likely the flow was to experience peak flow events [90]. τ_3 and τ_4 are related to peak data. The r_1 described the persistence of stream flow from one day to the next, while A and ω described the seasonal signal of the flow [26]. The equations for the 7FDSS are as follows:

$$\lambda_1 = \Sigma(X_i)/N \tag{4.1}$$

where X is the ordered daily stream flow record and N is the number of observations. Equation 4.1, represents the mean daily stream flow. Hosking and Wallis (1997) created L-moments to minimize the influence of sample size and outliers to the

computation of higher order statistics using

$$b_r = \frac{1}{n}\sum_{j=1}^{n}\frac{(j-1)(j-2)...(j-r)}{(n-1)(n-2)...(n-r)}x_{j,n}, \text{ where r = 1, 2, ..., n.} \tag{4.2}$$

Equation 4.2 was used to estimate values for τ:

$$\tau_2 = \frac{l_2}{l_1} \tag{4.3}$$

$$\tau_3 = \frac{l_3}{l_2} \tag{4.4}$$

$$\tau_4 = \frac{l_4}{l_2} \tag{4.5}$$

where

$$\begin{aligned} l_1 &= b_0 \\ l_2 &= 2b_1 - b_0 \\ l_3 &= 6b_2 - 6b_1 + b_0 \\ l_4 &= 20b_3 - 30b_2 + 12b_1 - b_0 \end{aligned} \tag{4.6}$$

The unbiased estimator b_r of the r^{th} probability weighted moment (Equation 4.2) is a function in the calculation of unbiased sample estimators of the first four L-moments (Equation 4.6) (l_1,l_2,l_3,l_4). Three of the four 7FDSS based on daily stream flow are listed in Equations 4.3-4.5. Equations 4.2 - 4.5 were taken from [88] (originally from [89].

The autoregressive lag-one correlation coefficient was calculated using the Yule-Walker method:

$$x_t - \mu = a_1(x_{t-1} - \mu) + ... + a_p(xt - p - \mu) + e_t \tag{4.7}$$

where the variance matrix of the innovations is calculated from the fitted coefficients and the autocovariance of x [36].The autoregressive lag one correlation coefficient is a measure of the relationship between the current daily stream flow and the previous daily stream flow [26]. In calculating r_1, the long-term monthly mean stream flow was subtracted from the daily stream flow in each month [26]. This calculation deseasonalized the time series. The transformed series was then standardized to have zero mean and unit variance [26].

The seasonal signal was represented by the amplitude and phase of the stream flows (Equation 4.8 and 4.9):

$$A = \sqrt{a^2 + b^2} \tag{4.8}$$

$$\omega = \tan^{-1}(\frac{-a}{b}) \tag{4.9}$$

where,

$$q_{zt} = a^* \sin(2\pi y) + b^* cos(2\pi y) \tag{4.10}$$

The standardized stream flow at day t is represented by q_{zt}. Parameters a and b were obtained by solving Equation 4.10 which were used in the equations for A and ω (Equation 4.8 and 4.9) [26].

The 7FDSS are advantageous as they are a pre-determined set of ERSS that does not need to be reduced from a set of correlated indices [26]. The 7FDSS are a parsimonious set of ERSS (Table 4.1). However, there is speculation that they do not adequately describe all ecological aspects of stream flow. The 7FDSS were originally created as a tool to classify the flow of ERSS while reducing the subjectivity of ERSS

chosen for a hydrological study in the continental United States (CONUS). In this research their applicability as a hydro-ecological tool is tested.

To determine whether these seven ERSS were within an acceptable range of uncertainty a +/- 30% bias was placed around OBS ERSS[49]. Using a range of uncertainty based on observed data established natural uncertainty, inherent to stream flow measurement, in comparison to model prediction bias [49]. Data within this range were considered to be reasonably estimated.

The 7FDSS have been shown to classify the flow just as well as a larger set of ERSS. However, a greater amount of ERSS will be calculated in the next chapters to ensure that the results from this phase are not only applicable to the 7FDSS. In this way this research will determine if they capture the full ecological characteristics of the stream flow [26]. Estimates in frequency, duration and rate of change are more difficult to estimate than changes in long term averages [46]. Thus the simulation of r_1, A and ω were of particular concern. The ability to simulate extreme high and low flows and the seasonal aspects of flow was of particular interest to this study. Comparisons between simulations were done using percent bias (Equation 4.11, below).

Table 4.1: Preliminary set of ERSS and Ecological Significance (Seven Fundamental Daily Stream Flow Statistics, 7FDSS) [26].

ERSS	**Ecological Significance**
Mean (λ_1)	Distribution of Daily flow
Variation (τ_2)	Distribution of Daily flow
Skewness (τ_3)	Distribution of Daily flow
Kurtosis (τ_4)	Distribution of Daily flow
Autoregressive Lag-One (r_1)	Duration and rate of change
Amplitude (A)	Seasonal Signal
Phase (ω)	Seasonal Signal

One objective of this research was to determine if ecologically relevant stream flow

statistics (ERSS) were well estimated in hydrological modelling simulations using both observed meteorological data and dynamically downscaled climate data (RCM data). ERSS were calculated from the stream flows described and simulated in the previous chapter of this thesis. Comparisons of ERSS were made between historical simulations using OBS and SIM. Each set of meteorological data inputs gave one ERSS point, as noted in Table 3.2. Comparisons were also made between OBS, MODEL and RCM data to determine which bias correction time scales and removal of which source of uncertainty (in the GCM and/or PRMS) simulated observed conditions (OBS) with minimal percent error or bias. Analysis was also done within the MODEL and RCM runs. These comparisons were made by visual comparison (boxplots and scatterplots) and percent bias:

$$Pbias_{i,s} = \frac{(ERSS_{i,s} - ERSS_{i,o})}{ERSS_{i,o}} \times 100\% \tag{4.11}$$

where $ERSS_{\mathrm{i,s}}$ represents statistic i, for stream flows from simulation s (e.g. SIM-BC, MODEL-BCM, RCM-BCS, etc.. . .), while $ERSS_{\mathrm{i,o}}$ is statistic i for the observed stream flow (OBS). $Pbias_{\mathrm{i,s}}$ represents the percent bias between the simulated $ERSS_{i,s}$ and observed $ERSS_{i,o}$. Comparisons were made between uncorrected indices (UC), and bias corrected indices (BC, BCS, BCM) and the OBS ERSS in all results (SIM, MODEL, RCM), using Equation 4.11.

The indices of interest (Table 4.1) were calculated through the R package "EflowStats" [91] for the historical period of water years 1956-2005. A minimum twenty year flow record was recommended to calculate the indices of interest [46]. A study by Kenard et al. (2009) showed that 90% of ERSS calculated using a 15 year flow record were within 30% of true values and 90% of ERSS were within 20% of

Land Use	Batsto	Maurice
Agriculture	7.4%	22.1%
Barren Land	0.1%	0.9%
Forest	60.0%	30.2%
Urban	5.6%	28.2%
Water	1.77%	1.2%
Wetlands	25.2%	17.5%

Table 4.2: Land Use as a Percentage of Total Basin Area for the Upper Maurice and Batsto River watersheds [74].

the true value using a 30 year flow record. There were minimal changes to both the Batsto and Maurice stream flows over the stream flow record which extended from 1927 in the Batsto River and 1932 in the Maurice River to 2005 compared to other rivers with larger infrastructure works [79]. Analyzing stream flows with minimal human alteration was advantageous because it was more likely observed changes to ERSS were due to data inputs (observed meteorological data, RCM data) and it was not necessary to consider pre- or post- impact conditions from an event.

The land use may impact the simulation of ERSS and account for differences between the Batsto and Maurice River watersheds, Table 4.2.

4.3 Results and Discussion

In phase 1 of this research the 7FDSS were calculated for each set of stream flows created by Daraio (2017), Table 3.2. Results are presented for the SIM simulations in the Batso and Maurice River watersheds first and then 7FDSS of the MODEL and RCM runs for each watershed are described.

4.3.1 PRMS Simulations driven by Observed Data

The 7FDSS were calculated for both watersheds and were analyzed to determine how the hydrological model PRMS simulated ERSS from observed meteorological data. This initial step was to determine how well the model simulated ERSS before adding additional uncertainty in the form of RCM data inputs. Error in the simulations could be attributed to the hydrological model. The stream flows were bias corrected to observed data (OBS) giving four sets of 7FDSS (SIM-UC, SIM-BC, SIM-BCS, SIM-BCM). The error was quantified by percent bias comparing the four sets of the 7FDSS to OBS. The results of the SIM simulation are shown graphically in Figure 4.1.

ERSS that described certain stream flow characteristics were expected to be within the range of uncertainty. Previous studies have shown that while magnitude ERSS were generally within the range of uncertainty, ERSS that represented other stream flow characteristics were not [8].

In the Batsto River and Maurice River watersheds the majority of the 7FDSS were within +/-30% error at all bias correction time scales as indicated by the data being within the dashed lines in Figure 4.1. Stream flow has a large natural variability, a 20-30% difference was observed between stream flow characteristics from a 75 year daily record to a 30 or 15 year daily record [92]. The +/-30% band of uncertainty placed model prediction bias into context with the natural variability of stream flow [49]. Mean daily stream flow (λ) and (τ_2) were within reasonable hydrological uncertainty at all time scales. This aligns with expected results [8], [49]. The PRMS model was calibrated to daily and mean monthly flows which explains the ability of λ_1 to be well-simulated and centred around 0%. Models that are calibrated to central tendency values, such as means, better predict central tendency statistics.

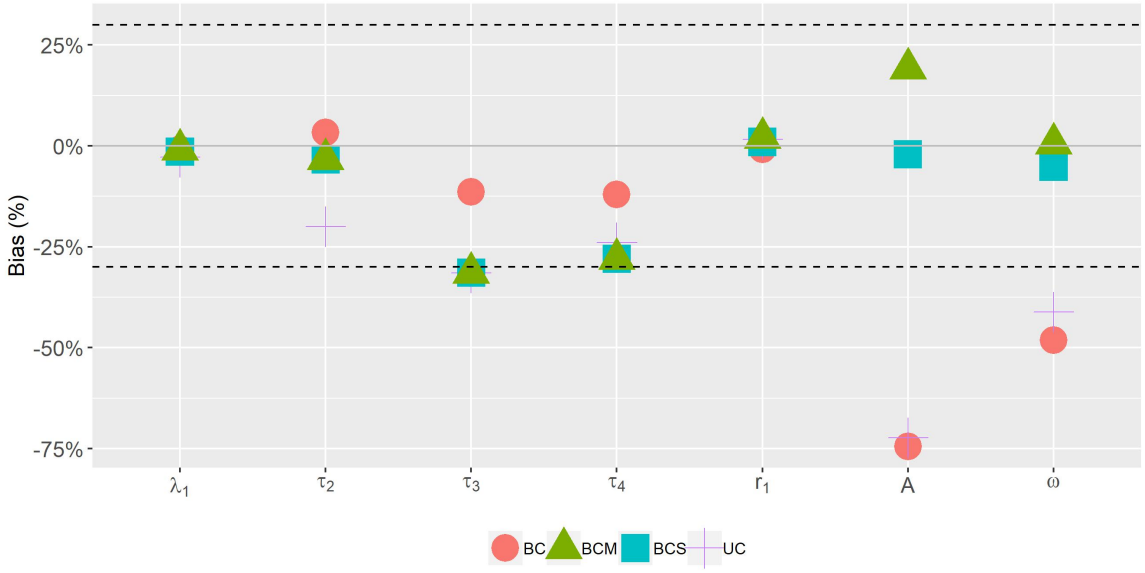

(a) Batsto

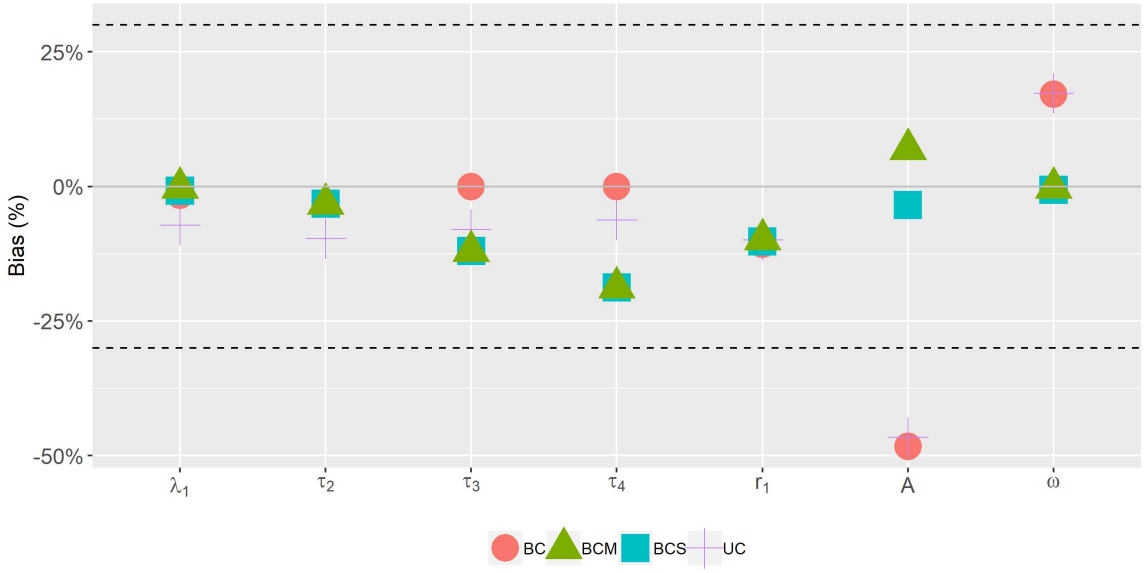

(b) Maurice

Figure 4.1: Percent Bias from the 7FDSS calculated from the historical climate simulation inputs into the PRMS hydrological model for the (a) Batsto River watershed and (b) Maurice River watershed. The dashed lines indicate +/-30% hydrological uncertainty.

The purpose of hydrological model calibration is to capture the variability and mean magnitude of stream flows, so λ_1 and τ_2 are expected to be well-simulated with or without bias correction [8]. In the SIM stream flows other ERSS were not as consistently well simulated.

Without bias correction (SIM-UC), τ_3 was outside hydrological uncertainty (+/-30%)in the Batsto River watershed, but not in the Maurice River watershed. Skewness (τ_3) with bias correction on seasonal and monthly time scales (SIM-BCS, SIM-BCM) had percent errors 1.4% outside of hydrological uncertainty in the Batsto River watershed. In the Batsto River watershed, τ_3 did not change from -31.4% with any bias correction except with bias correction on the full stream flow time series (SIM-BC). The percent bias of τ_3 only changed with full bias correction (BC). While τ_3 fell within the established hydrological uncertainty bounds for the Maurice River watershed, it did not in the Batsto.

In both watersheds kurtosis (τ_4) had a similar trend to τ_3 where SIM-BC was the simulation with minimal percent bias. Kurtosis (τ_4) was improved with bias correction at all time scales in both watersheds, but was not improved with bias correction at seasonal time scales (BCS, BCM). The daily stream flow statistics were still within hydrological uncertainty without bias correction. However, the seasonal ERSS had large bias values without certain types of bias correction. The bias correction on the smaller time scales did not prioritize τ_3 and τ_4. In one study it was found that τ_3 and τ_4 were very sensitive to the bias correction of precipitation [93]. This sensitivity may be applicable to stream flow as well.

Amplitude (A) and phase (ω) represented the seasonal aspect of the stream flow. In the Batsto River watershed uncorrected A and ω had percent errors of -72% and -41% respectively. In the Batsto River watershed SIM-BC these same ERSS had

percent errors of -74% and -48% respectively. In the Maurice River watershed a similar trend was observed, Figure 4.1. Full bias correction on the stream flow increased error for these ERSS. However, using seasonal and monthly time scales improved A and ω to be within hydrological uncertainty. Two of those ERSS were within 5%: A (BCS) and ω (BCM), of OBS values. Bias correction had little effect on λ_1 and r_1. ERSS τ_2 had reduced percent error with all bias correction methods (SIM-BC, SIM-BCS, SIM-BCM), compared to SIM-UC.

It was postulated that SIM-BCS and SIM-BCM would improve the prediction of all ERSS which was consistent with recent findings that the bias correction at smaller time scales improved model performance [84]. Bias correction at the smaller time scales did not have the expected improvement on τ_3 and τ_4 (Figure 4.1). However, improvement with SIM-BCS and SIM-BCM on the seasonal ERSS A and ω showed that these methods should be considered in hydrological model simulation of ERSS as simulation of the seasonal aspects of flow is where hydrological modelling has not been well simulated in past analysis [46].

The ERSS in the Maurice River watershed were better simulated compared to the Batsto River watershed when the respective hydrological models were driven by observed climate data (Figure 4.1). All ERSS, for uncorrected and bias corrected stream flows, were within hydrological uncertainty (+/- 30% error) with the exception of A which had a percent bias of approximately -50% in SIM-UC and SIM-BC. Only one ERSS (compared to two in the Batsto River watershed) was outside of accepted uncertainty in the Maurice River watershed. With SIM-BCM and SIM-BCS the simulation of A was improved to be within error. The Maurice River watershed was better simulated with hydrological modelling potentially due to the greater urbanization of the Maurice River watershed compared to the Batsto River watershed.

Calculating ERSS from a calibrated hydrological model with observed data inputs showed the bias inherent to the model. Removing the observed climate data as inputs into the PRMS model and replacing with RCM data added additional uncertainty. This change of climate inputs tested whether the calculation of ERSS could be done using RCM data within reasonable error with the potential to use this research for future predictions of ERSS for mitigation planning.

4.3.2 Downscaled GCM Simulations

To test the ability of downscaled climate data to simulate ERSS, the observed climate data inputs was removed from the PRMS model and were replaced with 40 RCM simulations. Bias correction was done resulting in 7 sets of stream flow per watershed (RCM-UC, MODEL-BC, MODEL-BCS, MODEL-BCM, RCM-BC, RCM-BCS, RCM-BCM). Each of the seven simulations had 40 7FDSS values due to the 40 dynamically downscaled climate (RCM) data inputs (Table 3.2).

Uncorrected Simulated ERSS driven by RCM data (RCM-UC)

In the Batsto watershed (Figure 4.2) λ_1 was simulated within +/- 30% hydrological uncertainty. The Maurice River watershed expressed similar behaviour (Figure 4.3) however, there was one outlier from climate data input CCSM4 r1i1p1 which had a percent bias of -31.2%. Mean error in variation (τ_2) was just outside hydrological uncertainty at -34% in the Batsto River watershed compared to -28.1% in the Maurice River watershed. Skewness (τ_3) was within hydrological uncertainty in the Maurice River watershed, but was mostly outside of hydrological uncertainty in the Batsto River watershed. Kurtosis (τ_4) experienced the same trend as τ_3 where the majority

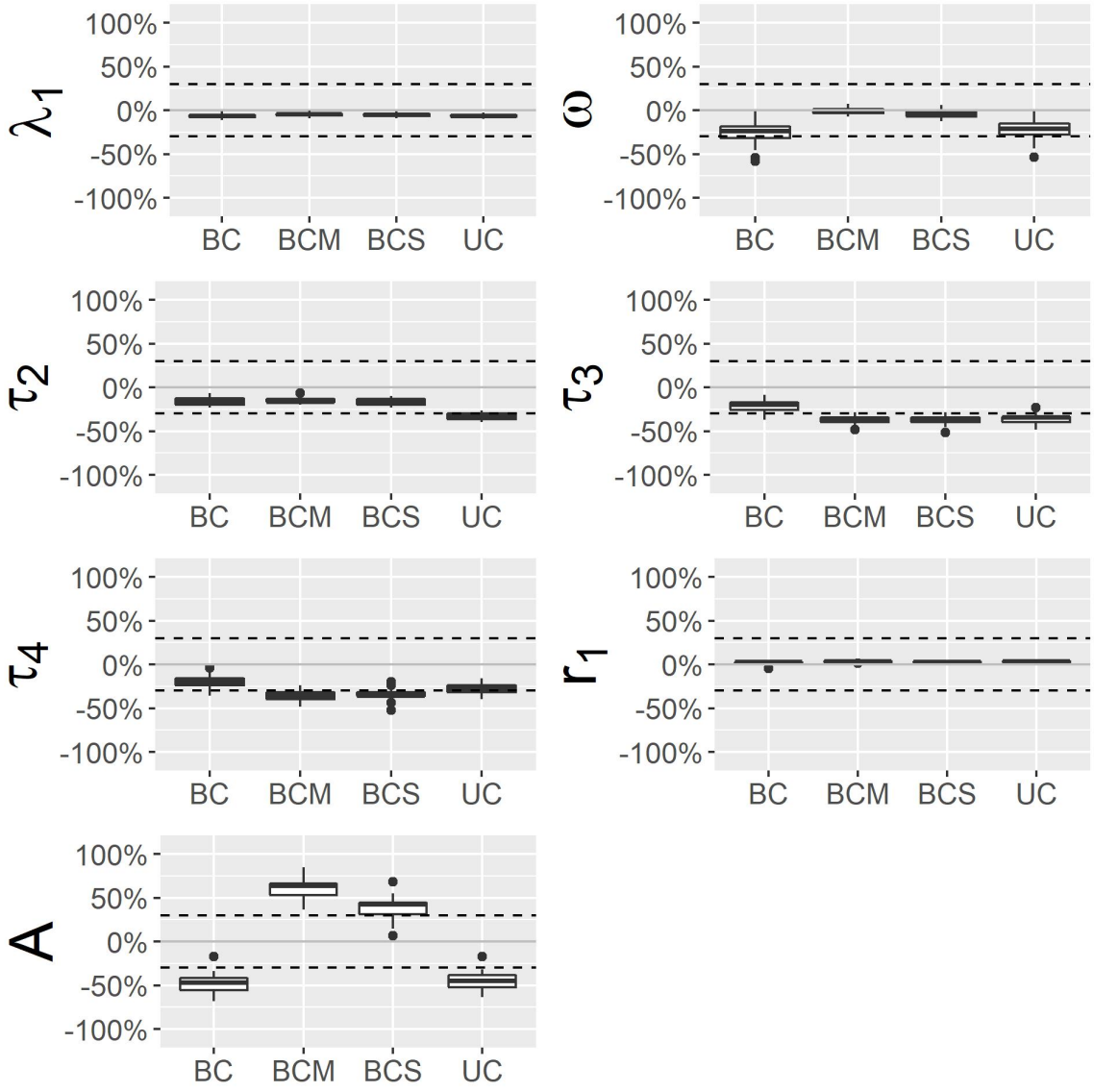

Figure 4.2: Percent Bias for the 7FDSS for the Batsto watershed with bias correction done on the MODEL driven streams.

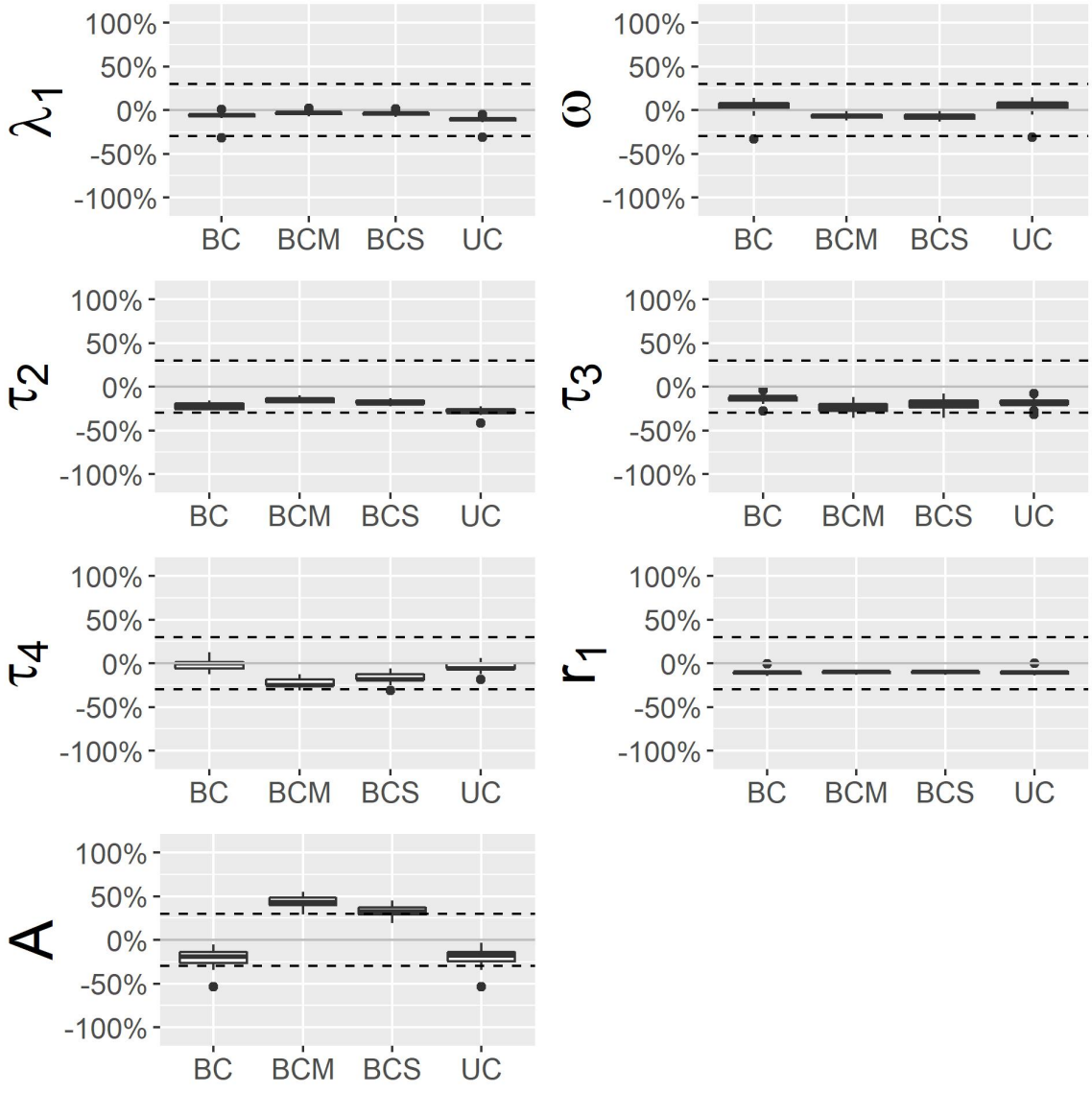

Figure 4.3: Percent Bias for the 7FDSS for the Maurice watershed with bias correction done on the MODEL driven streams.

of the simulation was within hydrological uncertainty in the Maurice River watershed, but not in the Batsto River watershed. The mean percent bias of τ_4 was -28.4% in the Batsto River watershed compared to -4.4% in the Maurice River watershed. The r_1 coefficient was simulated acurately without bias correction in both basins and was completely within hydrological uncertainty.

While many ERSS were simulated within reason for both watersheds, τ_3 and τ_4 were simulated differently per watershed. Given the similarity in characteristics between the two watersheds, this indicates that the simulation of these characteristics may be related to the urbanization of the Maurice River watershed compared to the Batsto. In the Batsto River watershed the average RCM-UC value for τ_3 was 0.22 compared to the OBS value of 0.35, while the RCM-UC value of τ_4 was 0.18 compared to OBS value of 0.18. The Maurice River watershed also had underestimated values, but was closer to observed values. The underestimation of τ_3 and τ_4 indicates that extreme events are being underestimated in the Batsto River watershed [90]. This was a concern starting this research as this result was found in the creation of the hydrological model [74]. This trend was also observed in the SIM results, which indicates that it was the hydrological model, not the RCM data inputs that were the result of the poorly simulated τ_3 and τ_4 in the Batsto River watershed.

As stated previously, two main ERSS of interest were amplitude (A) and phase (ω) as they represented the seasonal aspects of the stream flow signal which have not been well-simulated in hydrological models [46]. Using RCM data the mean percent error of A was -45.7% in the Batsto River watershed and -18.8% in the Maurice River watershed. The mean percent error of ω was -22.2% in the Batsto River watershed and -4.3% in the Maurice River watershed. This has implications for the modelling of undisturbed or minimally disturbed watersheds. Without bias correction, A and

ω in the Batsto River watershed exceeded the established uncertainty bounds more consistently across the range of simulations than in the Maurice River watershed. These results don't follow a similar pattern to the SIM results, where A and ω were poorly simulated in the Batsto River watershed and only A was poorly simulated in the Maurice River watershed. This indicates that the RCM data were a source of additional bias or uncertainty.

Model Corrected GCM Simulated Stream Flow (MODEL)

Mean daily flow (λ_1) did not change with MODEL bias correction (MODEL-BC, MODEL-BCS, MODEL-BCM). However, this was not unexpected as calibration of hydrological models by Daraio (2017) was done to daily mean and mean monthly flows. Bias correction at all time scales brought the error in τ_2 of the stream flows within acceptable range of uncertainty. These results were expected because there was minimal error on these ERSS from the hydrological model to begin with.

In the SIM results it was found that τ_3 and τ_4 only positively responded to SIM-BC. A similar outcome to the SIM results in the Batsto River watershed is noted in Figure 4.2 in regards to skewness (τ_3) and kurtosis (τ_4). The mean percent error of τ_3 in the Batsto River watershed were -21.5%, -37% and -37.6% in MODEL-BC, MODEL-BCS and MODEL-BCM respectively. The mean percent error of τ_4 in the Maurice River watershed were -0.01%, -16.7% and -22.7% in MODEL-BC, MODEL-BCS and MODEL-BCM respectively. While MODEL-BC improved the vast majority (Batsto) or all (Maurice) simulations of τ_3 and τ_4 to be within hydrological uncertainty, MODEL-BCM and MODEL-BCS increased the percent error. This agrees with past analysis that τ_3 and τ_4 of a time series is sensitive to bias correction [93]. Potentially, when trying to correct for the seasonal aspects of flow, the prediction of extreme

high and low flows are lost. The questions remains, whether they are lost to such an extent that the use of MODEL-BCS and MODEL-BCM should be disregarded. These results do not suggest so.

The seasonal aspects of flow also responded to MODEL-BCS and MODEL-BCM. ERSS ω and r_1 remained within hydrological uncertainty with the exception of a few outliers. While phase (ω) was corrected to be within the established range of hydrological uncertainty using BCM and BCS in both watersheds, amplitude did not have the same reaction. Instead, when MODEL-BCM and MODEL-BCS were applied, A went from being underestimated in both watersheds to being overestimated. The mean percent error of A was -47.9% in the MODEL-BC simulations and 38.8% and 60.4% in MODEL-BCS and MODEL-BCM simulations respectively in the Batsto River watershed. In the Maurice River watershed the percent errors of A were -19.6%, +32.7% and 43.1% for MODEL-BC, MODEL-BCS and MODEL-BCM respectively. In the RCM-UC and MODEL-BC simulations, A was more negative than -30% error, with MODEL-BCS and MODEL-BCM the error was greater than +30%. The change in amplitude is a difference in trend between the SIM results and the MODEL results. As the MODEL bias corrections were intended to correct for bias in the hydrological model. The change from a negative percent error to a positive percent error, between SIM and MODEL results (BCS and BCM), indicates that there is still uncertainty in the RCM data inputs that are not being accounted for.

In the Maurice River watershed, MODEL results followed a similar pattern to the Batsto (Figure 4.3). However, there were a greater number of outliers found in simulations of the Maurice River than in the Batsto River. While λ_1 had been within the range of uncertainty in past analyses there was one downscaled climate

projection that caused an outlier in the data provided from RCM CCSM4 r1i1p1. In MODEL-UC and MODEL-BC simulations of the Maurice River watershed, CCSM4 r1i1p1 had percent errors of -31.2% and -31.9% respectively.

Amplitude (A) responded similarly in the Batsto River and Maurice River watersheds when bias corrected in the MODEL simulations, however, A had greater mean percent error in the Batsto than in the Maurice. This agrees with the SIM analysis that urbanization may impact A's hydrological simulation. The majority of MODEL-UC and MODEL-BC ERSS were within hydrological uncertainty in the Maurice River watershed but underestimated from OBS, while the MODEL-UC and MODEL-BC ERSS were underestimated from OBS and outside of the range in the Batsto River watershed. In both watersheds using MODEL-BCS and MODEL-BCM overestimated A from OBS conditions to be outside the acceptable range of uncertainty.

Bias corrected GCM Simulated Stream Flow (RCM)

The RCM bias corrected simulations, corrected not only for hydrological model error (as in the MODEL simulations), but for additional bias from the RCM. Bias corrected RCM stream flows resulted in less biased predictions of ERSS compared to the MODEL simulations (Figure 4.4 and 4.5). This was exemplified by lower overall percent bias. Using RCM-BC, RCM-BCS and RCM-BCM all bias corrected ERSS were within hydrological uncertainty with the exception of A and ω. However, Amplitude A and ω in the RCM simulations generally showed improvement over the MODEL simulations.

The 7FDSS that represented the daily distribution (λ_1, τ_2, τ_3, τ_4) of flow experienced reductions in percent error using RCM bias correction. There was

approximately a 15% reduction in the percent bias of τ_2 from MODEL to RCM simulations using BCS and BCM. The mean percent error on τ_2 was -4.0% on RCM-BCS and -2.5% on RCM-BCM simulations in the Batsto River watershed. In the Maurice River watershed the coefficient of variation (τ_2) had a mean percent bias of -1.5% and -1.7% with RCM-BCS and RCM-BCM, respectively.

Data that described peak events were better simulated with RCM bias corrections. Skewness (τ_3) had percent bias of -25% with RCM-BCS and RCM-BCM. Kurtosis (τ_4) had percent bias of -23.9% and -26% with seasonal (RCM-BCS) and monthly (RCM-BCM) bias correction. Comparing Figure 4.2 and Figure 4.4, τ_3 and τ_4 have more of their data within hydrological uncertainty in the RCM simulations compared to MODEL simulations. Direct bias-correction of RCM driven simulated stream flow showed reduced bias for ERSS in the Maurice River watershed than the MODEL simulations.

Analysis of the 7FDSS that included seasonal characteristics of stream flow showed improvements in at least one of the ERSS. While ω did not change between RCM and MODEL simulations, A did. Instead of having percent bias greater than +30% with BCM and BCS (as in the MODEL simulations), the RCM-BCM and RCM-BCS resulted in A being within the established hydrological uncertainty bounds. Throughout MODEL and RCM simulation the percent bias of r_1 stayed consistently at 0%.

4.4 Summary

Model simulations using the 7FDSS resulted in some similarities among the flow characteristics. For example, seasonal characteristics of flow have often been found

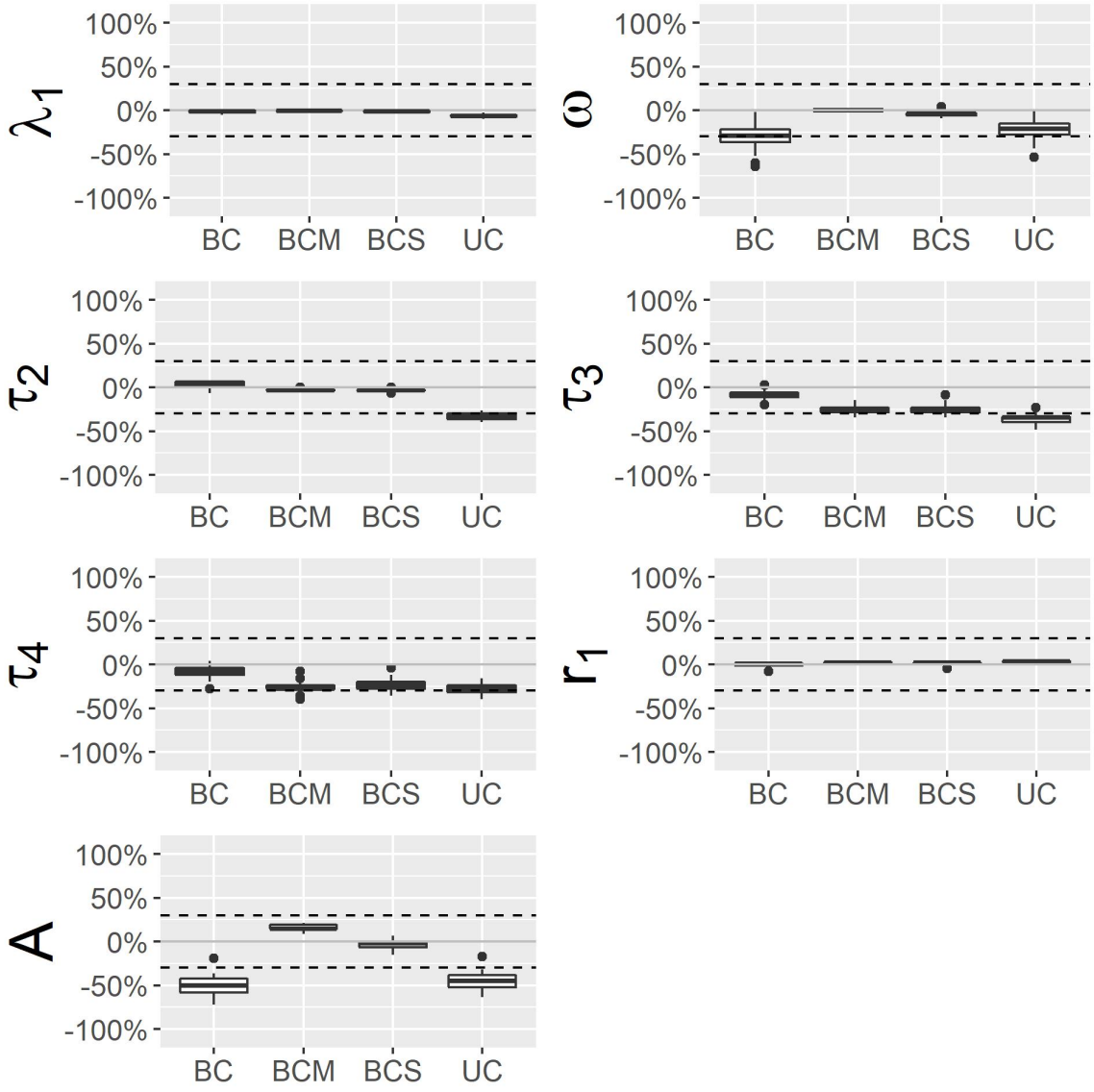

Figure 4.4: Percent Bias for the 7FDSS for the Batsto watershed with bias correction done on the RCM driven streams.

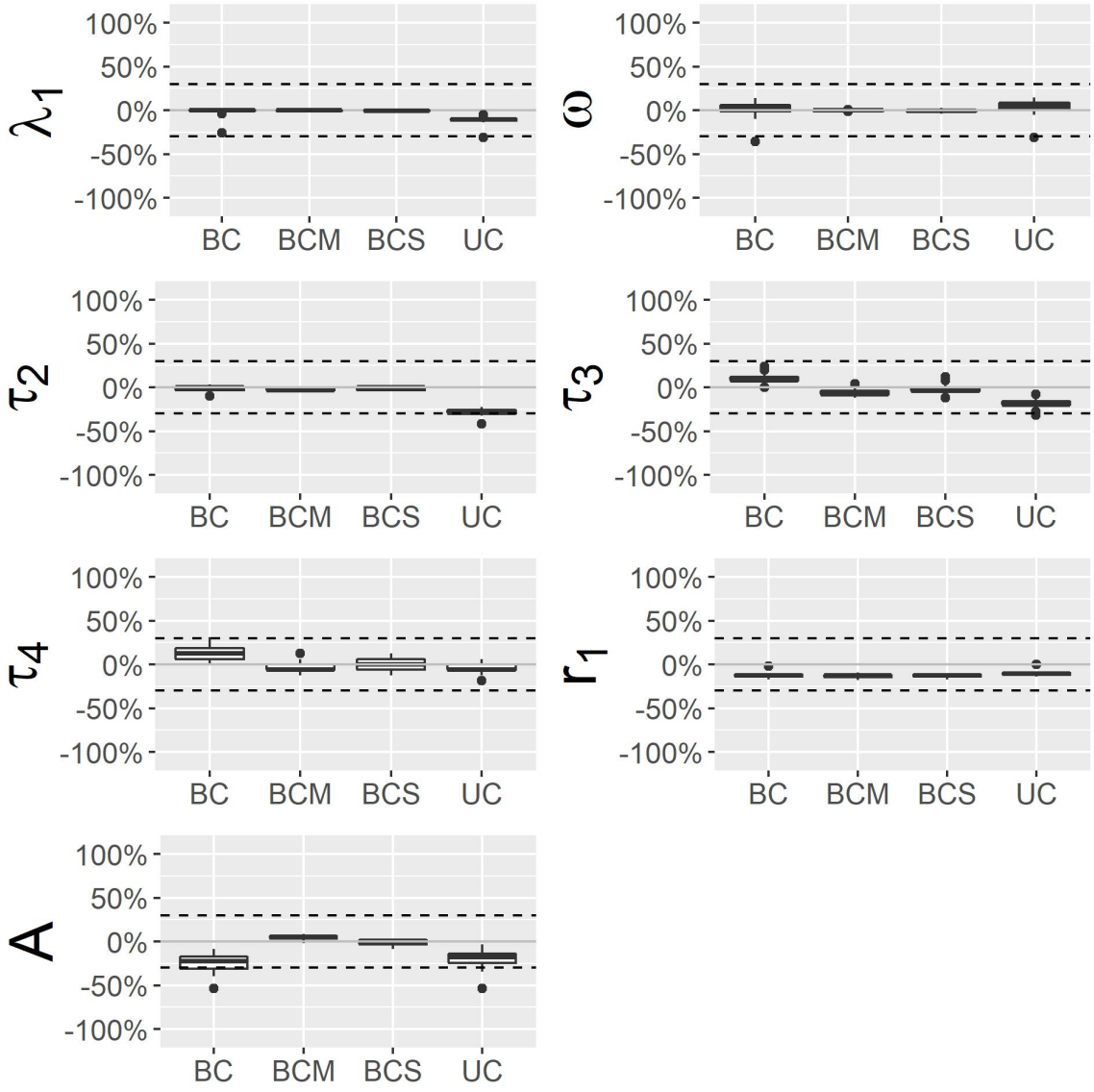

Figure 4.5: Percent Error for the 7FDSS for the Maurice watershed with bias correction done on the RCM driven streams.

to have higher uncertainty by hydrological models and that was true in this study with greater percent error found in A and ω without seasonal (BCS) and monthly (BCM) bias correction [46]. It was also found that the seasonal and monthly bias correction simulated the observed ERSS in the Batsto and Maurice River watersheds better then when bias correction included the RCM, thus decreasing the percent bias in ERSS representing all flow characteristics.

The need for bias correction on smaller time scales was speculated to be due to the choice of calibration criteria in the PRMS model. Caldwell et al. (2015) calibrated a PRMS model to annual, monthly, mean monthly and daily flow volumes and found that extreme high and low ERSS were poorly simulated [8]. Hydrological models from Daraio (2017) were calibrated to daily mean and mean monthly flows [74]. The calibration approach does not adequately account for the seasonal signal.

Bias correction at shorter time scales (BCS and BCM) was found to improve the simulation of the 7FDSS, both when using observed climate data (SIM) and downscaled climate data (MODEL, RCM). However, the difference between simulations in BCS and BCM was minimal. When simulating the stream flow Daraio (Under Review-b) found that there was no consistency between which shorter bias correction time scale outperformed the other (BCS or BCM) [84]. However, both BCS and BCM outperformed BC when simulating stream flows [84]. This was the primary finding of phase 1 of this research; ERSS from SIM-BCS and SIM-BCM better simulated the Batsto and Maurice River watersheds than SIM-UC or SIM-BC. The SIM simulation better represented observed conditions. Additionally, the observed meteorological data when used as an input to PRMS reduced the uncertainty associated with downscaled climate data.

The A and ω ERSS did not improve with bias correction on the full flow record

in the SIM, MODEL or RCM results, but did improve with BCS and BCM bias correction. While τ_3 and τ_4 showed only limited improvement with RCM-BCS or RCM-BCM bias correction and were best simulated with BC bias correction, they were still within the range of uncertainty with RCM-BCS and RCM-BCM.

The RCM produced the better simulations of ERSS compared to MODEL results as the bias corrected simulation reduced the overall uncertainty of the PRMS model when GCMs are included. The lower percent bias values across the RCM simulations compared to the MODEL simulations in the 7FDSS supported this conclusion. However, some natural variation may have been lost in the RCM simulations [15].

While the simulation of the 7FDSS in this analysis showed that ERSS were best simulated using RCM-BCS and RCM-BCM there is concern as to whether the 7FDSS describe the breadth of ecological changes associated with stream flow alteration in the Batsto and Maurice River watersheds. To determine whether this represents a consistent pattern, a larger selection of uncorrelated ERSS were used in phase 2 to describe the flow. Based on this preliminary phase of analysis, it was hypothesized that ERSS would be contain minimal uncertainty and be similar to observed conditions when the RCM was bias corrected on seasonal and monthly time scales compared to MODEL simulations. This method of bias correction provided acceptable uncertainty within all ERSS and did not favour only certain ERSS that represented specific aspects of flow.

Chapter 5

Phase 2: Analysis of ERSS selected through PCA

5.1 Introduction

In the previous chapter, the 7FDSS provided a simple set of non-redundant indices to determine the ability of dynamically downscaled climate data and hydrological models to estimate hydro-ecological indices [26]. The flow statistics related to the simulation of outlying flow events (τ_3 and τ_4) resulted in better simulated by RCM-BC while the seasonal statistics (A and ω) were better simulated by RCM-BCS and RCM-BCM. These results provided a good preliminary picture of the flow processes in the study basins (Maurice Batsto). However, the relevance of these ERSS to ecology is not well documented as the 7FDSS have been mainly used as a stream flow classification tool [26]. The 7FDSS only describe a broad picture of stream flow characteristics with a hydrodynamic focus (compared to an ecological focus). In addition, by only using 7 hydro-ecological indices the results may be overly simple and,

perhaps painted stream flow trends with a wide brush stroke. Important stream flow trends may have been missed by using only 7 ERSS. For more specific results, more ERSS were selected to describe the watersheds. Similar results were expected with seasonal ERSS being better simulated by RCM-BCS and RCM-BCM, and outlying flow characteristics being better simulated by RCM-BC.

Parsimonious sets of ERSS to define the region and simulations (objective 1) were calculated from 171 ERSS for each simulation (Table 3.2) using EFlowStats. Principal Component Analysis (PCA) was used following the approach outlined in Olden and Poff (2003) to select statistically significant ERSS [27]. The ERSS selected were then compared using statistical techniques and visual analysis (objectives 2 and 3).

5.2 Method

While the 7FDSS had been used as an initial set of measures to evaluate model simulation of hydro-ecological indices in RCM data, the full set of ERSS calculated by EflowStats is considered in this chapter. EflowStats calculates 171 ERSS [91], however, using all 171 indices to assess the variability and changes in ERSS would result in a high level of redundancy and could lead to issues with intercorrelation among flow variables. It is highly recommended across ecohydrology to calculate a smaller subset of the indices available [94]. A PCA in a regional analysis or modified regional analysis can e used to help identify a statistically significant subset of ERSS.

5.2.1 Principal Component Analysis

The function of a PCA is to reduce a large number of variables to a smaller number of uncorrelated variables [95]. In a regional analysis, a PCA is calculated on ERSS calculated from various stream flows of interest. In the modified regional analysis, watersheds with different modelling inputs (MODEL and RCM simulations) provided the inputs for a PCA (Table 3.2). Methods of analysis described in the literature review were not used because they are applicable when different watersheds are being compared, whereas in this study simulations of the watersheds are compared. Modified methods were used to determine statistically significant ERSS, and are described in this chapter. A PCA requires multiple data points (ERSS values) to be calculated. The SIM stream flows and the MODEL and RCM stream flow sets had the data points calculated differently between them.

Regional Analysis

In the SIM results, a regional analysis was performed where ERSS were calculated for both the Batsto and Maurice River watersheds as well as four other watersheds in the Pinelands. The Great Egg Harbor River at Folsom, NJ (USGS site 01411000) has an area of 147.9 km^2 and is an ecological sampling site for a study on stream flow and aquatic health interactions [96]. The Tuckahoe River at Head River (USGS site 01411300) has a drainage area of 79.8 km^2. The Mullica River near Batsto, NJ (USGS site 01409400) has a drainage area of 121.0 km^2. The Oswego River at Harrisville, NJ (USGS site 014000) has a drainage area of 187.8 km^2. The Great Egg Harbour, Mullica and Oswego sites are class B, while the Tuckahoe site is class C. Class B streams are stable with high base flows, while class C streams are moderately stable with moderately high base flows [34].Due to limitations in the flow record, data could

not be continuously taken from water years 1956-2005. The Batsto, Maurice, Great Egg and Oswego sites had data for the full water years 1956-2005 for all watersheds. The Tuckahoe site had a stream flow date range of water years 1971-2005, and the Mullica site had stream flow data from water years 1958-2005. All of these sites are in the Pinelands area; however, the majority are not completely within the PNR (Pinelands National Reserve). All sites have no or minor regulation and the entire record could be taken as a preliminary baseline, which is the same as the Batsto and Maurice River sites [79]. EflowStats was used to calculate 171 ERSS for each of these observed stream flow records. Using these five sites, a PCA was performed where each of the 171 indices represented a component.

Climate Change Analysis

To create a PCA for the MODEL and RCM results, a modified regional analysis was performed. The MODEL and RCM simulations had 40 data points each because there were 40 GCM simulations (Table 3.2). Instead of different watersheds being considered, as in a regional analysis, each stream flow record with a different RCM input was treated as a different watershed. EflowStats was used to calculate 171 ERSS for each stream flow calculated with a different RCM data input. The method to subset ERSS in this chapter (Phase 2) was based on work by Olden and Poff [27]. This is a novel approach because multiple basins were considered as well as multiple GCMs and multiple bias correction time scales.

Data Analysis

With a set of stream flows for each method of interest (SIM, MODEL, RCM), the data was quality controlled before PCA was performed. For example, ERSS

with extreme outliers and ERSS with small data ranges (<0.05) were removed to reduce noise from the data sets and judgement was also applied. The data was then checked for a normal distribution with the Shapiro-Wilk test, as PCA works best with a normal distribution (5.1) [97], [98]. The Shapiro-Wilk normality test is more appropriate for smaller data sets (< 50 samples). Therefore, it is applicable in this study because there are 40 GCM simulations (40 values for each ERSS) or 6 basins (6 values for each ERSS). For each set of ERSS, the Shapiro-Wilk test was calculated using:

$$W = \frac{(\sum_{i=1}^{n} a_i y_i)^2}{\sum_{i=1}^{n}(y_i - \bar{y})^2} \tag{5.1}$$

where

$$a_1, ..., a_n = \frac{m'V^{-1}}{\sqrt{m'V^{-1}V^{-1}m}}$$

where $m^{'}$ is the vector of expected values of standard normal order statistics, V is the corresponding covariance matrix and $y^{'}$ is the vector of ordered random observations. The two major components of the Shapiro-Wilk test are the W statistic and the p-value (significance) (Equation 5.1). A p-value of 0.05 was chosen. The null hypothesis was that the data is normally distributed. If the p-value of an ERSS set was less than 0.05 the null hypothesis was rejected and the data was considered not to have a normal distribution.

Not all ERSS data sets were normally distributed. Certain data sets that were found via the Shapiro-Wilk test to not follow a normal distribution were transformed using the Box-Cox method [99]:

$$y^{\lambda} = \begin{cases} \frac{y^{\lambda}-1}{\lambda}, (\lambda \neq 0) \\ log(\lambda), (\lambda = 0) \end{cases} \tag{5.2}$$

where λ is the transformation parameter and y is the dependant variable. The transformation was done by maximizing the W statistic in the Shapiro-Wilk test. This method of transformation has been found to be very effective in calculating the true Box-Cox transformation parameter, λ [100].

To make the contributions of each ERSS scale independent the Spearman's correlation matrix was calculated to equally weight the influence of each principal component. The Spearman's correlation matrix was then performed on the transformed ERSS (where all data was normalized) using [101]:

$$\begin{bmatrix} 1 & \rho_{12} & \rho_{13} & \dots & \rho_{1p} \\ \rho_{21} & 1 & \rho_{23} & \dots & \rho_{2p} \\ \rho_{31} & \rho_{32} & 1 & \dots & \rho_{3p} \\ \vdots & \vdots & \vdots & \ddots & \vdots \\ \rho_{p1} & \rho_{p2} & \rho_{p3} & \dots & 1 \end{bmatrix} \tag{5.3}$$

where,

$$\rho_{jk} = \frac{\Sigma_{i=1}^{n}(x_{ij} - \bar{x}_j)(x_{ik} - \bar{x}_k)}{\sqrt{\Sigma_{i=1}^{n}(x_{ij} - \bar{x}_j)}\sqrt{\Sigma_{i=1}^{n}(x_{ik} - \bar{x}_k)}}$$

and x and y represent the two ERSS sets whose correlation was calculated and i is the paired score.

A Spearman's correlation matrix was calculated for each ERSS set described in Chapter 3, Table 3.2, or observed stream flow for SIM analysis. The 171 ERSS were calculated by inputting stream flow data and peak flow data into EflowStats.

PCA was done on the set of 171 indices for each simulation and watershed to obtain the most representative statistics for the area. One PCA was done for SIM results, one was done for MODEL-BC, one for MODEL-BCS, etc. PCA takes a number of related variables and transforms them into a smaller set of uncorrelated variables [95]. Reducing so many indices was a numerical challenge as most PCA analyses typically do not start from such a large set of variables (171 ERSS) compared to observations (data points). Therefore, this research employed two functions to calculate PCAs.

The *prcomp* function in R was used to calculate the PCA on the ERSS sets and calculated the loadings and eigenvalues on the Spearman's correlation matrix. The function returned the standard deviation of the principal components (the square roots of the eigenvalues of the correlation matrix) and the loadings which were used as inputs for the stopping criterion [36].

Since PCA is usually meant to be performed on data with greater observations than variables the *prcomp* function was compared to the *SamplePCA* function from the ClassDiscovery package in R [36] to ensure the results from both functions agreed. The *SamplePCA* function is used to create a PCA more efficiently in scenarios with greater numbers of variables compared to data points; it was originally developed for biology microarray studies [36]. One component was calculated for every input variable, and thus resulted in 171 components.

The amount of principal components (PCs) determined the ERSS included in the analysis, reducing the large set of ERSS to a smaller, statistically significant ERSS set. The number of principal components was chosen using the broken stick method [102]:

$$b_k = \Sigma_{i=k}^{p} 1/i \tag{5.4}$$

Table 5.1: Stream flow categories [34].

	Definition
ma	Magnitude, Average flow conditions
ml	Magnitude, Low flow conditions
mh	Magnitude, High flow conditions
fl	Frequency, Low flow conditions
fh	Frequency, High flow conditions
dl	Duration, Low flow conditions
dh	Duration, High flow conditions
ta	Timing, Average flow conditions
tl	Timing, Low flow conditions
th	Timing, High flow conditions
ra	Rate of Change, Average flow conditions

where p is the number of variables and b_k is the size of the eigenvalue for the k^{th} component under the broken stick model [103]. The broken stick model was more easily able to be calculated through the *prcomp* function compared to the *SamplePCA* function which is why both functions were used.

In the broken stick method, a significant PC is identified if the observed eigenvalues are greater than the eigenvalues generated by the broken stick model (eigenvalues from random data) [102]. There is a standard Kaiser-Guttman approach of selecting as many principal components as eigenvalues greater than 0. However, this led to more PCs and an objective of this research was to be selective about choosing ERSS and finding parsimonious sets to reduce redundancy and confusion in interpretation. The broken stick method was also chosen as it has been used in similar studies [96], [103].

For each PC included based on the broken stick model, one component was chosen that represented a unique aspect of flow, ex. ma – magnitude average, fh – high frequency (Table 5.1). A full list of ERSS names and definitions from ERSS can be found in Appendix B [34].

The ERSS chosen had the greatest absolute loading for that PC and stream flow category, this replicated the method of Olden and Poff [27]. The percent error on these indices was then calculated and the data were analyzed for trends and patterns in how SIM, MODEL and RCM data represented observed conditions. Similar methods to determine the accuracy of the simulations from Chapter 4 were used in this analysis, such as the percent bias equation (Equation 4.11) and visual inspection. Some variation in ERSS were expected, a hydrological uncertainty of +/- 30% was used as context for inherent variability in stream flow and measurement [8], [49]. Each PCA led to a different set of ERSS chosen, therefore comparisons between basins SIM, MODEL and RCM simulations could not always be made directly.

The median absolute percent error (MdAPE) was used to compare the simulation of ERSS between simulations (SIM, MODEL, RCM). The MdAPE for each stream flow category was calculated using:

$$MdAPE = median(p_1, p_2, ...p_n) \tag{5.5}$$

where p_1 is the absolute $P_{bias_i,s}$ from Equation 4.11. The MdAPE can be calculated over the entire selected ERSS or using a subset of ERSS such as stream flow characteristics (e.g. only timing ERSS, only low flow ERSS). The median was used as a metric of average ERSS value because it is less sensitive to outliers. As the number of ERSS used in the analysis varied depending on simulation, the proportion of ERSS completely within the range of uncertainty was used as a measure of simulation accuracy. A lower MdAPE value indicated a better simulation.

The variability of the ERSS predictions was also of interest. Due to the differences in magnitude between ERSS, the data required standardization to compare the data

ranges between ERSS. To quantify the variation between ERSS, the standardized data range (SDR) was calculated for each ERSS set using [49]:

$$SDR = \frac{MAX(ERSS_{i,s}) - MIN(ERSS_{i,s})}{median(ERSS_{i,s})} \tag{5.6}$$

The SDR is the maximum ERSS value minus the minimum ERSS value divided by the median. The SDR for observed values (OBS) was calculated using the set of six stream flows from the regional analysis. The SDR for simulated data (MODEL and RCM) was calculated from the set of simulated stream flows. The SIM results could not have an SDR because each bias correction method produced only one ERSS point, whereas the models with RCM data produced 40 ERSS data points from the 40 RCM inputs.

The purpose of the SDR was to contextualize the variability of ERSS when using RCM data inputs in the PRMS model. The SDR represented the variability of an ERSS. The variability (predicted SDR) of a specific simulated ERSS was compared to the variability of an OBS ERSS (observed SDR). Ideally, the SDR of an observed ERSS would be equal to the SDR of a predicted ERSS. However, it was desirable that the variation of the ERSS from RCM data inputs be less than the variation of the ERSS from a regional analysis. This would show that the uncertainty of doing a regional analysis is greater than or equal to the uncertainty of using RCM data inputs and treating each RCM simulation as a separate watershed (modified regional analysis).

5.3 Results and Discussion

ERSS were selected and calculated for each simulation (Table 3.2) and statistical analysis techniques were done to determine which simulations had minimal error compared to OBS conditions. Quality control of the data is presented first, then results. Results are presented first for SIM, then results driven by RCM data are discussed in the next section of this chapter. Trends in the ERSS were analyzed to determine if there was consistency with the results from phase 1. It was expected that BCS and BCM bias correction on each simulation would have the minimal percent bias and MdAPE values for each stream flow characteristic and overall ERSS.

5.3.1 QA/QC

Using EflowStats, 171 ERSS were calculated for over 500 stream flows (Table 3.2). ERSS were systematically reduced prior to analysis following the steps outlined below.

Small data ranges or outliers caused certain ERSS to be removed in simulations of the stream flow. In all simulations ERSS *dl18, dl19, dl20, mh23* and *mh26* were removed because of a large amount of missing data (e.g., many 0's or NA's). ERSS *dl18* and *dl20* had a data set of 0 through the majority of the analysis. ERSS *dl19, mh23* and *mh26* had NA values in simulations. The low flow indices (*dl18, dl19, dl20*) were 0 because there were no zero flow days simulated in the record or pulse spells that low. The value on the high flow indices were due to there being no flows above seven times the median flow value. In the observed record (OBS) in the Batsto and Maurice watersheds, there were no zero flow days leading these ERSS (*dl18, dl19, dl20*) to be a set of 0's. In some simulations of ERSS *mh23* and *mh26* did not have

values attached to them (NA), this was due to a lack of extreme stream flow events in the simulation from the RCM. These ERSS, which are defined in Table 5.2 were removed from analysis.

Table 5.2: ERSS removed from analysis in first stage QA/QC due to a high proportion of missing values [34].

ERSS	**Definition**
dl18	Number of zero-flow days. Count the number of zero-flow days for the entire flow record. *Dl18* is the mean annual number of zero flow days per year. (number of days/year)
dl19	Variability in the number of zero-flow days. Compute the standard deviation for the annual number of zero flow days. *Dl19* is 100 times the standard deviation divided by the mean annual number of zero flow days. (%)
dl20	Number of zero-flow months. While computing the mean monthly flow values, count the number of months in which there was no flow over the entire flow record. (%)
mh23	High flow volume. The average volume of flow events above a threshold equal to seven times the median flow for the entire record. *Mh23* is the average volume defined by the median flow for the entire record. (days)
mh26	High peak flow. The average peak flow value for flow events over a threshold equal to seven times the median flow for the entire flow record. *Mh26* is the average peak flow divided by the median flow for the entire record. (dimensionless)

Outliers were removed from the data set on a case by case (simulation by simulation basis). The PCA was run for each simulation once and any ERSS with outliers was removed from analysis and re-run. ERSS that were consistently found to have outliers (*ta3, th1, tl4, dh6* and *dh23*), Table 5.3 were removed from analysis.

The Shapiro-Wilk test determined if the data were normally distributed on the

Table 5.3: ERSS removed due to outliers in various simulations [34].

ERSS	**Definition**
ta3	Seasonal predictability of flooding. The maximum number of flood days in any given 2-month period divided by the total number of flood days (flow events with flows > 1.67-year flood). (dimensionless)
th1	Julian date of annual maximum. Determine the Julian date that the maximum flow occurs for each year. Transform the dates to relative values on a circular scale (radians or degrees). Compute the x and y components for each year and average them across all years. Compute the mean angle as the arc tangent of y-mean divided x-mean. Transform the resultant angle back to Julian date. (Julian date)
tl4	Seasonal predictibility of non-low flow. Compute the number of days that flow is above the 5-year flood threshold as the ratio of number of days to 365 or 366 (leap year) for earch year. *Tl4* is the maximum of the yearly ratios. (dimensionless)
dh6	Variability of annual maximum daily flows. The standard deviation for the maximum 1-day moving averages, *dh6* is 100 times the standard deviation divided by the mean (%)
dh23	Flood duration. The flood threshold as a the flood equivalent for a flood recurrence of 1.67 years. Determine the number of days each year that the flow remains above the flood threshold. *Dh23* is the mean of the number of flood days for years in which floods occur. (days)

remaining ERSS. The Shapiro-Wilk normality test was done on all data sets (SIM, MODEL, RCM). The ERSS that needed to be normalized for each watershed are listed in Table 5.4.

Table 5.4: ERSS from the Batsto and Maurice River watersheds that required normalizing.

Batsto Simulation	**Number non-Gaussian**	**Maurice Simulation**	**Number non-Gaussian**
RCM-BCM	18	RCM-BCM	20
RCM-BCS	19	RCM-BCS	27
RCM-BC	23	MODEL-BCS	34
RCM-UC	29	MODEL-BCM	36
MODEL-BCM	34	RCM-BC	83
MODEL-BC	37	RCM-UC	95
MODEL-BCS	46	MODEL-BC	97

It was expected that there would be a pattern in the normalization due to the data inputs, however, an obvious trend was not found. In general, there were a higher number of ERSS that needed normalization in the MODEL runs than the RCM runs, Table 5.4. Only six ERSS needed to be normalized in the SIM runs. This showed that the RCM data drastically changed the distribution of stream flow characteristics.

Differences were apparent between results in the Batsto and Maurice simulations. In the Maurice River watershed there were fewer ERSS that needed to be normalized with seasonal and monthly bias correction on both the MODEL and RCM simulations (Table 5.4). To the authors knowledge there has not been any research on the effect of stream flow statistics to downscaled bias correction. This result could be a topic of future study.

Certain ERSS could not be normalized but were still included in the analysis. For example, in some simulations *th1* had a bimodal distribution of one of the ERSS (Figure 5.1). ERSS *th1* were bimodal in the Batsto runs UC, MODEL-BC,

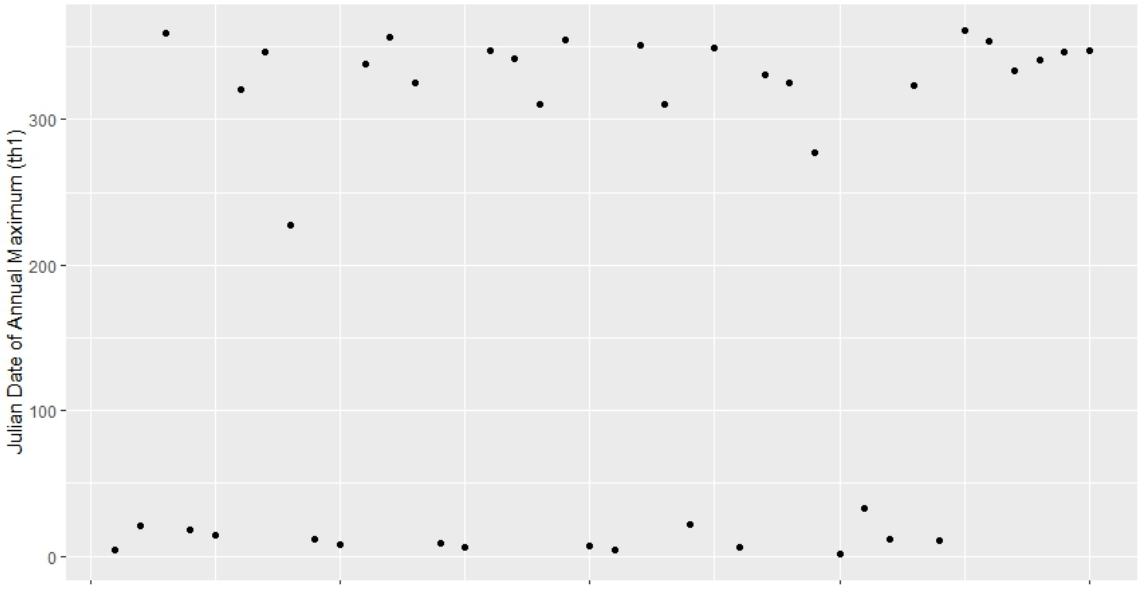

Figure 5.1: ERSS th1 simulated in the Batsto UC stream flow.

RCM-BC, but not on the remaining runs. In the Maurice simulations *th1* was bimodal in the RCM-UC simulation only. Certain ERSS could not be normalized in the Maurice River watersheds (*dh19, fh4 and fh7*) in the RCM-UC, MODEL-BCS and MODEL-BCM simulations because in the majority of simulations their values were 0. ERSS *dh19, fh4* and *fh7* represented high flows. A PCA was performed on the remaining ERSS to determine a subset of statistically significant minimally correlated indices.

Other ERSS that were not able to be normalized were *dh19, fh4* and *fh7*. These ERSS couldn't be normalized in the Maurice MODEL-BCS and Maurice MODEL-BCM simulations because the majority of the data series were 0 value. These ERSS represented high flow duration, dependant on flow values equal to seven times the median flow over the entire record. These ERSS (*dh19, fh4, fh7*) had non-zero values in the OBS Maurice record. As was seen in the previous paragraph, from the removal of outliers, models of the Maurice poorly simulated flows that high.

Phase 1 showed that RCM simulations had minimized percent error with monthly and seasonal bias correction. Therefore, it was expected that the watersheds would have minimal percent bias with BCS and BCM bias correction in the SIM simulations. It was also expected that extreme high and low flow ERSS would be best simulated by BC in the SIM results but would be reasonably well simulated with SIM-BCS and SIM-BCM, according to the results from phase 1.

5.3.2 PRMS Simulations driven by Observed Data

Quality control of the data removed between 8-15 ERSS sets from each simulation. Removing so few indices alone did not create an uncorrelated set of ERSS to describe the stream flow characteristics, that was the function of the PCA. Principal Component Analysis (PCA) run on the remaining ERSS and a parsimonious set of ERSS were obtained that described the full range of stream flow characteristics of the watershed simulations.

In the SIM simulation the ERSS was calculated for 4 similar watersheds (Great Egg, Tuckahoe, Mullica, Oswego, Batsto, Maurice) in the Pinelands Ecoregion in addition to the Batsto and Maurice River watersheds. PCA performed on the ERSS from the six watersheds to obtain a parsimonious set of ERSS that still described the stream flow characteristics. The set of ERSS selected from the SIM runs were compared across all SIM simulations (SIM-UC, SIM-BC, SIM-BCS, SIM-BCM).

There were two significant principal components found by performing PCA on the ERSS from the six observed stream flow gauges. One ERSS that represented a unique stream flow characteristic was selected for each principal component based on the absolute value of the loading. The MdAPE across all ERSS (regardless of stream

flow characteristic) were compared across all BC time scales and the MdAPE was calculated across specific stream flow characteristics and compared across BC time scales. The ERSS selected based on PCA are in Table 5.5.

In the Batsto River watershed the overall MdAPE was found to be 19.6% in the SIM-UC simulations (Figure 5.2a). Using bias correction at smaller time scales improved the results, MdAPE changed for BC (9.2%), BCS (10.1%) and BCM (7.3%) (Table 5.6). Similar results were found in the Maurice River watershed (Figure 5.2b, Table 5.7). While the 'best' simulation (minimized MdAPE) was different for the two watersheds - SIM-BCM for the Batsto and SIM-BCS for the Maurice, this showed that bias correction at smaller time scales improved the simulation of ERSS compared to the UC and BC simulations. These results are consistent with phase 1 of this research.

[1]

The simulation of individual stream flow characteristics was different than the simulation of the overall selected ERSS (Table 5.1). The impact of bias correction on the SIM ERSS is shown in Figure 5.2. Bias correction reduced the MdAPE over all ERSS flow aspects compared to SIM-UC, with the exception of the timing ERSS in SIM-BC (14.1%) compared to SIM-UC (11.7%) in the Batsto River watershed. Thus the expected trend that bias correction (at any time scale) improved the prediction of ERSS was followed in most scenarios. However, the effect of bias correction at smaller time scales (SIM-BCS, SIM-BCM) had mixed results. Tables 5.6 and 5.7 show which simulations reproduced the observed stream flow characteristics with minimized MdAPE. Overall, the hypothesis that bias correction at smaller time scales (BCS and BCM) improved the simulation of ERSS held in the Maurice watershed but not the

[1]Note that *fh3* in the Maurice River Watershed is not displayed because the observed value was 0

Table 5.5: Selected ERSS and definitions by PCA from a regional analysis in the Pinelands [34].

ERSS	**Definition**	**ERSS**	**Definition**
ma7	Ratio of the 20% Exceedance Values to 80% Exceedance Values for the Entire Flow Record (dimensionless)	*dl15*	90 percent exceedance of the entire flow record (dimensionless)
ma26	Variability of February Flow Values (%)	*dh11*	Annual maximum of 1-day moving average flows divided by the median for the entire record (dimensionless)
ml7	Mean of Minimum Flows in July across all yeards (f^3/s)	*dh24*	Flood free days (days)
ml21	Variability across annual minimum flows (%)	*ta2*	Predictability (dimensionless)
mh16	High flow discharge index (dimensionless)	*ta3*	Seasonal predictability of flooding (dimensionless)
mh21	High flow volume index (days)	*tl1*	Julian date of annual minimum (Julian date)
fl1	Low flood pulse count (number of events/year)	*tl3*	Seasonal predictability of low flow (dimensionless)
fl3	Frequency of low pulse spells (number of events/year)	*th1*	Julian date of annual maximum (Julian date)
fh1	Average number of flow events with flows above a 75th percentile threashold (number of events/year)	*th2*	Variability in Julian date of annual maximum (Julian date)
fh3	Average number of days per year that the flow is above a threashold equal to three times the median flow of the entire record (number of days/year)	*ra5*	Number of day rises (dimensionless)
dl1	Annual minimum daily flow (f^3/s)	*ra7*	Change of flow (f^3/s)

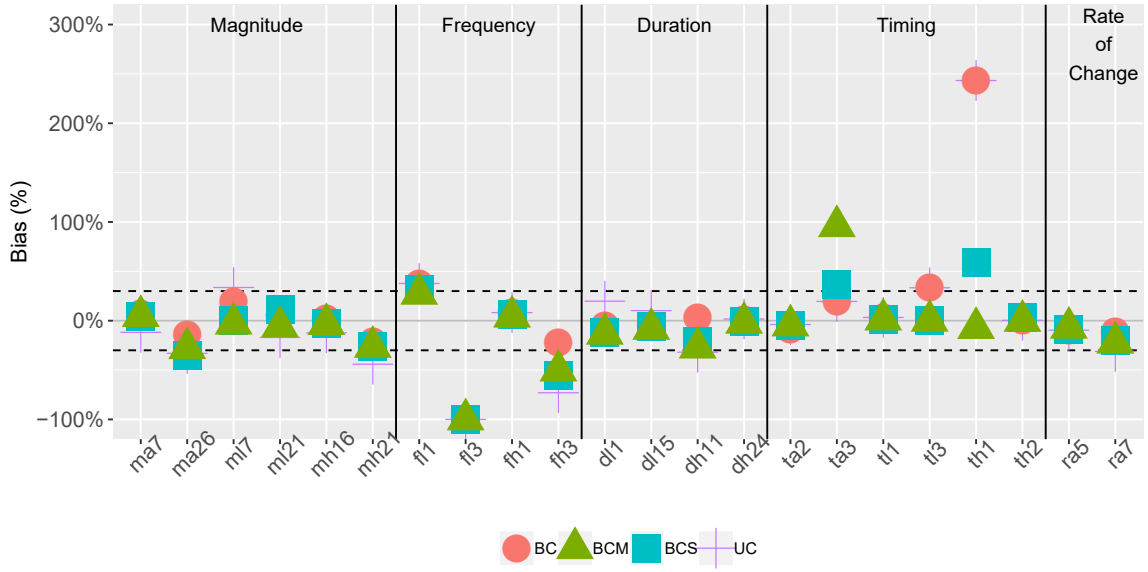

(a) Batsto watershed

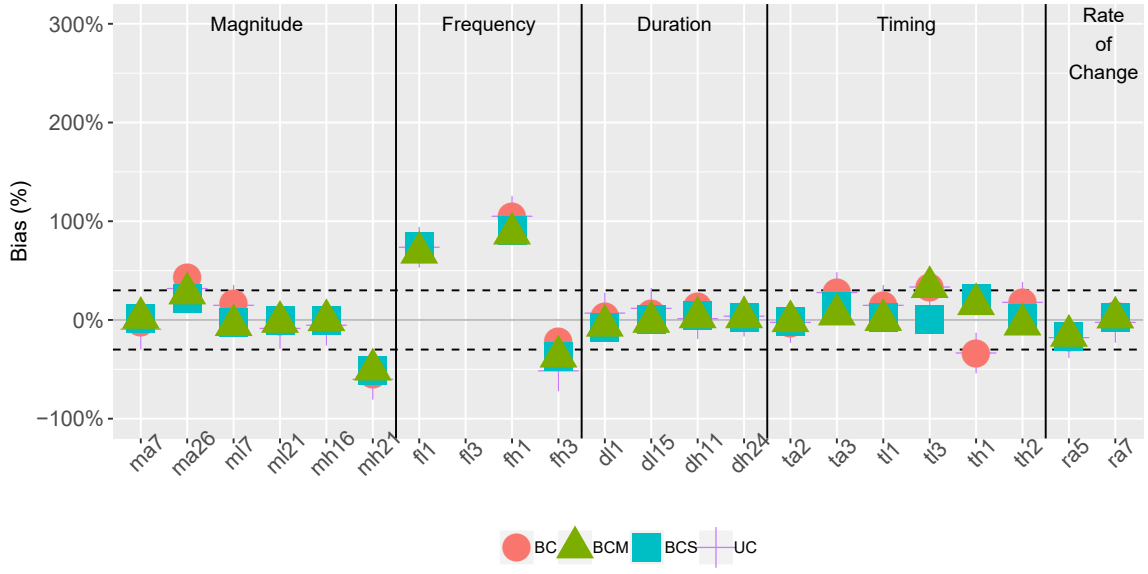

(b) Maurice watershed

Figure 5.2: Percent Bias between PCA Selected ERSS in the (a) Batsto and (b) Maurice River watersheds - SIM simulations with UC, BC, BCS and BCM bias correction. Dashed lines show +/- 30% hydrological uncertainty.

Table 5.6: MdAPE Values of the Batsto River watershed modelled with observed data (SIM results) and bias correction.

	SIM-UC	**SIM-BC**	**SIM-BCS**	**SIM-BCM**
All ERSS	19.6%	9.2%	10.1%	7.3%
Magnitude	25.1%	10.4%	7.9%	5.3%
Frequency	55.4%	29.9%	43.4%	38.9%
Duration	15.0%	4.3%	8.6%	10.7%
Timing	11.7%	14.1%	3.9%	3.0%
Rate of Change	20.4%	10.4%	14.3%	14.7%

Table 5.7: MdAPE Values of the Maurice River watershed modelled with observed data (SIM results) and bias correction.

	SIM-UC	**SIM-BC**	**SIM-BCS**	**SIM-BCM**
All ERSS	14.8%	16.4%	2.5%	5.2%
Magnitude	12.1%	9.7%	1.9%	3.7%
Frequency	73.6%	73.6%	74.2%	68.2%
Duration	5.4%	5.0%	3.3%	2.7%
Timing	22.8%	22.8%	1.8%	5.1%
Rate of Change	10.2%	11.5%	9.6%	9.3%

Batsto watershed.

The timing and frequency ERSS were poorly simulated in the Batsto River watershed. Various timing and frequency ERSS were simulated in this analysis and the definitions of the ERSS are in Table 5.5. In the Batsto watershed, two ERSS indices representing timing had large percent errors, *ta3* and *th1* in the SIM simulations. In SIM-UC and SIM-BC *th1* equaled 303, which indicated that annual maximum was at the end of October, while based on observed data (*th1* = 88) this occurred at the end of March. The bias in simulation caused the MdAPE of the timing ERSS to increase in the SIM-UC and SIM-BC simulations. With seasonal and monthly bias correction *th1* was much closer to the OBS value. However, when applying bias correction at these smaller time scales *ta3* did not improve in the Batsto River watershed but *ta3* did improve in the Maurice River watershed with SIM-BCS and SIM-BCM. *Ta3* was based on stream flows calculated for two months and the MdAPE was outside the range of uncertainty in the Batsto River watershed SIM-BC and SIM-BCS simulations. This indicated that *ta3* was impacted by the watershed and potentially related to urbanization. ERSS *ta3* represented seasonal predictability of flooding. It is possible that as the Batsto River watershed is less urbanized, the area may have unknown hydrological processes which impact the ERSS. The processes may not be as well simulated in the Batsto River watershed due to porous soils. Porous soils lead to greater stream flow and ground water recharge and less surface runoff [74]. PRMS is limited in it's ability to model groundwater-surface water interactions, and errors in simulation most likely propogated to the calculation of ERSS [15]. As shown in Figure 5.2, ERSS were generally better predicted in the Maurice River watershed compared to the Batsto River watershed with the exception of frequency ERSS.

Frequency ERSS were not well represented in any SIM watershed simulation.

Frequency ERSS were expected to have large percent errors as hydrological models in past analysis were not able to simulate rate and frequency of daily rise and falls in stream flow [32]. Caldwell et al. (2015) found frequency ERSS regularly outside of the range of uncertainty [8]. The frequency ERSS were outside the range of uncertainty in both watersheds (Figure 5.2). In the SIM-UC ERSS on the Batsto River watershed, the frequency ERSS were poorly simulated with a MdAPE of 55.4%. In the Maurice River watershed the frequency ERSS were also poorly simulated with an MdAPE of 73.6% in SIM-UC. Neither watershed showed substantial improvement with bias correction on the simulation of frequency ERSS. All other MdAPE values were less than 30% in SIM-UC in both watersheds. This may indicate that PRMS has difficulty in simulating stream flow frequency. Simulation of frequency ERSS remains elusive as frequency ERSS are highly variable and uncertainty is high [46]. This would likely impact stream flows simulated with RCM data.

ERSS *fl3* was poorly simulated in the Batsto with a percent bias of -100%. However, this was due to the fact that only one low flow event was simulated compared to 0 low flow events. In the Maurice watershed the *fl1* and *fh1* ERSS had large percent errors outside of the range of uncertainty in all SIM stream flows. In the Maurice watershed there were 0 low flow events and 0 low flow events simulated in all SIM and because of the percent bias calculation (Eq. 4.11) (0/0) the value was undefined and no points are shown on Figure 5.2. ERSS *fl1* was overestimated in the Maurice River watershed (SIM-UC) and bias correction did not improve the prediction of *fl1*. ERSS *fl1* represented a low flood pulse count. It is not surprising that it was poorly simulated as, again, frequency aspects of stream flow have not been well simulated in past analysis nor extreme high or low flows [8], [32]. *Fh1* represented high flood pulse count which was well simulated in the Batsto but not the Maurice.

Fh1 was approximately twice as high in the SIM simulations in the Maurice River watershed compared to the OBS value. There was potentially misrepresentation of runoff processes in the model of the Maurice River watershed causing errors in high flow simulation [15]. The SIM results showed the internal error in the model, and the bias in PRMS by calculating ERSS from observed stream flow conditions.

In the Batsto and Maurice River watersheds all ERSS were best simulated by SIM-BCM or SIM-BCS, respectively. The majority of timing ERSS followed the expected trend, but *ta3* did not. Frequency ERSS was poorly simulated in both the Batsto and Maurice River watersheds with the minimal MdAPE of 29.9% (SIM-BC) and 68.2% (SIM-BCM) respectively. Future calculations of frequency ERSS must be treated with caution as bias correction could not correct for the simulation of frequency ERSS.

5.3.3 Downscaled GCM Simulations

Simulating the watersheds with observed data and bias correction at different time scales resulted in the majority of stream flow characteristics being best simulated with monthly and seasonal bias correction. However, frequency ERSS had large MdAPE value and were not well-simulated. Substituting observed data, RCM data then drove the PRMS model (RCM-UC) and bias correction was performed to correct for model error (MODEL) and RCM error (RCM).

Uncorrected Simulated ERSS driven by RCM data (RCM-UC)

There were three significant principal components in the RCM-UC simulations in the Batsto River watershed based on the results of the broken stick method. In the

RCM-UC simulation in the Batsto River watershed the first component represented 78.0% of the variance (Figure 5.3). The three PCs had a cumulative proportion of variance of 89.2%. In the Maurice River watershed RCM-UC simulation there were four principal components. The first component represented 70.5% of the variation and the four principal components had total cumulative variation of 90.7%. One ERSS was selected from each PC that represented each major aspect of the flow regime resulting in 27 ERSS for the Batsto River watershed and 33 ERSS for the Maurice River watershed RCM-UC simulations. The simulation of these ERSS are shown in Figure 5.4.

Overall, in uncorrected simulations the ERSS that represented duration and timing well simulated OBS conditions. The proportion of ERSS within +/-30% bias was greater than the proportion outside. All flow categories had ERSS outside of hydrological uncertainty.

However, the majority of ERSS were within the range of uncertainty in the Batsto and Maurice RCM-UC simulations (Figure 5.4). In the Batsto River watershed the MdAPE of all selected ERSS was 27.3%. The MdAPE of all selected ERSS in the Maurice watershed was 28.0%. Both basins had similar percent bias without considering bias correction. However, there was variation in how well different types of ERSS were simulated.

The MdAPE for each stream flow characteristic in the Batsto River watershed was 33.3%, 23.4%, 26.5%, 8.8% and 34.1% for the magnitude, frequency, duration, timing and rate of change ERSS, respectively in the RCM-UC simulations (Table 5.8). Likewise the MdAPE values in the Maurice River watershed were 17.9%, 57.9%, 30.9%, 14.4% and 31.3% for the magnitude, frequency, duration, timing and rate of change ERSS, respectively (Table 5.9).

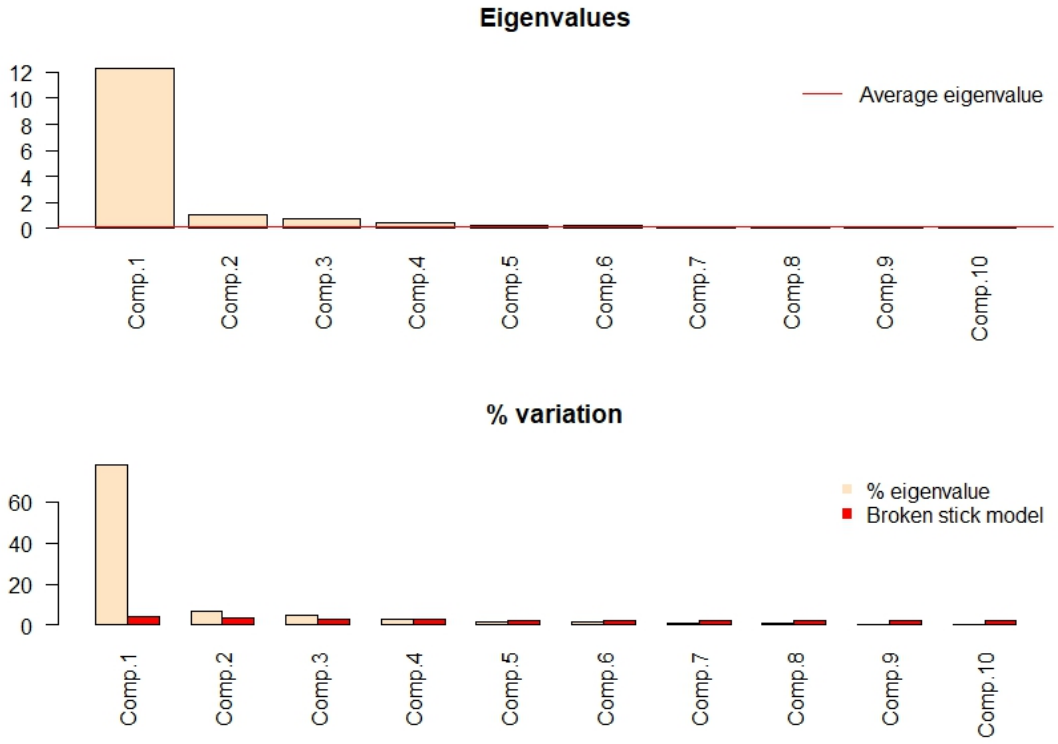

Figure 5.3: First 10 Components of the RCM-UC Simulations in the Batsto River watershed.

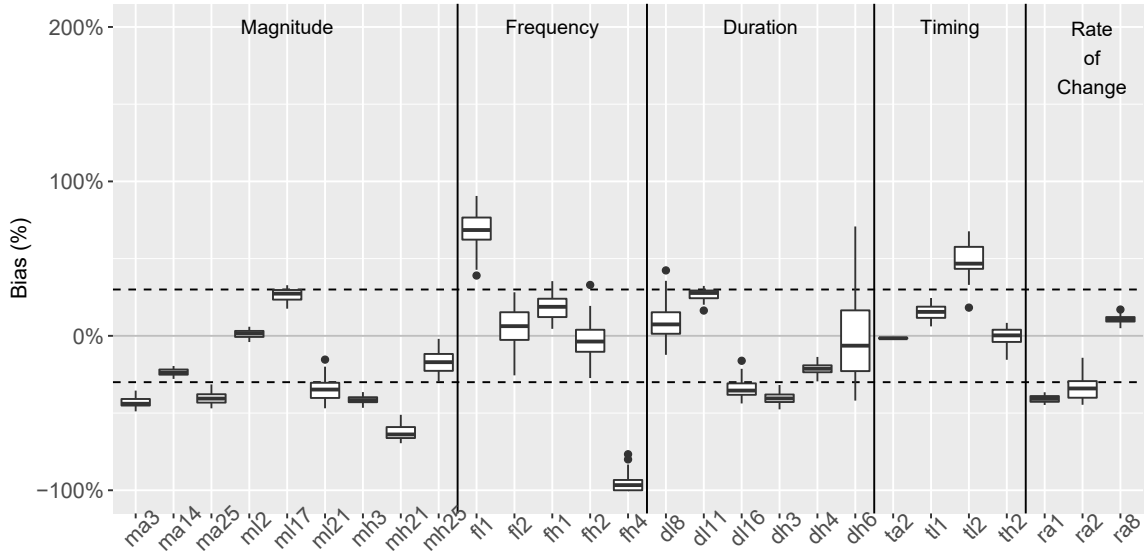

(a) Batsto watershed

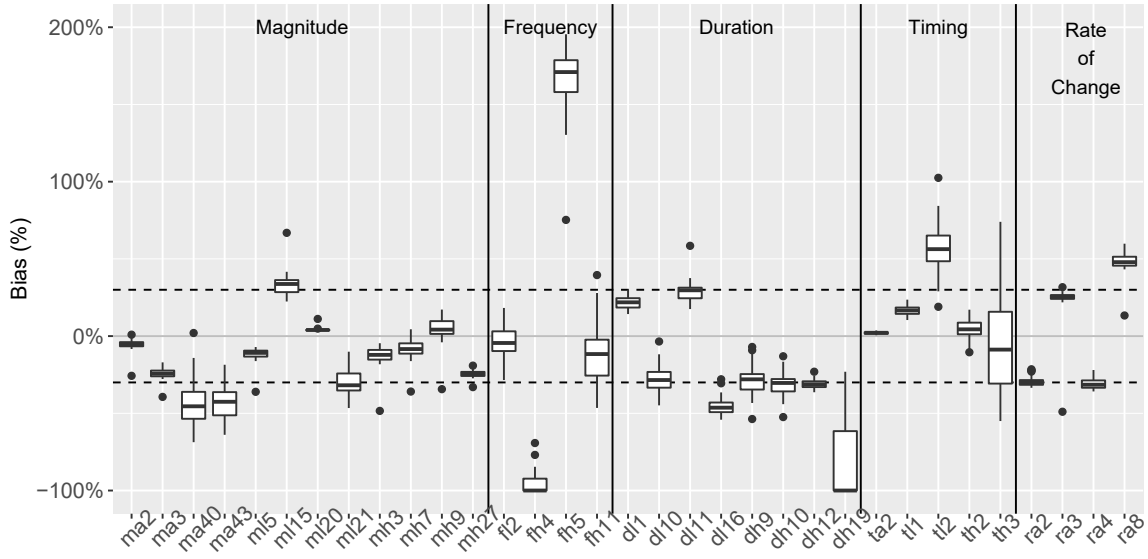

(b) Maurice watershed

Figure 5.4: Percent Bias between PCA Selected ERSS in the (a) Batsto River watershed and (b) Maurice River watershed - RCM-UC simulations and observed. Dashed lines show +/- 30% hydrological uncertainty.

The timing ERSS were best simulated with MdAPE in both watersheds without bias correction (RCM-UC). This result was different than the SIM results which had a large MdAPE value on the timing ERSS due to two ERSS (*th1* and *ta3*). These ERSS were not selected for analysis based on the PCA and thus the MdAPE for the timing ERSS was smaller.

Two ERSS flow characteristics had MdAPE outside the range of uncertainty in the Batsto River watershed: magnitude (33.3%) and rate of change (34%). However, the magnitude ERSS in the Maurice River watershed was within the accepted range of uncertainty in RCM-UC, with MdAPE of 17.9%. Approximately five magnitude ERSS in the Batsto River watershed had data outside the range of uncertainty (Figure 5.4a) leading to poor simulation of the magnitude ERSS. Typically, magnitude ERSS are better simulated compared to other ERSS characteristics [8].

Due to only three rate of change ERSS being included in the analysis a smaller amount of ERSS outside the range of uncertainty gave a greater MdAPE value for the rate of change ERSS in the Batsto River watershed. Rate of change ERSS are very sensitive to errors in daily flow simulation [32]. The Maurice River watershed had a larger amount of rate of change ERSS included in the analysis and less than half of the ERSS had data within the range of uncertainty in the RCM-UC results.

The largest MdAPE of the RCM-UC simulations in the Batsto River watershed were in the ERSS that represented frequency, *fh4* (96.7%) and *fl1* (68.5%), a consistent trend with past results that frequency ERSS would not be well simulated [32]. The frequency ERSS were also poorly simulated in the Maurice River watershed. This was also found in the SIM results, where the Maurice River watershed had frequency ERSS with an MdAPE of 73.6%, Table 5.7.

The standardized data ranges (SDR) showed the variability between the OBS

stream flows and the RCM-UC simulations (Appendix C). In the Batsto River watershed 11 ERSS of 28 had larger variability compared to OBS conditions. In the Maurice River watershed 10 of 34 ERSS had larger variability compared to OBS conditions. Overall the simulation of the ERSS using RCM data underestimated the variability. However, one third of the ERSS had overestimated variability, indicating that perhaps some improvement is required to the PRMS model to better fit the ERSS. The ERSS with under and overestimated variability were spread across stream flow characteristics and were not constrained to one stream flow characteristic (e.g. timing).

There was error and uncertainty in the simulation of stream flows using RCM data, additional methods to reduce this error should be considered in future analysis. Magnitude ERSS, which are considered to be the most reasonably simulated ERSS were outside of the range of uncertainty in the Batsto River watershed which supports the hypothesis that improvement in the simulation of ERSS using dynamically downscaled climate data. The variability of the ERSS could also be better simulated by RCM data. Bias correcting for the PRMS error (MODEL) may be enough to reduce ERSS to within the range of uncertainty.

Model Corrected GCM Simulated Stream Flow (MODEL)

Bias correction was done on the stream flows directly to the observed data (MODEL) (Figure 5.5 and 5.6). The purpose of this form of bias correction was to remove the error due to PRMS. Seasonal bias correction (MODEL-BCS) minimized percent error across all ERSS in both watersheds. However, frequency and rate of change ERSS in MODEL simulations in both basins resulted in large deviations from OBS conditions.

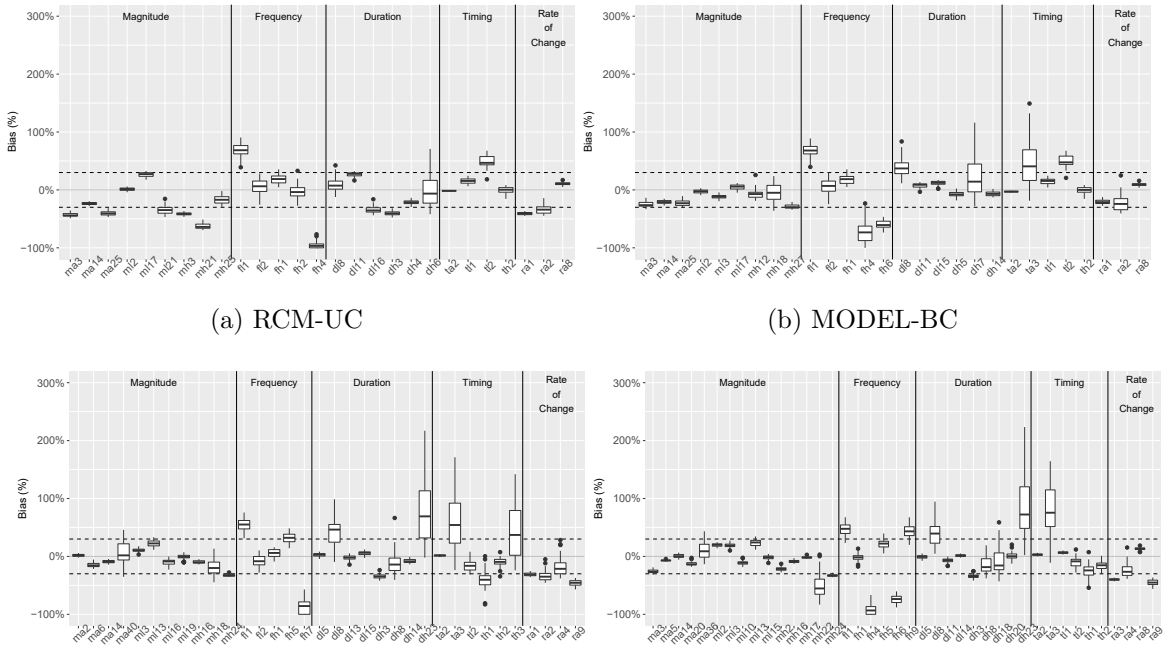

(a) RCM-UC

(b) MODEL-BC

(c) MODEL-BCS

(d) MODEL-BCM

Figure 5.5: Percent Bias between PCA selected ERSS in the Batsto River Watershed - MODEL simulations with (a) RCM-UC, (b) BC, (c) BCS and (d) BCM bias correction. Dashed lines show +/- 30% hydrological uncertainty.

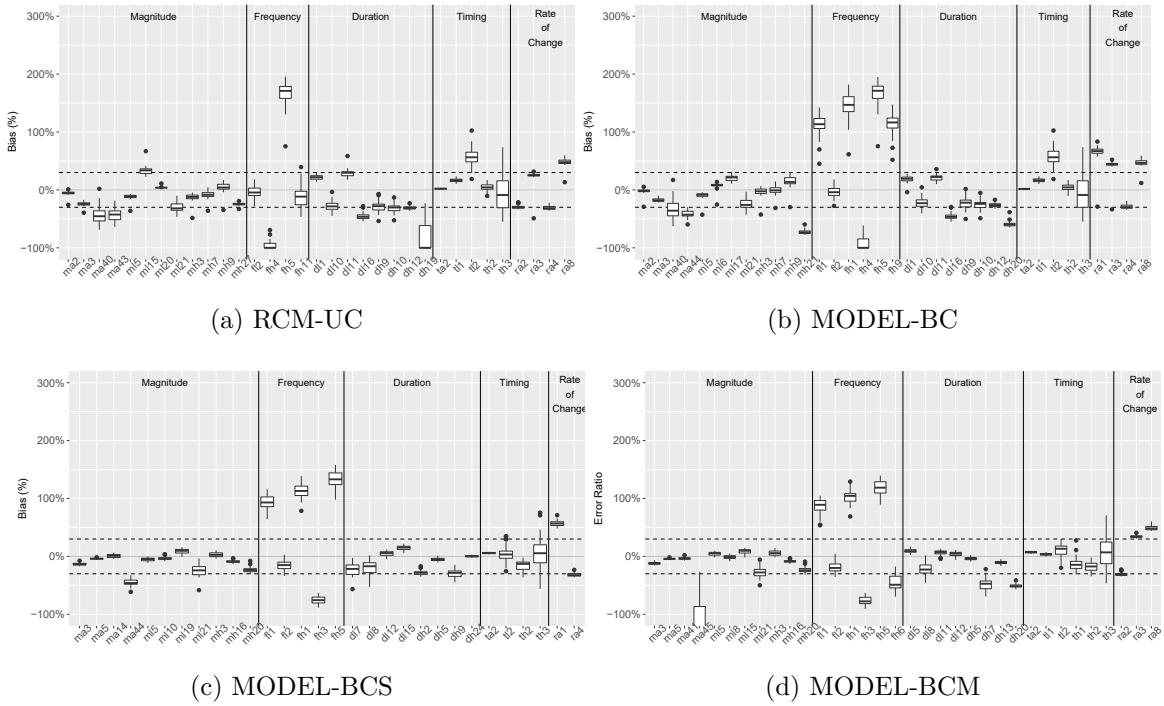

(a) RCM-UC

(b) MODEL-BC

(c) MODEL-BCS

(d) MODEL-BCM

Figure 5.6: Percent Bias between PCA selected ERSS in the Maurice River Watershed - MODEL simulations with (a) RCM-UC, (b) BC, (c) BCS and (d) BCM bias correction. Dashed lines show +/- 30% hydrological uncertainty.

The Batsto River watershed MODEL-BCS simulation had 15.8% MdAPE and the Maurice River watershed MODEL-BCS simulation had 14.3% MdAPE across all ERSS (Table 5.8 and 5.9). This showed improvement from the approximately 28% MdAPE in RCM-UC in both watersheds. While the overall ERSS were better simulated in MODEL-BCS, some stream flow characteristics were simulated better than others.

Bias correction at all time scales decreased the MdAPE of magnitude and duration ERSS to be below 30%, and in most scenarios, below 15%. Magnitude and duration ERSS had minimal MdAPE with MODEL-BCS and MODEL-BCM in the Batsto and Maurice River watersheds, respectively (Table 5.8 and 5.9). This was consistent with the results from phase 1. MODEL-BCS provided the lowest MdAPE for the timing ERSS in the Maurice River watershed however, the RCM-UC simulation had the lowest MdAPE for the Batsto River watershed. While the timing ERSS did not have the lowest MdAPE with smaller bias correction time scale - the expected trend from phase 1, the timing ERSS were still well simulated in MODEL-BCS (18.9% MdAPE) and MODEL-BCM (11.5% MdAPE). The frequency and rate of change ERSS were more poorly simulated.

Table 5.8: MdAPE Values of the Batsto River watershed with bias correction on the PRMS model (MODEL simulations).

	RCM-UC	**MODEL-BC**	**MODEL-BCS**	**MODEL-BCM**
All ERSS	27.3%	17.0%	15.8%	19.3%
Magnitude	33.3%	15.6%	10.8%	14.4%
Frequency	23.4%	52.5%	31.6%	44.1%
Duration	26.5%	10.7%	10.7%	12.1%
Timing	8.8%	13.5%	18.9%	11.5%
Rate of Change	34.1%	17.7%	33.3%	37.1%

Using any form of bias correction in the MODEL simulations increased the

Table 5.9: MdAPE Values of the Maurice River watershed with bias correction on the PRMS model (MODEL simulations).

	RCM-UC	**MODEL-BC**	**MODEL-BCS**	**MODEL-BCM**
All ERSS	28.0%	24.5%	14.3%	16.0%
Magnitude	17.9%	14.9%	8.3%	8.3%
Frequency	57.9%	113.1%	92.6%	81.2%
Duration	31.0%	25.5%	13.7%	10.1%
Timing	14.4%	14.0%	8.0%	9.5%
Rate of Change	31.1%	44.7%	42.2%	34.3%

MdAPE in the frequency and timing ERSS in the Batsto River watershed (Figure 5.5b - 5.6d). The MdAPE of the frequency ERSS increased in the Maurice River watershed with bias correction whereas the MdAPE of the timing ERSS decreased (the expected result). This indicated that frequency ERSS did not follow the expected trend in both watersheds and further bias correction or other methods may be needed. The difference in the trend of the timing ERSS may be a result of differences between the watersheds. The two watersheds have differences in urbanization, land use and soils [15].

Frequency and rate of change ERSS are sensitive to errors in the simulation of daily stream flow from hydrological models [32]. MODEL bias correction did not improve the simulation of frequency ERSS. The frequency ERSS did not follow the expected pattern (Table 5.8 and 5.9); MdAPE increased with MODEL-BCS and MODEL-BCM in both watersheds. The MODEL simulations were intended to reduce the error from the hydrological model and this was found in the magnitude and duration ERSS across the board. However, the frequency and rate of change ERSS in both watersheds and the timing ERSS in the Batsto River watershed did not have their percent bias reduced by MODEL bias correction. This may indicate that the RCM data inputs have inherent bias and doing bias correction to reduce model error

made the simulations worse in some ways.

The rate of change ERSS were reasonably simulated in the Batsto River watershed with MODEL-BC (17.7% MdAPE) but in no other simulations. All other simulations of rate of change ERSS in both watersheds were over 30%. The rate of change ERSS in the SIM runs had lower percent bias. While there may be some inherent bias in the hydrological model, this may indicate that the RCM simulations were tested to see if a large proportion of bias in the rate of change ERSS came from RCM data inputs.

It was desirable that the variability of the MODEL or RCM simulations were less than the variability of ERSS in the regional analysis (6 observed stream flows). The SDR of the MODEL simulations showed that there was reduced variability in the stream flow characteristics compared to the OBS ERSS (Appendix C - Table 2 and Table 3). In the Batsto River watershed MODEL-BC simulations 20 of 28 ERSS had reduced variability in the simulated results compared to OBS ERSS. In the Maurice River watershed 21 of 34 ERSS had reduced variability in the MODEL-BC simulations compared to the OBS simulations. In the Batsto River watershed the proportion of ERSS that had overestimated variability went down, while in the Maurice River watershed the proportion increased with smaller bias correction time scales. However, the proportion of ERSS with overestimated variability was around 30% in all MODEL simulations. The simulated stream flow record, in past analysis, could not fully capture the observed variation in FDCs in either basin but variation at low exceedance levels was underestimated in the Batsto watershed, while variation at high exceedance levels was underestimated in the Maurice watershed [15]. The variation of low and high flow ERSS is explored in phase 3.

Bias correction on the MODEL simulations increased the MdAPE in certain

characteristics, the opposite of the desired effect. The rate of change, frequency and timing ERSS did not consistently follow the same trend as phase 1 or the SIM ERSS in phase 2. This may point to internal error in the RCM.

Bias corrected GCM Simulated Stream Flow (RCM)

The following section describes the results from creating the ERSS from stream flows that were bias corrected on the RCM (see Figures 5.7 - 5.8 for ERSS used in this analysis). The main results and deviations from expected trends are discussed. Bias correction improved the simulation of ERSS for the Batsto watershed at all timescales and minimized error compared to using no bias correction (RCM-UC) or bias correction only for the PRMS model (MODEL), Table 5.10 and 5.11.

Bias correction in this section removed both the error from the PRMS model and corrected for the remainder of the bias from the RCM. This improved the simulations of ERSS over MODEL results (Table 5.10 and 5.11). While the MdAPE indicated that RCM-BCS and RCM-BCM minimized percent error across all ERSS, the shorter timescales did not show the greatest improvement across all flow characteristics. RCM bias correction simulations results in simulated ERSS with minimized error, as lower percent errors were found in all ERSS in the RCM bias corrected simulations compared to the MODEL simulations.

In the RCM-UC simulations all ERSS had percent errors between -100 and 100%. However, when applying bias correction certain ERSS developed ranges of percent errors of 350% while the majority of the ERSS were within the range of uncertainty. This affected the MdAPE of certain stream flow characteristics more than others.

The magnitude ERSS had the lowest range of uncertainty in the Batsto River

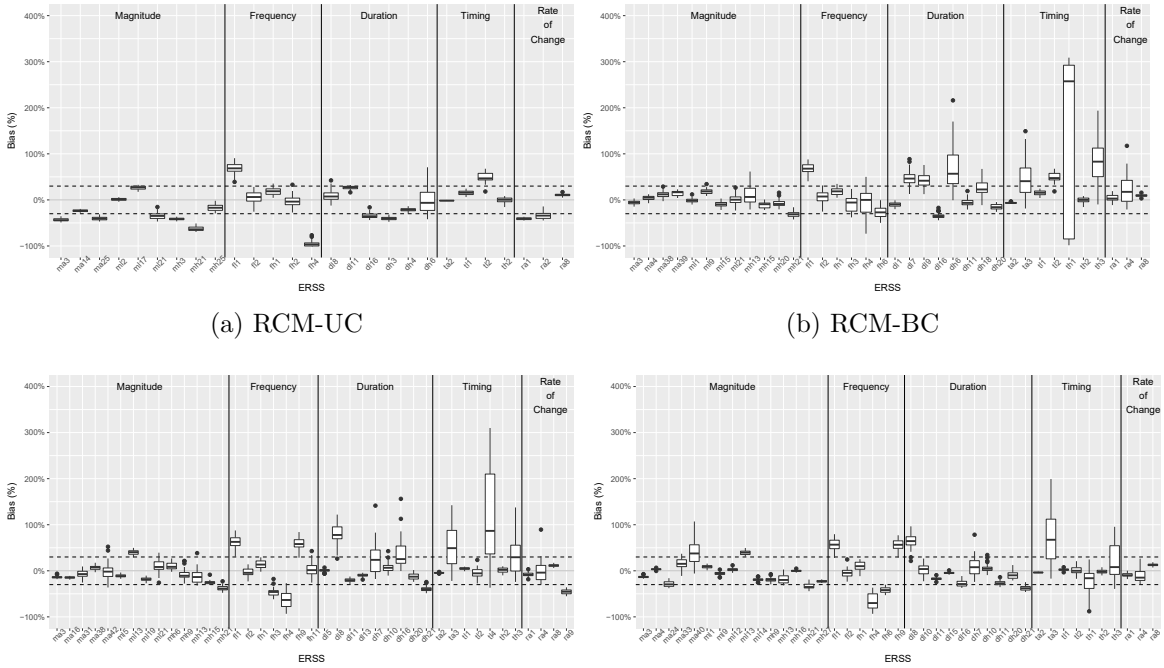

(a) RCM-UC

(b) RCM-BC

(c) RCM-BCS

(d) RCM-BCM

Figure 5.7: Percent Bias between PCA selected ERSS in the Batsto River Watershed - RCM simulations with (a) RCM-UC, (b) BC, (c) BCS and (d) BCM bias correction. Dashed lines show +/- 30% hydrological uncertainty.

Table 5.10: MdAPE Values of the Batsto River watershed with bias correction on the RCM (RCM simulations).

	RCM-UC	**RCM-BC**	**RCM-BCS**	**RCM-BCM**
All ERSS	27.3%	15.7%	14.0%	16.2%
Magnitude	33.3%	9.5%	14.3%	16.5%
Frequency	23.4%	21.9%	40.9%	43.4%
Duration	26.5%	25.4%	17.6%	18.0%
Timing	8.8%	24.1%	8.0%	5.6%
Rate of Change	34.1%	9.1%	12.9%	12.1%

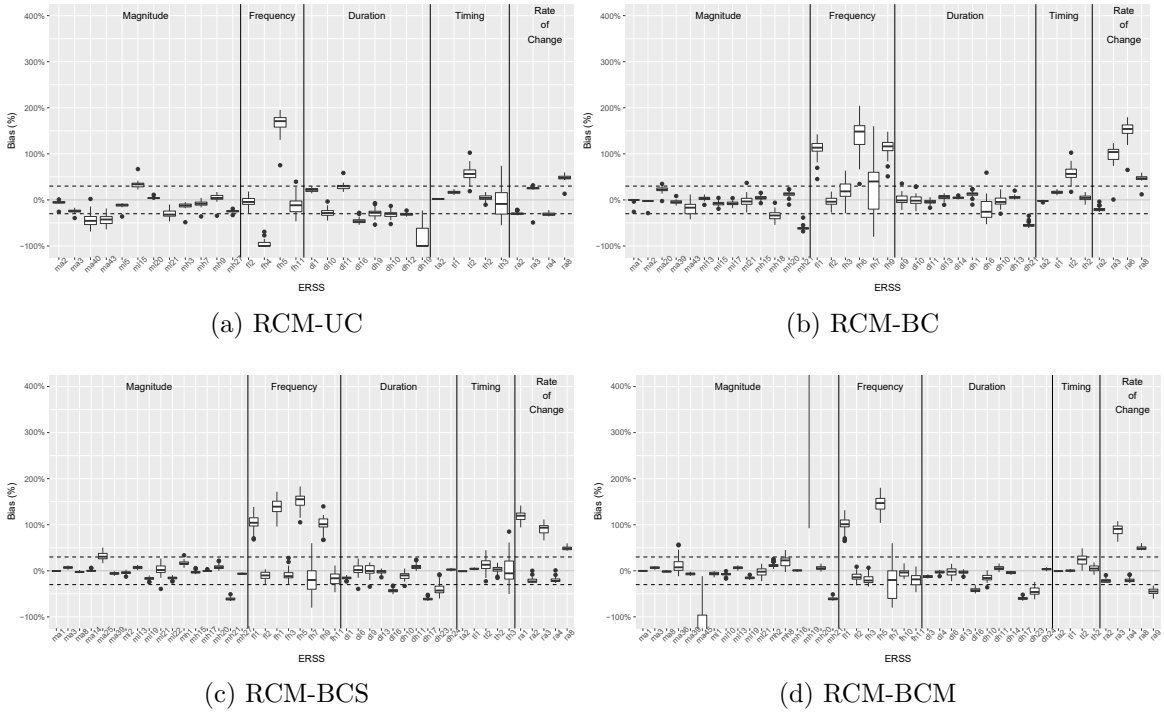

(a) RCM-UC

(b) RCM-BC

(c) RCM-BCS

(d) RCM-BCM

Figure 5.8: Percent Bias between PCA selected ERSS in the Maurice River Watershed - RCM simulations with (a) RCM-UC, (b) BC, (c) BCS and (d) BCM bias correction. Dashed lines show +/- 30% hydrological uncertainty.

Table 5.11: MdAPE Values of the Maurice River watershed with bias correction on the RCM (RCM simulations).

	RCM-UC	**RCM-BC**	**RCM-BCS**	**RCM-BCM**
All ERSS	28.0%	13.3%	12.1%	11.8%
Magnitude	17.9%	8.2%	6.6%	8.3%
Frequency	57.9%	80.0%	71.6%	22.6%
Duration	31.0%	7.6%	12.3%	8.5%
Timing	14.4%	13.0%	5.6%	2.0%
Rate of Change	31.1%	57.6%	48.4%	44.6%

watershed simulated by RCM-BC (Table 5.10), this was not the consistent with the results from phase 1. There were four principal components on the RCM-BC simulations and five in the RCM-BCS and RCM-BCM simulations. Having the additional principal components led to increased ERSS which skewed results. However, after accounting for the increased principal components, the simulation of certain ERSS was shown to be better or worse depending on the simulation. The selection of ERSS *ma40*, *ml13* and *mh21* may have skewed the results in the Batsto watershed. These three ERSS were selected only in the RCM-BCS and RCM-BCM simulations and skewed the expected results. ERSS *ma40* is the skewness of monthly flow values. Skewness of the daily flow values was not as well represented in the Batsto watershed (Figure 4.4 in Phase 1) so this may have extended to the monthly skewness as well. ERSS *ml13* described the variability across minimum monthly flows and *mh21* represented the high flow volume index - the average volume divided by the median flow for the entire record. These ERSS were not well simulated which led to the increased MdAPE value in the magnitude ERSS in the RCM-BCS and RCM-BCM simulations in the Batsto River watershed. Selection of ERSS through the modified regional analysis method played a role in the ability of RCM data to simulate ERSS, however, visual observation put the results into context.

Shrestha et al.(2014) [68] found that a hydrological model did not simulate duration ERSS well, however, in this study duration ERSS were better simulated compared to certain other stream flow characteristics. The duration ERSS were best simulated in the Batsto River watershed with RCM-BCS, with an MdAPE of 17.6%. However, the percent error was similar in RCM-BCM (18.0% MdAPE). In the Maurice River watershed, the MdAPE was lowest in the RCM-BC simulation (7.6%); however MdAPE for duration ERSS was lowest in all RCM bias correction

simulations (RCM-BCS: 12.3% and RCM-BCM: 8.5%) compared to the RCM-UC simulation (30.1% MdAPE). The duration ERSS had a expected trend that was consistent with the results from phase 1, that bias correction at smaller time scales improved the prediction of ERSS.

The timing ERSS generally was consistent with phase 1, where bias correction at smaller time scales decreased the MdAPE values. With the exception of the Batsto River watershed which had a greater MdAPE value in the RCM-BC simulation compared to the RCM-UC simulation (Table 5.10).

In the Batsto River watershed the MdAPE of the frequency ERSS was lower in RCM-BC with 21.9% MdAPE. While in the Maurice River watershed the MdAPE of the frequency ERSS was lower in the RCM-BCM simulation with 22.6% MdAPE. This was different from what was observed in the watersheds with MODEL results, where both watersheds showed low MdAPE in the RCM-UC simulations. This indicated that there was error in the RCM that could be corrected for frequency ERSS to be better simulated. However, the other RCM bias corrections had greater MdAPE in frequency ERSS compared to RCM-UC (Table 5.10 and 5.11). This may indicate that selection of ERSS may have impacted the results of the simulation. Frequency ERSS were examined in more detail.

In the Batsto watershed RCM-BC, *fl1* was the only frequency ERSS with flows outside the range of uncertainty (Figure 5.7). The following paragraph is a discussion of the frequency ERSS, specifically in the RCM simulations of the Batsto River watershed as these simulations did not follow the results from phase 1. In the simulation of RCM-BCS and RCM-BC not only was *fl1* poorly simulated but due to a greater amount of significant principal components ERSS *fh3*, *fh4* and *fh9*, which also had large percent errors, were selected for analysis. *Fh3* and *fh4* were selected for

analysis in RCM-BC but had smaller percent errors. ERSS *fl1* was poorly simulated in all bias corrected watersheds, and represented low flood pulse count, the average number of low flow events below the 25th percentile of the flow record. ERSS *fh3* and *fh4* represented the high pulse count, based on the number of days the flow was above 3 and 7 times the median flow, respectively. Seasonal and monthly bias correction of the RCM were unable to bring these flow metrics within the desired range of uncertainty for the simulation of *fh3* and fh4. ERSS *fh9* was representative of flood frequency and was the average number of flow events above a 75% exceedance value. This led to the minimized MdAPE in the RCM-BC for frequency ERSS just by comparison as there were fewer frequency ERSS included in the analysis of other simulations. The selection of *fh9* in RCM-BCS and RCM-BCM contributed to increased MdAPE in the frequency ERSS. However, *fh3* and *fh4* also contributed and these ERSS were sensitive to the bias correction time scale. It is possible that bias correction at these time scales reduced some of the natural variation of the hydrological model impacting the calculation of these ERSS [15].

In the Maurice River watershed (Figure 5.8) in both RCM-BC and RCM-BCS approximately 50% of the frequency ERSS were simulated with large data ranges, and in some cases over 100% error. In the Maurice River watershed the frequency ERSS that were poorly simulated for RCM-BC were *fl1, fh6,* and *fh9* and for RCM-BCS were *fl1, fh1, fh5,* and *fh9*. In RCM-BCM *fl1* and *fh5* (average number of flow events above the median flow) were still simulated poorly; the other ERSS that had large percent errors and increased the MdAPE value of the frequency ERSS were not selected. The lower amount of significant PCAs on certain frequency ERSS affected the simulation of the ERSS more than the simulation of frequency ERSS with a bias correction time scale. The uncorrected (RCM-UC) and RCM-BC simulations

had fewer significant PCs resulting in fewer ERSS being included in the analysis, but had a larger MdAPE value than RCM-BCM. Comparing the graphs in Figure 5.8 , the individual frequency ERSS experienced less variation between RCM-UC, RCM-BC, RCM-BCS and RCM-BCM. This indicated that while selection of the frequency ERSS had a larger effect on the MdAPE of frequency ERSS compared to changes that occurred due to bias correction.

The rate of change ERSS had a low MdAPE value in the Batsto River watershed RCM-BC simulation (9.1%) compared to other RCM simulations, Table 5.10. However, the MdAPE of rate of change ERSS were within the range of uncertainty in all RCM bias corrected simulations in the Batsto River watershed. In the Maurice River watershed the smallest MdAPE value was in the RCM-UC simulation but the value was outside the accepted range of uncertainty (31.1%). Neither of these results reflected the expected trend that rate of change ERSS would be best simulated with bias correction on the RCM at smaller time scales. While the MdAPE in the Batsto River watershed may be lower in the RCM-BC simulations, as shown in Figure 5.7, rate of change was actually better simulated in the RCM-BCM simulation as all values were within the accepted range of uncertainty. Data were analyzed in a variety of ways in this study to determine the best simulation method. In the Batsto River watershed RCM-BCS had an outlier in the simulation of ERSS: *ra9*. ERSS *ra9* represented variability in reversals. It was not selected in other simulations. It had been shown that the rate of daily rises and falls has not been well simulated which may have contributed to the increased MdAPE value [32].

In the Maurice watershed the rate of change ERSS were better simulated in the RCM-UC simulation. This was most likely due to the selection of ERSS. ERSS *ra8* was not well simulated in any runs in the Maurice River watershed (Figure 5.8b).

ERSS *ra8* represented the average number of days per year when the flow changed direction. As referenced in the previous paragraph, reversals were not well simulated so it was expected that *ra8* would be simulated poorly. ERSS *ra1, ra3* and *ra6* were included in the RCM-BC, RCM-BCS and RCM-BCM analysis which may have skewed how well the rate of change ERSS were simulated due to the inclusion of an increased amount of rate of change ERSS. ERSS *ra1* and *ra3* were complimentary ERSS and were the rise and fall rate, respectively. They were the average change of flow for days when the change was only positive (*ra1*) or negative (*ra3*). ERSS *ra6* is similar to *ra1*, and calculated the median of the log of the change of flow for days when the change was positive. Rate of change ERSS were not well simulated in the MODEL simulations either, this may indicate structural errors in the PRMS model. Rate of change ERSS are very susceptible to large uncertainties [46].

The SDR of the RCM results showed that with bias correction a greater proportion of ERSS had reasonable variability (Appendix C - Tables 7-9 and Tables 13-15). In the RCM-UC simulations approximately 68% of selected ERSS had underestimated variability compared to OBS variability in both basins. Underestimated variability of simulated ERSS compared to OBS ERSS was desirable as it showed that using dynamically downscaled data in a hydrological model had less variation than a regional analysis. The proportion of ERSS with underestimated variability increased in both watersheds with bias correction. It was surmised that RCM-BC would reduce natural variation of the hydrological model [15]. In this study however, it was found that the natural variation was reduced within reason with bias correction and improved with bias correction that had timing considerations (RCM-BCS, RCM-BCM).

5.4 Summary

ERSS were selected using PCA for each simulation of interest (Table 3.2). Due to the varying number of principal components in the SIM, MODEL and RCM simulations there were different amounts and different ERSS that could be compared between the observed conditions and simulated conditions. In the future, one set of ERSS containing all flow characteristics relevant to the Pinelands would be useful as a comparison between simulations. Using a different subset of PCA selected ERSS for each watershed was tedious for the purposes of comparison but had the benefit of showing that the trends in data were not biased by the selection of the ERSS. While there was a set of ERSS found that had ecological relevance to the Pinelands it did not contain all flow characteristics. This set of ERSS was analyzed in phase 3.

Bias correction on the seasonal and monthly timescales on the RCM generally led to lower percent error in the simulations. This result was consistent with what was found in phase 1 of this research. However, the individual flow characteristics in the Batsto and Maurice watersheds did not appear to follow the same trends, particularly the frequency and rate of change ERSS which will need to be more carefully simulated in future, this includes better model calibration, better input data, among other improvements. Having ERSS better simulated in RCM-UC or RCM-BC often indicated a problem with the simulation of that stream flow characteristic as opposed to this method as a whole. The simulation of frequency and rate of change ERSS has been problematic in past studies, additional research is still necessary to simulate these ERSS well in modelled basins [32], [46].

There was a similar range of uncertainty across a regional analysis as there was across SIM, MODEL and RCM results. Previous studies of regional analysis showed

between -100% and 300% across various modelling programs [8], [49] with the majority of ERSS within a +/- 30% range. Similar results were found in this analysis. In a comparison of the standardized data ranges the RCM and MODEL simulations had smaller standardized data ranges than the six watershed regional analysis.

Bias correction did have some positive effects, however, work still needs to be done to consistently improve the prediction of ERSS. While the inherent problem with modelling is that calibration on one characteristic cannot predict all characteristics accurately, it is important that they are within a reasonable range of error [49]. This phase of research focused on the simulation of the five fundamental aspects of stream flow. In phase 3 the ability of RCM data to simulate ERSS relevant to the Pinelands indices were explored with a focus on the simulation of low flow ERSS.

Chapter 6

Phase 3: Analysis of ERSS Relevant to Pinelands Ecology

6.1 Introduction

It was beneficial to examine the simulation of ERSS relevant to the Pinelands Ecoregion as these ERSS may be used in mitigation measures and management plans in the future. These ERSS of relevance only covered two stream flow characteristics (magnitude and duration) at average and low flows. Low flows are of importance to the Pinelands Ecoregion due to a strong groundwater component [94]. The selected ERSS (Table 6.1 were able to be examined in more detail and more easily across simulations (Table 3.2).

This phase of research differs from phase 2 where parsimonious sets of ERSS were determined through a new methodology. Whereas, in phase 3, a pre-determined set was used. Phase 3, is more concerned with objective 2 and 3, comparing simulated ERSS. Phase 3 was implemented to determine if there were differences in how low

flow ERSS were simulated compared to average flow ERSS. It was generally found that low flow ERSS were more poorly simulated compared to average flow ERSS.

Kennen & Riskin (2010) took 163 hydrological variables from HIT (the precursor to EflowStats) and used a conservative screening criteria to reduce the variables to an uncorrelated set of indices that were used in fish-assemblage flow-ecology response models [104]. A PCA was used to reduce a large subset of environmental variables; these results were combined with fish sampling results of the Pinelands along with water quality data which reduced these ERSS to a set of 18 ERSS that were related to aquatic health of the Pinelands [104]. No timing, frequency or rate of change ERSS were included in the analysis because they were uncorrelated ($\rho < 0.5$) with anthropogenic indicators [104]. All the ERSS in Table 6.1 were correlated with ecological response in Pineland streams [104].

6.2 Method

In this phase of research, a smaller amount of ERSS were compared across simulations compared to phase 2. This allowed for additional trends to be evaluated. Similar methods of analysis were used in phase 3 and phase 2. MdAPE, percent bias and visual inspection methods determined whether low flow ERSS had minimal error compared to average flow ERSS.

The indices in Table 6.1 were compared across SIM, RCM and MODEL simulations to determine how RCM data simulated ERSS. In phase 2 of this analysis, frequency, timing and rate of change ERSS were more poorly simulated compared to magnitude and duration ERSS. Removing frequency, timing and rate of change ERSS from the analysis allowed for more detailed observations to be made on the

Table 6.1: Indices important to the aquatic health of the Pinelands [104].

	Definition
ma1	Mean of all the daily mean flow values for the entire flow record(f^3/s)
ma12	Mean of all January flow values over the entire record (f^3/s)
ma13	Mean of all February flow values over the entire record (f^3/s)
ma14	Mean of all March flow values over the entire record (f^3/s)
ma15	Mean of all April flow values over the entire record (f^3/s)
ma16	Mean of all May flow values over the entire record (f^3/s)
ma17	Mean of all June flow values over the entire record (f^3/s)
ma19	Mean of all August flow values over the entire record (f^3/s)
ma20	Mean of all September flow values over the entire record (f^3/s)
ma21	Mean of all October flow values over the entire record (f^3/s)
ma22	Mean of all November flow values over the entire record (f^3/s)
ma23	Mean of all December flow values over the entire record (f^3/s)
ml5	Mean of the minimums of all May flow values over the entire record (f^3/s)
ml8	Mean of the minimums of all August flow values over the entire record (f^3/s)
ml9	Mean of the minimums of all September flow values over the entire record (f^3/s)
ml13	Variability (coefficient of variation) across minimum monthly flow values (%)
ml16	Median of annual minimum flows (dimensionless)
dl1	Mean of annual minimum of 1-day average flow (f^3/s)
dl4	Mean of annual minimum of 30-day moving average flow (f^3/s)
dl5	Mean of annual minimum of 90-day moving average flow (f^3/s)

data. Phase 3 was used primarily to compare the simulation of low flow ERSS to average flow ERSS as these low flow ERSS were determined to be especially relevant to the Pinelands Ecoregion [94]. The duration and magnitude ERSS of interest were compared graphically, through percent bias, and MdAPE. Using the SDR all simulated ERSS had reasonable variability compared to OBS values, so the SDR was not examined in detail in this phase.

6.3 Results and Discussion

The ERSS from Table 6.1 were calculated for each stream flow in Table 3.2. The performance of the simulations to estimate these ERSS were compared across watersheds and bias correction time scales. ERSS from SIM were examined first followed by MODEL and RCM.

6.3.1 PRMS Simulations driven by Observed Data

The simulations of the ERSS driven by observed climate in PRMS are shown for the Batsto River Watershed (Figure 6.1a) and the Maurice River Watershed (Figure 6.1b).

In the Batsto and Maurice River watersheds the overall ERSS had an MdAPE between 14% and 20% in the uncorrected (UC) simulations (Table 6.2 and 6.3). With all forms of bias correction the simulation of both watersheds improved; the MdAPE decreased with shorter bias correction time scales. The MdAPE with monthly bias correction was 1.1% in both the Batsto and Maurice River Watersheds. Removing the other stream flow characteristics from analysis appeared to make the trends much

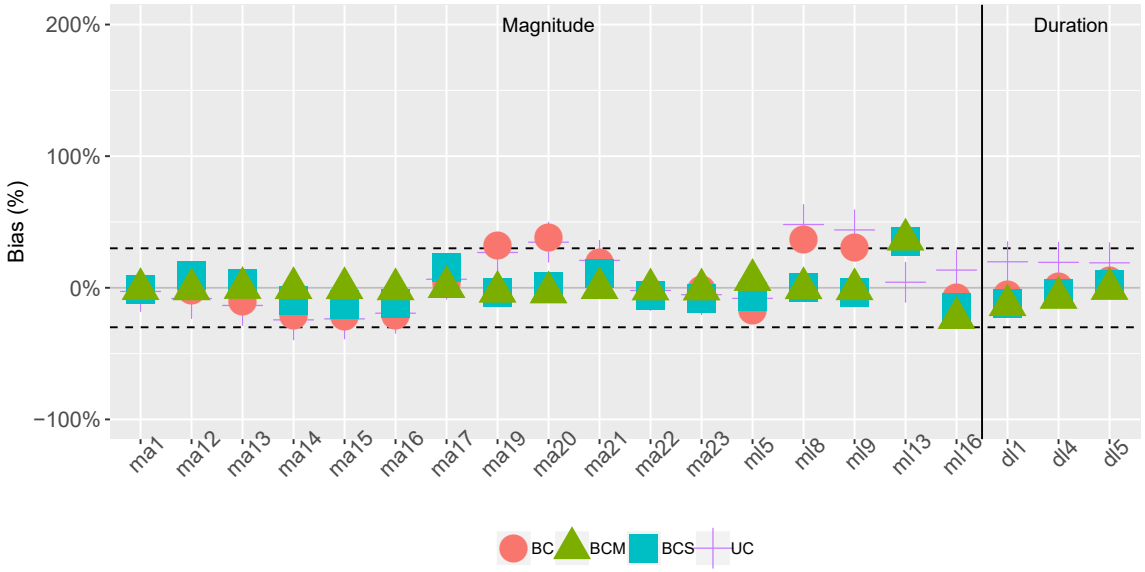

(a) Batsto River watershed

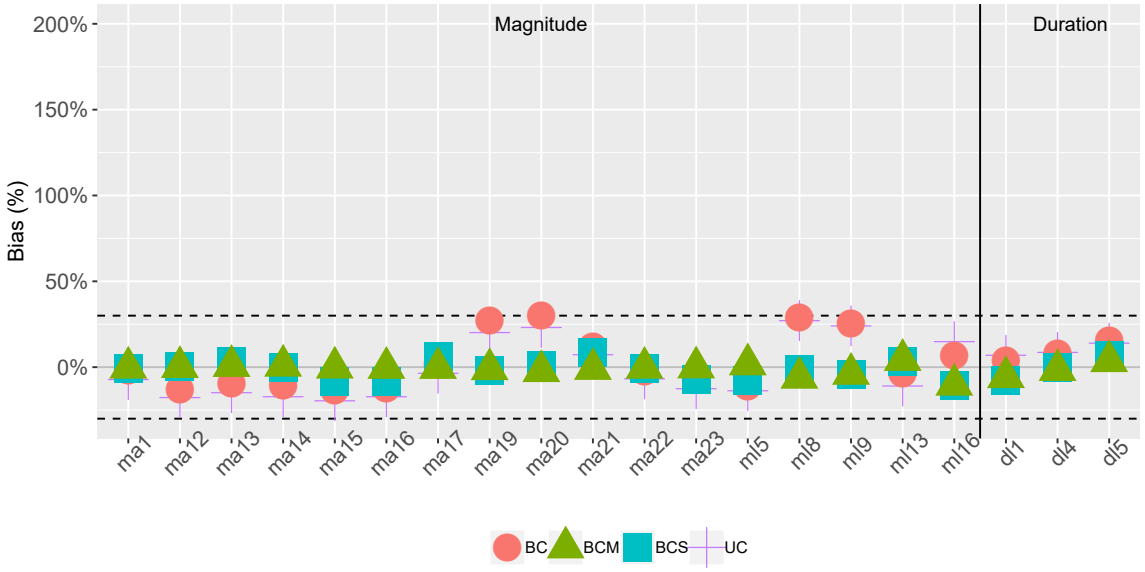

(b) Maurice River watershed

Figure 6.1: Percent Bias between Pinelands ERSS in the (a) Batsto and (b) Maurice River Watershed - SIM simulations with SIM-UC, SIM-BC, SIM-BCS and SIM-BCM bias correction. Dashed lines show +/- 30% hydrological uncertainty.

more apparent. Overall, based on the MdAPE values, the phase 3 SIM ERSS were better simulated than the phase 2 SIM ERSS. In the phase 3 results only the Batsto Watershed has SIM ERSS outside of the range of uncertainty. This agreed with the phase 2 analysis that showed the Batsto River watershed had greater error in simulation of ERSS. However, both stream flow characteristics improved with bias correction at short time scales.

Table 6.2: MdAPE Values of the Batsto River watershed modelled with observed data (SIM results) and bias correction.

	SIM-UC	**SIM-BC**	**SIM-BCS**	**SIM-BCM**
All ERSS	19.1%	13.7%	7.5%	1.1%
Magnitude	13.5%	19.1%	8.1%	1.1%
Duration	19.3%	5.2%	4.1%	7.7%

Table 6.3: MdAPE Values of the Maurice River watershed modelled with observed data (SIM results) and bias correction.

	SIM-UC	**SIM-BC**	**SIM-BCS**	**SIM-BCM**
All ERSS	14.4%	11.1%	3.8%	1.1%
Magnitude	14.9%	11.4%	3.4%	0.9%
Duration	8.6%	8.1%	6.6%	3.5%

Indices representing magnitude and duration decreased as bias correction time scales decreased in both watersheds with one exception. In the Batsto River watershed, the duration ERSS had a greater MdAPE value in the SIM-BCM simulation compared to the SIM-BC and SIM-BCS values (Table 6.2). However, in the Batsto River watershed, SIM-BCM had duration ERSS completely within the range of uncertainty and SIM-BCS simulation had the lowest duration MdAPE (4.1%). Neither bias correction method at small time scales (between BCS and BCM) was expected to outperform the other [84].

While magnitude and duration ERSS were consistently shown to be better

simulated with bias correction at smaller time scales, there was a concern that low flow ERSS would not be as well simulated [9], [94]. Of the 20 ERSS selected in the analysis, eight described low flow conditions (*ml5, ml8, ml9, ml13, ml16, dl1, dl4, dl5*). There were no high flow ERSS in this analysis as they did not meet the screening criteria. The low flow ERSS were not consistently better or more poorly simulated in the watersheds according to the MdAPE with any specific form of bias correction (Table 6.4 and 6.5).In Tables 6.4 and 6.5 low flow and average flow ERSS improved with bias correction at decreased time scales. It was expected that low flow ERSS would be consistently poorly simulated compared to average flow ERSS. However, it was found in the SIM-BC and SIM-BCS simulations in the Batsto River watershed and the SIM-UC and SIM-BC simulations in the Maurice River watershed that the low flow ERSS were better simulated compared to the average flow ERSS.

Table 6.4: MdAPE values of Average Flow and Low Flow ERSS in the Batsto River watershed with observed data (SIM results) and bias correction.

	SIM-UC	**SIM-BC**	**SIM-BCS**	**SIM-BCM**
Average Flow ERSS	16.4%	14.6%	8.6%	1.0%
Low Flow ERSS	19.1%	12.3%	5.5%	6.8%

Table 6.5: MdAPE values of Average Flow and Low Flow ERSS in the Maurice River watershed with observed data (SIM results) and bias correction.

	SIM-UC	**SIM-BC**	**SIM-BCS**	**SIM-BCM**
Average Flow ERSS	16.1%	11.4%	2.5%	0.4%
Low Flow ERSS	13.9%	9.7%	5.4%	4.0%

6.3.2 Downscaled GCM Simulations

The SIM results in phase 3 showed that there was minimal error in the hydrological model for the magnitude and duration ERSS. Bias correction further improved the

simulation of magnitude and duration ERSS. Driving the hydrological model with RCM data showed similar results. Only bias correcting to remove model error gave percent errors within the range of uncertainty for all ERSS. However, bias correcting to remove additional error from the RCM data gave lower overall error but did produce outliers.

Uncorrected Simulated ERSS driven by RCM data (RCM-UC)

Using RCM data, the selected ERSS were generally well simulated. The Batsto and Maurice watersheds followed similar trends in the simulation of ERSS, Figure 6.2, indicated that these magnitude and duration ERSS were not as affected by differences in land use. Certain ERSS were not well-simulated without bias correction. In both watersheds *ml8, ml9* and *ml16*, could use improvement; these are all low flow indices. Using RCM data the low flow indices tended to be poorer simulated compared to average flow ERSS.

Ml8 and *ml9* had the majority of their estimates from simulated data outside the range of uncertainty in both watersheds, while *ml16* had approximately 75% of the estimates of this ERSS outside of the range of uncertainty in the Maurice River watershed. *Dl1* also had a majority of data outside of uncertainty in the Batsto River watershed. All of these ERSS were low flow indices and indicated that low flow ERSS could use improvement when simulating stream flow with RCM data. This is in contrast to the SIM results, where low flow ERSS were well simulated with observed climate data. *Ml8* and *ml9* were the mean minimum flows across August and September, respectively. Magnitude of flows are often related month to month, so it is logical that both of these ERSS were similarly poor simulated. ERSS *ml16* was the median of annual minimum flows and *dl1* was the mean of minimum 1-day

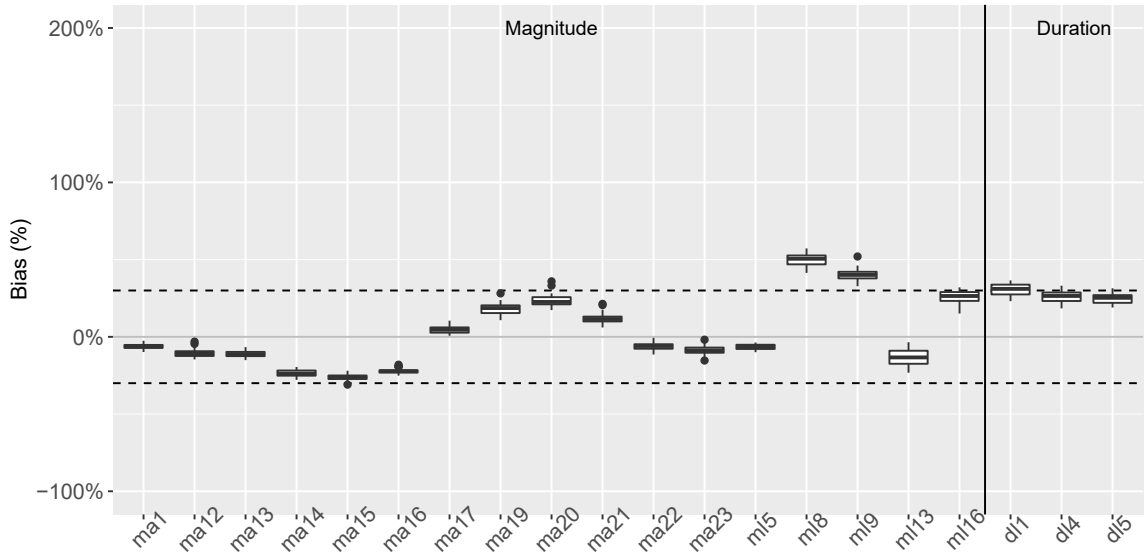

(a) Batsto River watershed

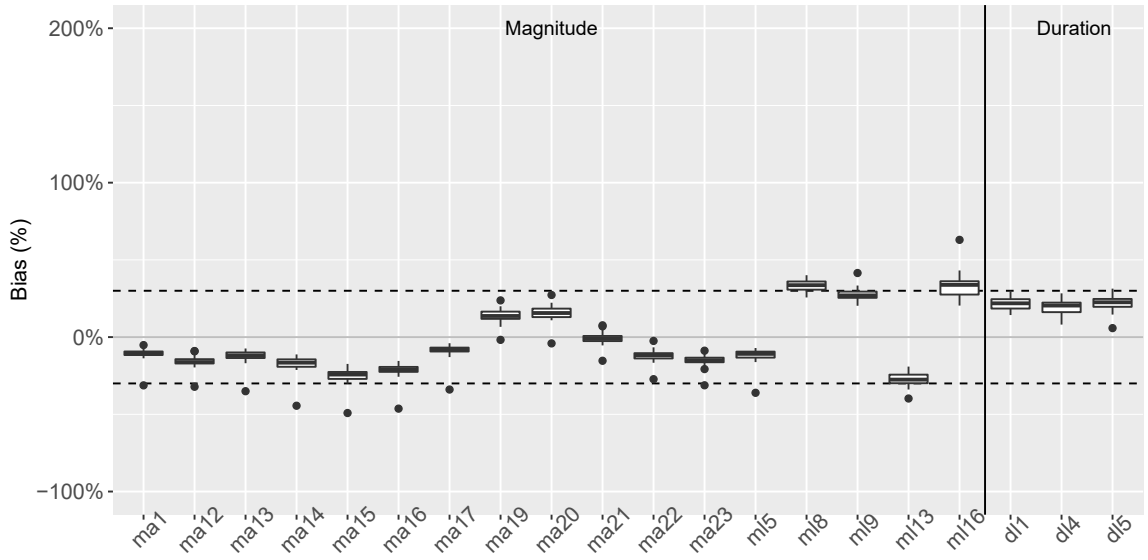

(b) Maurice River watershed

Figure 6.2: Percent Bias between Pinelands ERSS in the (a) Batsto River Watershed and (b) Maurice River Watershed - RCM-UC simulations and observed. Dashed lines show +/- 30% hydrological uncertainty.

average flows for each year. The poor simulation of low flows is consistent with past analysis [9], [10].

By comparing the two watersheds (Figure 6.2) the Maurice River watershed had more outliers in the individual ERSS than the Batsto River watershed. These outliers were caused by RCM CCSM4 r1i1p1. In future analysis this model may not be included. Previously, in phase 1, RCM CCSM4 r1i1pi was found to cause larger percent errors in the Maurice River watershed.

Model Corrected GCM Simulated Stream Flow (MODEL)

The selected ERSS were simulated, correcting for bias from PRMS (Figure 6.3 and 6.4). When bias correction was done using the stream flows determined from the PRMS model (MODEL) in both watersheds, it was found that MODEL-BCM led to a smaller overall MdAPE. Based on the results from phase 1 and phase 2, that bias correction at shorter time scales would better estimate ERSS. The MdAPE of the MODEL-BCM simulation was 4.4% and 5.5% in the Batsto and Maurice River watersheds, respectively (Table 6.6 and 6.7).

All simulations had an MdAPE less than 30%. However, again, it was found that in each stream flow characteristic a decreased time scale had (the desired effect of) a decrease in MdAPE.

Table 6.6: MdAPE Values of the Batsto River watershed with bias correction on the PRMS model (MODEL simulations).

	RCM-UC	**MODEL-BC**	**MODEL-BCS**	**MODEL-BCM**
All ERSS	20.4%	10.5%	8.2%	4.4%
Magnitude	14.7%	13.5%	9.3%	5.4%
Duration	27.1%	8.6%	3.1%	3.1%

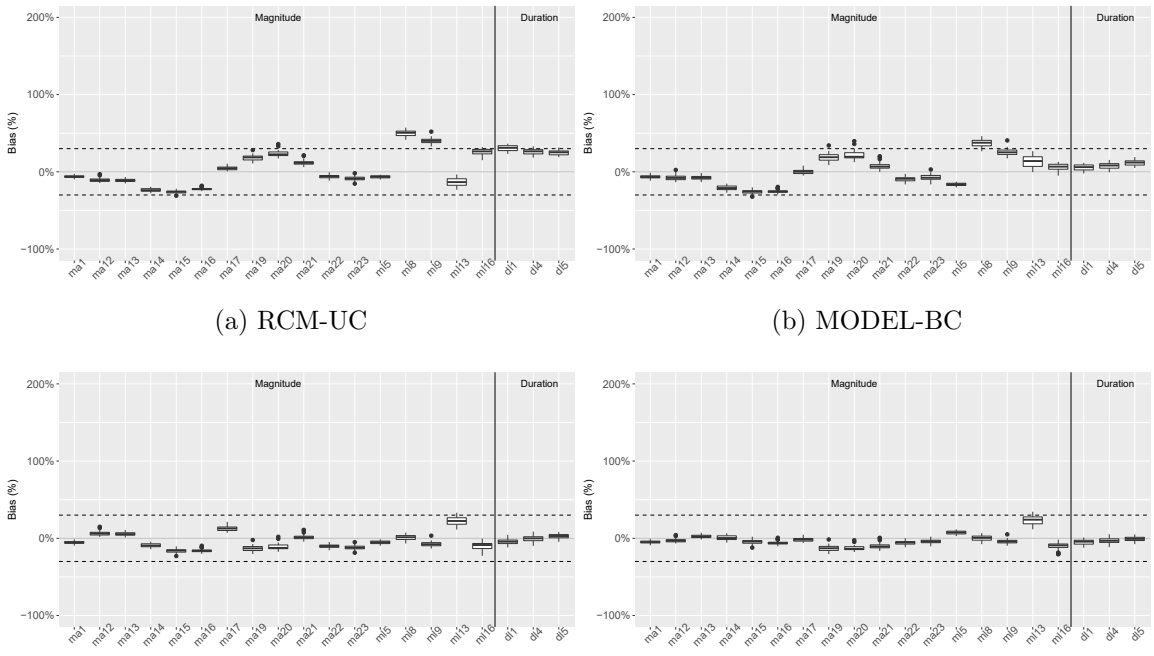

(a) RCM-UC

(b) MODEL-BC

(c) MODEL-BCS

(d) MODEL-BCM

Figure 6.3: Percent Bias between Pinelands ERSS in the Batsto River Watershed - MODEL simulations with (a) RCM-UC, (b) BC, (c) BCS and (d) BCM bias correction. Dashed lines show +/- 30% hydrological uncertainty.

Table 6.7: MdAPE Values of the Maurice River watershed with bias correction on the PRMS model (MODEL simulations).

	RCM-UC	**MODEL-BC**	**MODEL-BCS**	**MODEL-BCM**
All ERSS	16.4%	18.0%	6.9%	5.5%
Magnitude	15.8%	13.2%	5.5%	4.8%
Duration	21.2%	21.2%	9.6%	8.1%

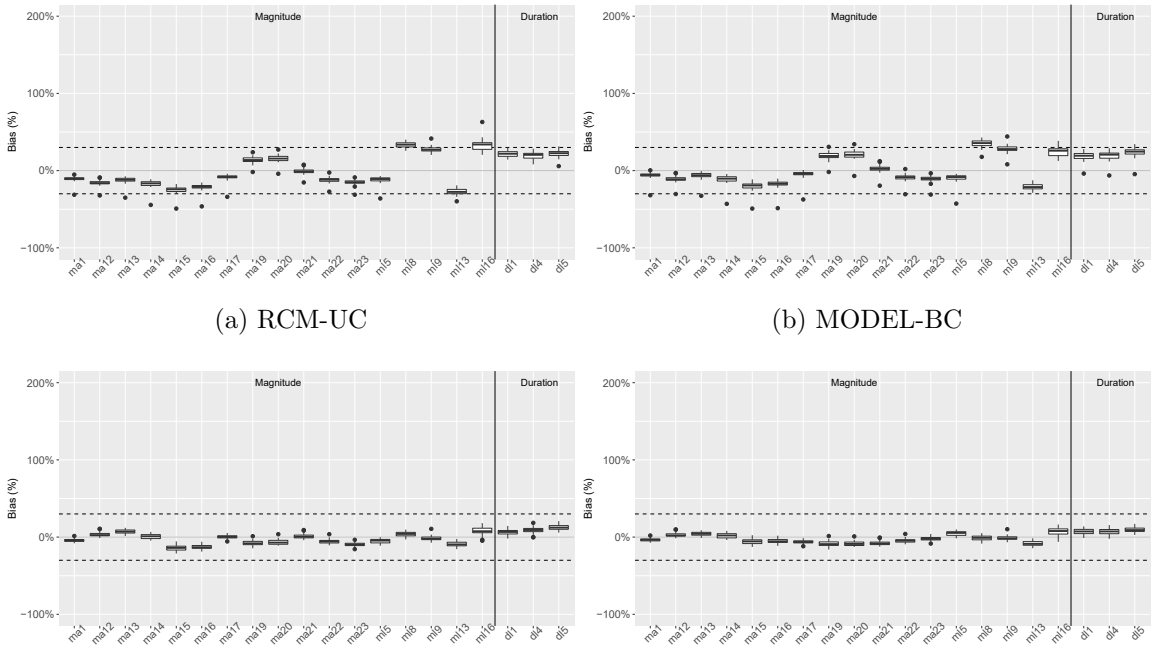

(a) RCM-UC

(b) MODEL-BC

(c) MODEL-BCS

(d) MODEL-BCM

Figure 6.4: Percent Bias between Pinelands ERSS in the Maurice River Watershed - MODEL simulations with (a) RCM-UC, (b) BC, (c) BCS and (d) BCM bias correction. Dashed lines show +/- 30% hydrological uncertainty.

In the the uncorrected simulations the low flow ERSS were more poorly simulated than the average flow ERSS: 27.0% MdAPE versus 12.3% MdAPE in the Batsto watershed and 24.9% MdAPE versus 13.8% MdAPE in the Maurice watershed (Table 6.8 and 6.9). However, when bias correction was applied that difference decreased. In fact, MODEL-BCS in the Batsto Watershed better simulated the low flow ERSS (5.4% MdAPE) versus the average flow ERSS (10.0% MdAPE).

With bias correction on the full stream flow record (MODEL-BC), the ERSS that were previously of concern (*ml8, ml9, ml13, ml16* and *dl1*), did show minor improvement but still had the majority of data outside of hydrological uncertainty. However, in both watersheds, MODEL-BCS and MODEL-BCM had all data within the range of uncertainty. This showed that these ERSS were minimally affected by any residual bias from the RCM.

Table 6.8: MdAPE Values Average Flow and Low Flow ERSS in the Batsto River watershed with bias correction on the PRMS model (MODEL simulations).

ERSS	**RCM-UC**	**MODEL-BC**	**MODEL-BCS**	**MODEL-BCM**
Average Flow	12.3%	10.5%	10.0%	5.1%
Low Flow	27.0%	13.0%	5.4%	5.2%

Table 6.9: MdAPE Values Average Flow and Low Flow ERSS in the Maurice River watershed with bias correction on the PRMS model (MODEL simulations).

ERSS	**RCM-UC**	**MODEL-BC**	**MODEL-BCS**	**MODEL-BCM**
Average Flow	13.8%	10.7%	5.7%	5.0%
Low Flow	24.9%	23.2%	6.8%	6.3%

Bias corrected GCM Simulated Stream Flow (RCM)

The MODEL simulations corrected for bias from the hydrological model, the RCM simulations corrected for any remaining residual bias from the RCMs. The RCM

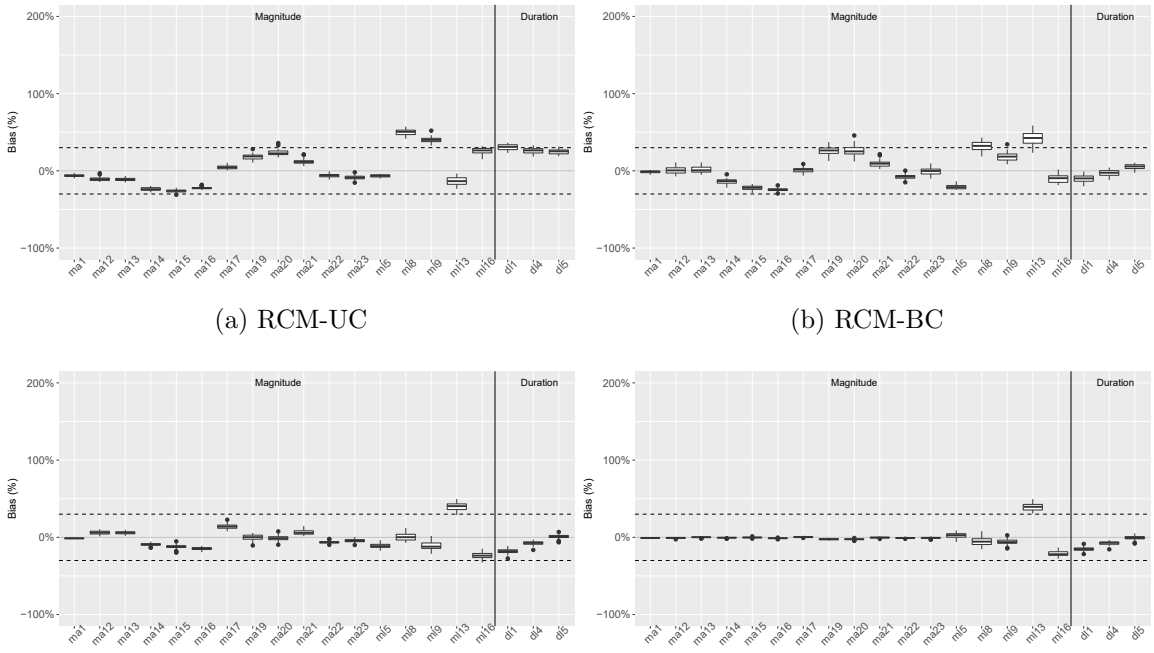

(a) RCM-UC

(b) RCM-BC

(c) RCM-BCS

(d) RCM-BCM

Figure 6.5: Percent Bias between Pinelands ERSS in the Batsto River Watershed - RCM simulations with (a) RCM-UC, (b) BC, (c) BCS and (d) BCM bias correction. Dashed lines show +/- 30% hydrological uncertainty.

driven results were bias corrected to the observed data (RCM). In both watersheds in the RCM simulations it was found that shorter BC time scales had the desired effect of decreased MdAPE (Table 6.5 and 6.6). This trend was also found in the MODEL results, with the RCM results the MdAPE values were even lower.

While the magnitude ERSS had decreased MdAPE with decreased bias correction time scales. The duration ERSS were best simulated with RCM-BC simulations on the Batsto River (6.1% MdAPE), however, similar MdAPE values were found in RCM-BCS (7.2%) and RCM-BCM (7.1%). All ERSS, except one, in the Batsto River watershed were within the range of uncertainty in RCM-BCS and RCM-BCM compared to RCM-BC. The Maurice River watershed had duration ERSS best simulated by RCM-BCM (7.4% MdAPE) (Table 6.10 and 6.11).

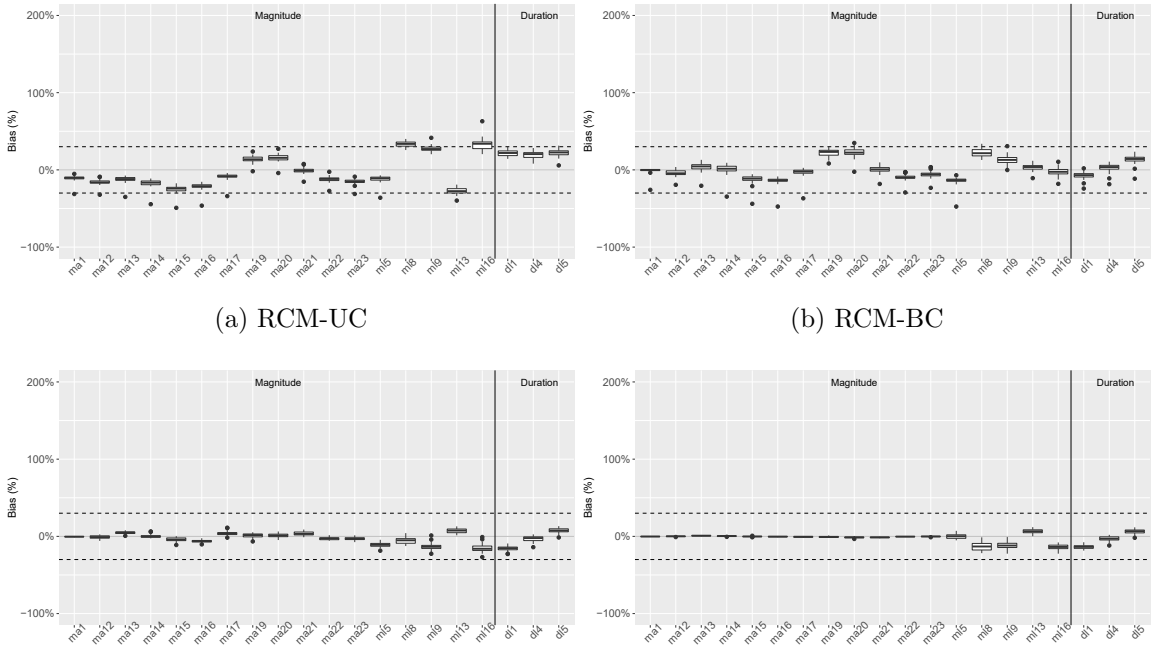

(a) RCM-UC

(b) RCM-BC

(c) RCM-BCS

(d) RCM-BCM

Figure 6.6: Percent Bias between Pinelands ERSS in the Maurice River Watershed - RCM simulations with (a) RCM-UC, (b) BC, (c) BCS and (d) BCM bias correction. Dashed lines show +/- 30% hydrological uncertainty.

Table 6.10: MdAPE Values of the Batsto River watershed with bias correction on the RCM (RCM simulations).

	RCM-UC	**RCM-BC**	**RCM-BCS**	**RCM-BCM**
All ERSS	20.4%	9.7%	6.9%	1.4%
Magnitude	14.7%	14.3%	7.7%	1.1%
Duration	27.1%	6.1%	7.2%	7.1%

Table 6.11: MdAPE Values of the Maurice River watershed with bias correction on the RCM (RCM simulations).

	RCM-UC	**RCM-BC**	**RCM-BCS**	**RCM-BCM**
All ERSS	16.4%	6.3%	4.1%	1.1%
Magnitude	15.8%	7.7%	4.1%	0.7%
Duration	21.2%	7.7%	8.4%	7.4%

All ERSS were within the range of uncertainty in the RCM-BCS and RCM-BCM simulations (like the MODEL results), with the exception of ERSS *ml13* in the Batsto River watershed. ERSS *ml13* described the variability across minimum monthly flow values. In the Maurice River watershed this measure of variability was within uncertainty. The variability in minimum monthly flows (*ml13*) for the Batsto River watershed was overestimated in all RCM simulations. This outlier was not observed in the MODEL simulations, but was narrowly inside the uncertainty in the MODEL simulations (Figure 6.3. This indicated that the additional error was introduced with the bias correction of the RCM. Bias correction on the RCM may sometimes add additional error into particular ERSS by reducing the simulation of natural variation, in particular for intra-annual variation however, consideration of timing in bias correction should have reduced this error [15]. It is possible that even accounting for seasonal and monthly bias correction, the wrong corrections were being applied. This may be due to simulation of key events occurring at different times than expected [15]. While this one ERSS was outside of the RCM, this should not take away from the improvement that the RCM bias correction gave to the simulation of Table 6.1 ERSS.

Table 6.12: MdAPE Values Average Flow and Low Flow ERSS in the Batsto River watershed with bias correction on the RCM (RCM simulations).

ERSS	**RCM-UC**	**RCM-BC**	**RCM-BCS**	**RCM-BCM**
Average Flow	12.3%	9.3%	6.5%	0.7%
Low Flow	27.0%	15.1%	12.1%	8.2%

Using RCM bias correction, the low flow ERSS always had greater percent error than the average flow ERSS (Table 6.12 and 6.13). However, decreased bias correction time scales did decrease MdAPE values in low flow ERSS. This same trend was found in MODEL results. In comparing the simulation low flow ERSS between MODEL

Table 6.13: MdAPE Values Average Flow and Low Flow ERSS in the Maurice River watershed with bias correction on the RCM (RCM simulations).

ERSS	**RCM-UC**	**RCM-BC**	**RCM-BCS**	**RCM-BCM**
Average Flow	13.8%	6.7%	2.7%	0.4%
Low Flow	24.9%	9.7%	9.7%	8.7%

results and RCM results, it is shown in Tables 6.8, 6.9, 6.12, and 6.13 that there was a difference in how low flow ERSS were simulated compared to average flow ERSS. In the MODEL results, at smaller BC time scales, MdAPE of average and low flow ERSS were similar. However, in the RCM simulations, at smaller BC time scales the MdAPE of average flow ERSS was much smaller than the MdAPE of low flow ERSS. The MdAPE of low flow ERSS was lower in the MODEL simulations at lower time scales compared to RCM simulations at lower time scales. The RCM bias correction better simulated ERSS at average flow than low flows and this should be considered in future analysis.

6.4 Summary

Magnitude and duration ERSS were found to be the only stream flow characteristics relevant in the Pinelands Ecoregion that met a conservative screening criteria by Kennen & Riskin (2010) [104]. Analyzing only this small subset of these ERSS allowed for more detailed analysis of the simulations, in particular the simulations of low flow ERSS. Biological interpretation of these results will be included in future analysis. It was expected and found (similar to phase 1) that all ERSS were better simulated by the RCM-BCS and RCM-BCM simulations. However, low flow ERSS were better simulated by the MODEL simulations. In MODEl-BCS, MODEL-BCM, RCM-BCS and RCM-BCM, generally, all data were within the range

of uncertainty. Bias correction at smaller time scales, compared to the full record, improved the simulation of magnitude and duration ERSS in SIM, MODEL and RCM simulations.

Chapter 7

Conclusions

Ecologically Relevant Stream flow Statistics (ERSS) were calculated for two New Jersey rivers that were simulated by PRMS and driven with 1) observed climate data and 2) RCM data. This was to determine if ERSS could be captured with RCM data, and if bias correction could be used to improved the simulation of ERSS. The evidence presented in this research supported the hypothesis.

Three different methods (in three phases) were used to determine a parsimonious set of ERSS for each waterway and simulation. Three different methods were used so that the selection of ERSS would not unfairly bias the results. The simulation of ERSS was first tested on stream flows from hydrological models driven by observed climate data. Bias correction at different time scales was done on simulated stream flows with observed climate data to correct for errors in the hydrological model (SIM). ERSS were then calculated from stream flows driven by RCM data. The stream flows were then bias corrected directly to the observed data (MODEL) and the RCM model driven results were bias corrected directly to the observed data (RCM). The MODEL simulations were to correct for biases in the hydrological model. To correct

for remaining bias from the RCM, bias correction was performed on the stream flows from dynamically downscaled data (RCM).

The two watersheds of interest - the Batsto and the Maurice, were both located in the Pinelands. The watersheds were very similar however, the Maurice River watershed was slightly more urbanized compared to the Batsto, Table 4.2. Overall, it was found that the PRMS simulations of the Maurice River watershed better estimated ERSS compared to the Batsto. Land use and urbanization may have contributed to the percent bias in the simulation of ERSS.

Phase 1

Simulating the 7FDSS gave preliminary evidence that the hypothesis was supported; that bias correcting stream flows will improve hydrologic simulations ability to capture flow indices and improve the performance of GCM driven models to represent these indices. The seasonal aspects of flow were best simulated by RCM-BCS and RCM-BCM. While certain daily aspects of flow (τ_3 and τ_4) were better simulated by RCM-BC but were still reasonably simulated by RCM bias correction at smaller time scales. From phase 1, a secondary hypothesis was presented that bias correction at smaller time scales on the RCM would have the most positive impact on the simulation of all ERSS. This hypothesis was generally supported in other phases of this research.

The SIM and RCM results had a greater percentage of ERSS within the range of uncertainty (+/- 30%) compared to the MODEL simulations. Application of downscaled data has a high level of uncertainty [58]. Results suggest that ERSS were almost completely within the range of uncertainty in the RCM-BCS simulations and this indicated that doing bias correction on the RCM at smaller time scales

improved the prediction of ERSS. It also showed that RCM bias correction reduced variation in the simulations [15]. Without a consideration of timing the reduction of variability is potentially inaccurate [15]

The Batsto and the Maurice watersheds showed similar results in SIM, MODEL and RCM bias correction where bias correction on the RCM at shorter time scales led to minimized percent error. The Maurice watershed had more outliers and the Batsto River watershed had greater percent error. There was concern that the simulation of certain characteristics of the Maurice River stream flow (compared to the Batsto) would not be well simulated due to the misrepresentation of runoff processes from greater urban development [15]. However, greater error was found in the simulation of the Batsto River watershed most likely due to structural errors in the PRMS model, potentially caused by the groundwater component.

Phase 2

In phase 2 of the analysis PCAs were used to create sets of ERSS that described each simulation of stream flow using a set of RCM data. This method gave different ERSS for each simulation that described the five primary stream flow characteristics. While it may have been beneficial to just select one set of ERSS to compare across watersheds, this method showed which ERSS best defined the stream flows with different bias correction methods.

Overall, similar results from phase 1 were found in phase 2; RCM-BCS and RCM-BCM showed the greatest improvement on the simulation of ERSS. However, upon further examination certain ERSS were found to be poorly simulated even with bias correction at the smallest time scale on the RCM. The simulation of frequency and rate of change ERSS need to be improved [32]. These ERSS are very sensitive

to minor errors in stream flow simulation. The type of bias correction used in this study did not improve the simulation of frequency ERSS. The simulation of certain ERSS, particularly frequency ERSS has been a concern and has been highlighted in many recent papers [8].

It was found that MODEL results gave more consistent and expected simulations than RCM results. More ERSS followed the expected pattern (from phase 1), compared to the RCM simulations. Using the RCM simulations changed the variability of the simulated flow. However, when examining the SDR, it was clear that the simulation of ERSS using RCM data was done with reasonable accuracy compared to a regional analysis.

Phase 3

Phase 3 of this study examined only two stream flow characteristics that had been well simulated in phase 2 - magnitude and duration ERSS. These ERSS were determined to be ecologically relevant to the Pinelands Ecoregion [104]. Phase 3 tested the simulation of low flow magnitude and duration ERSS compared to average flow.

Without bias correction, it was found that average flow ERSS were consistently better simulated than low flow ERSS. MODEL simulations, and not RCM simulations, predicted low flow ERSS the best, while RCM simulations predicted average flow ERSS the best. However, both simulations at short bias correction time scales predicted this set of 18 ERSS generally within the range of uncertainty.

There were limitations to this research. The biases in the Batsto River watershed model in the summer and autumn add to the uncertainty of the stream flow

simulations which limit the applicability of this hydro-ecological work stemming from Daraio's (2017) research. Further work is required to interpret the biological significance of these simulations of hydro-ecological indices. The biological perspective will be explored in upcoming publications.

The hypothesis of this research was that bias correcting stream flows will improve the ability of hydrological simulations to capture flow indices and improve the performance of GCM driven models to represent these indices. From the results of phase 1, 2 and 3 this hypothesis was generally supported, with the exception of frequency and rate of change ERSS, which were still poorly simulated (phase 2) with bias correction.

Overall, the goal was achieved to create parsimonious sets of ERSS and compare ERSS between simulations of the Batsto and Maurice River watersheds. This work showed that using RCM data is reasonable for the simulation of ERSS as long as proper bias correction is performed. However, the simulation of frequency ERSS needs to be carefully considered for future modelling studies and requires further research. The simulation of ERSS using RCM data has importance to climate change predictions and therefore mitigation measures. More detailed analysis of the flow regime and ecological characteristics are necessary as there are projected change to these stream flows [15]. Future work should include the simulation of these ERSS for future time periods and completing bias correction based on the results presented here.

This research has implications for the choice of ERSS used in future studies and management applications in the Pinelands streams. The simulation of certain ERSS must be treated with caution. Management of hydro-ecological resources is a balance of competing interests. The ability to simulate and model future ERSS with minimal

uncertainty will result in more informed management decisions. Bias correction at shorter time scales is a valuable tool when dealing with potential future ecologically damaging scenarios to create predictions with minimal uncertainty.

Bibliography

[1] N. L. Poff, J. D. Allan, M. B. Bain, J. R. Karr, K. L. Prestegaard, B. D. Richter, R. E. Sparks, and J. C. Stromberg, *The Natural Flow Regime*, 1997.

[2] W. J. Junk, P. B. Bayley, and R. E. Sparks, "The flood pulse concept in river-floodplain systems," in *International Large River Symposim*, T. Mailund, Ed., vol. 106, Ottawa, Dec. 1989, pp. 110–127.

[3] O. Moog, "Quantification of daily peak hydropower effects on aquatic fauna and management to minimize environmental impacts," *Regulated Rivers: Research & Management*, vol. 8, no. 1-2, pp. 5–14, May 1993.

[4] J. D. Allan, *Stream ecology : structure and function of running waters*, eng. London ; New York: Chapman Hall, 1995.

[5] A. H. Arthington, A. Bhaduri, S. E. Bunn, S. E. Jackson, R. E. Tharme, D. Tickner, B. Young, M. Acreman, N. Baker, S. Capon, A. C. Horne, E. Kendy, M. E. McClain, N. L. Poff, B. D. Richter, and S. Ward, "The brisbane declaration and global action agenda on environmental flows (2018)," *Frontiers in Environmental Science*, vol. 6, p. 45, 2018.

[6] T. Dunne, *Water in environmental planning*, eng. San Francisco: W. H. Freeman, 1978.

[7] P. Däll and J. Zhang, "Impact of climate change on freshwater ecosystems: A global-scale analysis of ecologically relevant river flow alterations," *Hydrology and Earth System Sciences*, vol. 14, no. 5, pp. 783–799, 2010.

[8] P. V. Caldwell, J. G. Kennen, G. Sun, J. E. Kiang, J. B. Butcher, M. C. Eddy, L. E. Hay, J. H. Lafontaine, E. F. Hain, S. A. Nelson, and S. G. Mcnulty, "A comparison of hydrologic models for ecological flows and water availability," *Ecohydrology*, vol. 8, no. 8, pp. 1525–1546, 2015.

[9] F. Chiew, H. Zheng, and N. Potter, "Rainfall-Runoff Modelling Considerations to Predict Streamflow Characteristics in Ungauged Catchments and under Climate Change," *Water*, vol. 10, no. 10, p. 1319, Sep. 2018.

[10] O. Huziy, L. Sushama, M. N. Khaliq, R. Laprise, B. Lehner, and R. Roy, "Analysis of streamflow characteristics over Northeastern Canada in a changing climate," *Climate Dynamics*, vol. 40, no. 7-8, pp. 1879–1901, 2013.

[11] N. L. Poff, B. D. Richter, A. H. Arthington, S. E. Bunn, R. J. Naiman, E. Kendy, M. Acreman, C. Apse, B. P. Bledsoe, M. C. Freeman, J. Henriksen, R. B. Jacobson, J. G. Kennen, D. M. Merritt, J. H. O'Keeffe, J. D. Olden, K. Rogers, R. E. Tharme, and A. Warner, "The ecological limits of hydrologic alteration (ELOHA): A new framework for developing regional environmental flow standards," *Freshwater Biology*, vol. 55, no. 1, pp. 147–170, 2010.

[12] D. J. Baker, A. J. Hartley, J. W. Pearce-Higgins, R. G. Jones, and S. G. Willis, "Neglected issues in using weather and climate information in ecology and biogeography," *Diversity and Distributions*, vol. 23, no. 3, pp. 329–340, 2017.

[13] J. H. Christensen, T. R. Carter, M. Rummukainen, and G. Amanatidis, "Evaluating the performance and utility of regional climate models: The PRUDENCE project," *Climatic Change*, vol. 81, no. SUPPL. 1, pp. 1–6, 2007.

[14] M. Troin, D. Caya, J. A. Velázquez, and F. Brissette, "Hydrological response to dynamical downscaling of climate model outputs: A case study for western and eastern snowmelt-dominated Canada catchments," *Journal of Hydrology: Regional Studies*, vol. 4, pp. 595–610, 2015.

[15] J. A. Daraio, "Assessing Climate Change impacts on Stream Flows Using Flow Duration Curves," *American Water Resources Association*, 2019.

[16] S. R. Carpenter, E. H. Stanley, and M. J. Vander Zanden, "State of the World's Freshwater Ecosystems: Physical, Chemical, and Biological Changes," *Annual Review of Environment and Resources*, vol. 36, no. 1, pp. 75–99, 2011.

[17] T. Cui, T. Yang, C. Y. Xu, Q. Shao, X. Wang, and Z. Li, "Assessment of the impact of climate change on flow regime at multiple temporal scales and potential ecological implications in an alpine river," *Stochastic Environmental Research and Risk Assessment*, vol. 32, no. 6, pp. 1849–1866, 2018.

[18] S. Kim, H. Noh, J. Jung, H. Jun, and H. S. Kim, "Assessment of the impacts of global climate change and regional water projects on streamflow characteristics in the Geum River Basin in Korea," *Water (Switzerland)*, vol. 8, no. 3, 2016.

[19] D. L. Ficklin, J. T. Abatzoglou, S. M. Robeson, S. E. Null, and J. H. Knouft, "Natural and managed watersheds show similar responses to recent climate change," *Proceedings of the National Academy of Sciences*, vol. 115, no. 34, pp. 8553–8557, 2018.

[20] E. M. Demaria, R. N. Palmer, and J. K. Roundy, "Regional climate change projections of streamflow characteristics in the Northeast and Midwest U.S.," *Journal of Hydrology: Regional Studies*, vol. 5, pp. 309–323, 2016.

[21] S. Pool, M. J. P. Vis, R. R. Knight, and J. Seibert, "Streamflow characteristics from modelled runoff time series - importance of calibration criteria selection," *Hydrology and Earth System Sciences Discussions*, pp. 1–27, 2017.

[22] N. Truong, H. Nguyen, and A. Kondoh, "Land Use and Land Cover Changes and Their Effect on the Flow Regime in the Upstream Dong Nai River Basin, Vietnam," *Water*, vol. 10, no. 9, p. 1206, Sep. 2018.

[23] K. Hassaballah, Y. Mohamed, S. Uhlenbrook, and K. Biro, "Analysis of streamflow response to land use and land cover changes using satellite data and hydrological modelling: Case study of Dinder and Rahad tributaries of the Blue Nile (Ethiopia-Sudan)," *Hydrology and Earth System Sciences*, vol. 21, no. 10, pp. 5217–5242, 2017.

[24] M. Castillo, H. Morales, E. Valencia, J. Morales, and J. Cruz-Motta, "The effects of human land use on flow regime and water chemistry of headwater streams in the highlands of Chiapas," *Knowledge and Management of Aquatic Ecosystems*, no. 407, p. 09, 2012.

[25] L. Yang, Q. Feng, Z. Yin, R. C. Deo, X. Wen, J. Si, and C. Li, "Separation of the Climatic and Land Cover Impacts on the Flow Regime Changes in Two Watersheds of Northeastern Tibetan Plateau," *Advances in Meteorology*, vol. 2017, 2017.

[26] S. A. Archfield, J. G. Kennen, D. M. Carlisle, and D. M. Wolock, "An objective and parsimonious approach for classifying natural flow regimes at a continental scale," *River R*, vol. 30, no. 2, pp. 1166–1183, 2014.

[27] J. D. Olden and N. L. Poff, "Redundancy and the choice of hydrologic indices for characterizing streamflow regimes," *River Research and Applications*, vol. 19, no. 2, pp. 101–121, 2003.

[28] The Nature Conservancy, *Indicators of Hydrologic Alteration*, 2017.

[29] A. Lee, S. Cho, D. K. Kang, and S. Kim, "Analysis of the effect of climate change on the Nakdong river stream flow using indicators of hydrological alteration," *Journal of Hydro-Environment Research*, vol. 8, no. 3, pp. 234–247, 2014.

[30] R. Mathews and B. D. Richter, "Application of the indicators of hydrologic alteration software in environmental flow setting," *Journal of the American Water Resources Association*, vol. 43, no. 6, pp. 1400–1413, 2007.

[31] M. Pfeiffer and M. Ionita, "Assessment of hydrologic alterations in Elbe and Rhine Rivers, Germany," *Water (Switzerland)*, vol. 9, no. 9, p. 19, 2017.

[32] B. D. Richter, J. V. Baumgartner, R. Wigington, and D. P. Braun, "How much water does a river need ? Discussion : Who does what ?" *Freshwater Biology*, pp. 231–249, 1997.

[33] J. A. Henriksen, G. Kennen, J, and S. Nieswand, "Users Manual for the Hydroecological Integrity Assessment Process Software (including the New Jersey Assessment Tools)," Tech. Rep., 2006.

[34] J. G. Kennen, J. Henriksen, and S. Nieswand, "Development of the Hydroecological Integrity Assessment Process for Determining Environmental Flows for New Jersey Streams," 2007.

[35] J. Thompson, S. Archfield, J. Kennen, and J. Kiang, "Eflowstats: An r package to compute ecologically-relevant streamflow statistics," in *AGU Fall Meeting Abstracts*, 2013.

[36] R Development Core Team, *R: A language and environment for statistical computing*, Vienna, Austria, 2008.

[37] K. L. Wahl, W. O. Thomas, and R. M. Hirsch, "The stream-gaging program of the us geological survey," US Geological Survey, Tech. Rep., 1995.

[38] US EPA, "Chapter 1: Stream Design Flow for Steady-State Modeling," in *Technical Guidance Manual for Performing Wasteload Allocation: Book VI Design Condtions*, 79, 1986.

[39] G. A. Nnaji, W. Huang, M. W. Gitau, and C. Clark, "Frequency analysis of minimum ecological flow and gage height in suwannee river, florida," *Journal of Coastal Research*, vol. 68, no. sp1, pp. 152–159, 2014.

[40] M. C. Molles, C. S. Crawford, L. M. Ellis, H. M. Valett, and C. N. Dahm, "Managed flooding for riparian ecosystem restoration," *BioScience*, vol. 48, no. 9, pp. 749–756, 1998.

[41] B. D. Richter and H. E. Richter, "Prescribing flood regimes to sustain riparian ecosystems along meandering rivers," *Conservation Biology*, vol. 14, no. 5, pp. 1467–1478, 2000.

[42] M. L. Scott, G. T. Auble, and J. M. Friedman, "Flood dependency of cottonwood establishment along the missouri river, montana, usa," *Ecological Applications*, vol. 7, no. 2, pp. 677–690, 1997.

[43] K. D. Fausch, Y. Taniguchi, S. Nakano, G. D. Grossman, and C. R. Townsend, "Flood disturbance regimes influence rainbow trout invasion success among five holarctic regions," *Ecological Applications*, vol. 11, no. 5, pp. 1438–1455, 2001.

[44] N. A. Sievert, C. P. Paukert, Y. P. Tsang, and D. Infante, "Development and assessment of indices to determine stream fish vulnerability to climate change and habitat alteration," *Ecological Indicators*, vol. 67, pp. 403–416, 2016.

[45] L. E. Hay and M. P. Clark, "Use of statistically and dynamically downscaled atmospheric model output for hydrologic simulations in three mountainous basins in the western United States," *Journal of Hydrology*, vol. 282, no. 1-4, pp. 56–75, 2003.

[46] O. Vigiak, S. Lutz, A. Mentzafou, G. Chiogna, Y. Tuo, B. Majone, H. Beck, A. de Roo, A. Malagó, F. Bouraoui, R. Kumar, L. Samaniego, R. Merz, C. Gamvroudis, N. Skoulikidis, N. P. Nikolaidis, A. Bellin, V. Acuňa, N. Mori, R. Ludwig, and A. Pistocchi, "Uncertainty of modelled flow regime for flow-ecological assessment in Southern Europe," *Science of the Total Environment*, vol. 615, pp. 1028–1047, 2018.

[47] H. Mcmillan, T. Krueger, and J. Freer, "Benchmarking observational uncertainties for hydrology: Rainfall, river discharge and water quality," *Hydrological Processes*, vol. 26, no. 26, pp. 4078–4111, 2012.

[48] T. T. Hailegeorgis and K. Alfredsen, "Regional Statistical and Precipitation-Runoff Modelling for Ecological Applications: Prediction of Hourly Streamflow in Regulated Rivers and Ungauged Basins," *River Research and Applications*, vol. 33, no. 2, pp. 233–248, Feb. 2017.

[49] J. C. Murphy, R. R. Knight, W. J. Wolfe, and W. S. Gain, "Predicting ecological flow regime at ungaged sites: a comparison of methods," *River Research and Applications*, vol. 29, no. 5, pp. 660–669, Jun. 2013.

[50] C. A. Santos, C. Almeida, T. B. Ramos, F. A. Rocha, R. Oliveira, and R. Neves, "Using a hierarchical approach to calibrate SWAT and predict the semi-arid hydrologic regime of northeastern Brazil," *Water (Switzerland)*, vol. 10, no. 9, 2018.

[51] N. J. Potter, M. Ekström, F. H. Chiew, L. Zhang, and G. Fu, "Change-signal impacts in downscaled data and its influence on hydroclimate projections," *Journal of Hydrology*, vol. 564, no. May, pp. 12–25, 2018.

[52] R. Benestad, *Downscaling Climate Information*. Oxford University Press, Jul. 2016, vol. 1.

[53] P. C. D. Milly, J. Betancourt, M. Falkenmark, R. M. Hirsch, Z. W. Kundzewicz, D. P. Lettenmaier, and R. J. Stouffer, "Stationarity Is Dead: Whither Water Management?" *Science*, vol. 319, no. 5863, pp. 573–574, Feb. 2008.

[54] Intergovernmental Panel on Climate Change, "Climate Change 2014," Tech. Rep., 2014.

[55] National Ocean and Atmospheric Administration, *Climate Model Downscaling*, 2018.

[56] F. Fung, A. Lopez, and M. New, *Modelling the Impact of Climate Change in Water Resources*. 2011, p. 187.

[57] J. Chen, F. P. Brissette, and R. Leconte, "Uncertainty of downscaling method in quantifying the impact of climate change on hydrology," *Journal of Hydrology*, vol. 401, no. 3-4, pp. 190–202, 2011.

[58] G. Bürger, S. R. Sobie, A. J. Cannon, A. T. Werner, and T. Q. Murdock, "Downscaling extremes: An intercomparison of multiple methods for future climate," *Journal of Climate*, vol. 26, no. 10, pp. 3429–3449, 2013.

[59] R. L. Wilby and T. M. L. Wigley, "Downscaling general circulation model output: a review of methods and limitations," *Progress in Physical Geography*, vol. 21, no. 4, pp. 530–548, 1997.

[60] K. Tabor and J. W. Williams, "Globally downscaled climate projections for assessing the conservation impacts of climate change," *Ecological Applications*, vol. 20, no. 2, pp. 554–565, Mar. 2010.

[61] J. H. Christensen, "Prediction of Regional scenarios and Uncertainties for Defining European Climate change risks and Effects," Tech. Rep., 2005, pp. 1–269.

[62] M. Glotter, J. Elliott, D. McInerney, N. Best, I. Foster, and E. J. Moyer, "Evaluating the utility of dynamical downscaling in agricultural impacts projections," *Proceedings of the National Academy of Sciences*, vol. 111, no. 24, pp. 8776–8781, 2014.

[63] G. R. Fahad, R. Nazari, J. Daraio, and D. J. Lundberg, "Regional Study of Future Temperature and Precipitation Changes Using Bias Corrected Multi-Model Ensemble Projections Considering High Emission Pathways," *Journal of Earth Science & Climate Change*, vol. 8, no. 8, 2017.

[64] U. Nations, *Intergovernmental Panel on Climate Change (IPCC)*.

[65] K. E. Taylor, "CMIP5: models design," vol. 2009, no. January 2011, pp. 1–33, 2009.

[66] C. Teutschbein, F. Wetterhall, and J. Seibert, "Evaluation of different downscaling techniques for hydrological climate-change impact studies at the catchment scale," *Climate Dynamics*, vol. 37, no. 9-10, pp. 2087–2105, 2011.

[67] D. Maraun, M. Widmann, J. M. Gutiérrez, S. Kotlarski, R. E. Chandler, E. Hertig, J. Wibig, R. Huth, and R. A. Wilcke, "VALUE: A framework to validate downscaling approaches for climate change studies," *Earth's Future*, vol. 3, no. 1, pp. 1–14, Jan. 2015.

[68] R. R. Shrestha, D. L. Peters, and M. A. Schnorbus, "Evaluating the ability of a hydrologic model to replicate hydro-ecologically relevant indicators," *Hydrological Processes*, vol. 28, no. 14, pp. 4294–4310, 2014.

[69] S. Hempel, K. Frieler, L. Warszawski, J. Schewe, and F. Piontek, "A trend-preserving bias correction – The ISI-MIP approach," *Earth System Dynamics*, vol. 4, no. 2, pp. 219–236, 2013.

[70] R. M. Vogel and N. M. Fennessey, "Flow duration curves. i: New interpretation and confidence intervals," *Journal of Water Resources Planning and Management*, vol. 120, no. 4, pp. 485–504, Jul. 1994.

[71] D. Kim, I. W. Jung, and J. A. Chun, "A comparative assessment of rainfall-runoff modelling against regional flow duration curves for ungauged catchments," *Hydrology and Earth System Sciences*, vol. 21, no. 11, pp. 5647–5661, 2017.

[72] G. Blöschl, M. Sivapalan, H. Savenije, T. Wagener, and A. Viglione, *Runoff prediction in ungauged basins: synthesis across processes, places and scales.* Cambridge University Press, 2013.

[73] T. Ranatunga, S. T. Tong, and Y. J. Yang, "An approach to measure parameter sensitivity in watershed hydrological modelling," *Hydrological Sciences Journal*, pp. 1–17, Aug. 2016.

[74] J. A. Daraio, "Potential climate change impacts on streamflow and recharge in two watersheds on the new jersey coastal plain," *Journal of Hydrologic Engineering*, 2017.

[75] Y. Yokoo and M. Sivapalan, "Towards reconstruction of the flow duration curve: Development of a conceptual framework with a physical basis," *Hydrology and Earth System Sciences*, vol. 15, no. 9, pp. 2805–2819, 2011.

[76] M. Yaeger, E. Coopersmith, S. Ye, L. Cheng, A. Viglione, and M. Sivapalan, "Exploring the physical controls of regional patterns of flow duration curves - part 4: A synthesis of empirical analysis, process modeling and catchment classification," *Hydrology and Earth System Sciences*, vol. 16, no. 11, pp. 4483–4498, 2012.

[77] S. Dhungel, D. G. Tarboton, J. Jin, and C. P. Hawkins, "Potential Effects of Climate Change on Ecologically Relevant Streamflow Regimes," *River Research and Applications*, vol. 32, no. 9, pp. 1827–1840, 2016.

[78] N. J. D. of Fish and Wildlife). (2015). The pinelands national reserve, [Online]. Available: `https://www.nj.gov/pinelands/reserve/` (visited on 07/18/2019).

[79] R. A. Esralew and R. J. Baker, "Determination of Baseline Periods of Record for Selected Streamflow-Gaging Stations in New Jersey for Determining Ecologically Relevant Hydrologic Indices (ERHI)," pp. 1–70, 2008.

[80] S. L. Markstrom, R. S. Regan, L. E. Hay, R. J. Viger, R. M. T. Webb, R. A. Payn, and J. H. LaFontaine, "PRMS-IV , the Precipitation-Runoff Modeling System, Version 4," *U.S. Geological Survey Techniques and Methods, Book 6: Modeling Techniques*, p. 158, 2015.

[81] D. L. Blodgett, N. L. Booth, T. C. Kunicki, J. I. Walker, and R. J. Viger, *USGS Geo Data Portal*, 2011.

[82] M. M. Kalcic, I. Chaubey, and J. Frankenberger, "Defining Soil and Water Assessment Tool (SWAT) hydrologic response units (HRUs) by field boundaries," *International Journal of Agricultural and Biological Engineering*, vol. 8, no. 3, pp. 1–12, 2015.

[83] L. E. Hay and M. Umemoto, "Multiple-objective stepwise calibration using Luca," *U. S. Geological Survey Open-File Report*, no. 2006-1323, p. 25, 2006.

[84] J. A. Daraio, "Bias Correction of Simulated Stream Flows from Calibrated Hydrologic Models to Evaluate and Improve Long-Term Simulations Key Points :,"

[85] M. Garnier, D. M. Harper, L. Blaskovicova, G. Hancz, G. A. Janauer, Z. Jolánkai, E. Lanz, A. L. Porto, M. Mándoki, B. Pataki, J. L. Rahuel, V. J. Robinson, C. Stoate, E. Tóth, and G. Jolánkai, "Climate Change and European Water Bodies, a Review of Existing Gaps and Future Research Needs: Findings of the ClimateWater Project," *Environmental Management*, vol. 56, no. 2, pp. 271–285, 2015.

[86] D. Maraun and M. Widmann, *Statistical Downscaling and Bias Correction for Climate Research*. Cambridge University Press, 2018.

[87] L. Gudmundsson, J. B. Bremnes, J. E. Haugen, and T. Engen-Skaugen, "Technical Note: Downscaling RCM precipitation to the station scale using statistical transformations - A comparison of methods," *Hydrology and Earth System Sciences*, vol. 16, no. 9, pp. 3383–3390, 2012.

[88] M. Moujahid, L. Stour, A. Agoumi, and A. Saidi, "Regional approach for the analysis of annual maximum daily precipitation in northern Morocco," *Weather and Climate Extremes*, vol. 21, no. July, pp. 43–51, 2018.

[89] J. R. M. Hosking and J. R. Wallis, *Regional Frequency Analysis*. Cambridge: Cambridge University Press, 1997.

[90] J. S. Rice, R. E. Emanuel, J. M. Vose, and S. A. C. Nelson, "Continental U.S. streamflow trends from 1940 to 2009 and their relationships with watershed spatial characteristics," *Water Resources Research*, vol. 51, no. 8, pp. 6262–6275, Aug. 2015.

[91] J. Mills and D. Blodgett, *Eflowstats: Hydrologic indicator and alteration stats*, R package version 5.0.0, 2017.

[92] M. J. Kennard, S. J. Mackay, B. J. Pusey, J. D. Olden, and N. Marsh, "Quantifying uncertainty in estimation of hydrologic metrics for ecohydrological studies," *River Research and Applications*, vol. 26, pp. 137–156, 2009. arXiv: `arXiv:1011.1669v3`.

[93] J. Chen, F. P. Brissette, D. Chaumont, and M. Braun, "Finding appropriate bias correction methods in downscaling precipitation for hydrologic impact studies over North America," *Water Resources Research*, vol. 49, no. 7, pp. 4187–4205, 2013.

[94] J. Kennen, private communication, 2018.

[95] J. E. Jackson, *A User's Guide to Principal Components*. Chicago: John Wiley & Sons, 1991.

[96] J. G. Kennen, K. Riva-Murray, and K. M. Beaulieu, "Determining hydrologic factors that influence stream macroinvertebate assemblages in the northeastern US," *Ecohydrology*, vol. 3, no. February, pp. 88–106, 2010.

[97] S. S. Shapiro and M. B. Wilk, "An analysis of variance test for normality (complete samples)," *Biometrika*, vol. 52, no. 3/4, pp. 591–611, 1965.

[98] B. McCune and J. B. Grace, *Analysis of Ecological Communities*. May 2002.

[99] G. Box and D. Cox, "An analysis of transformations," *Journal of the Royal Statistical Society*, vol. 45, no. 2, pp. 211–252, 1964.

[100] Ö. Asar, O. Ilk, and O. Dag, "Estimating Box-Cox power transformation parameter via goodness of fit tests," *Communications in Statistics - Simulation and Computation*, pp. 1–17, 2013.

[101] C. Spearman, "The proof and measurement of association between two things," *The American journal of psychology*, vol. 15, no. 1, pp. 72–101, 1904.

[102] S. Frontier, "Étude de la décroissance des valeurs propres dans une analyse en composantes principales: Comparaison avec le modele du bâton brisé," *Journal of Experimental Marine Biology and Ecology*, vol. 25, no. 1, pp. 67–75, 1976.

[103] Jackson D. A., "Stopping rules in principal components analysis: a comparison of heuristical and statistical approaches," *Ecology*, vol. 74, no. 8, pp. 2204–2214, 1993.

[104] M. L. Riskin and J. G. Kennen, "Evaluating Effects of Potential Changes in Streamflow Regime on Fish and Aquatic-Invertebrate Assemblages in the New Jersey Pinelands," 2010.

Appendices

Appendix A

Terms

Glossary

range of uncertainty also known as hydrological uncertainty, a +/- 30% placed around the observed stream flow ERSS determined as a reasonable range of ERSS..

RCM data dynamically downscaled climate data.

simulations The stream flows or ERSS calculated from Table 3.2, the stream flows were calculated by Daraio (Under Review-b) [1].

Acronyms

-BC Bias Correction for the entire stream flow record.

-BCM Bias Correction on a monthly time scale.

-BCS Bias Correction on a seasonal time scale.

7FDSS Seven Fundamental Daily Stream Flow Statistics.

BC Bias Correction.

CMIP5 Coupled Model Intercomparison Project Phase 5.

ERSS Ecologically Relevant Stream flow Statistics, also, Hydro-Ecological Indices.

FDC Flow Duration Curve.

GCM General Circulation Model.

IPCC Intergovernmental Panel on Climate Change.

MdAPE Median Absolute Percent Error.

MODEL- Stream flows that were determined from the PRMS model and then bias corrected to the observed data.

OBS Observed, recorded stream flow or ERSS for the gauges of interest.

PCA Principal Component Analysis.

PRMS Precipitation Runoff Modelling System.

RCM- Stream flows that had the RCM model driven results bias corrected to the observed data.

RCM Regional Climate Model.

SDR Standardized Data Range.

SIM Simulated Stream Flow from inputting observed climate data into PRMS.

USGS United States Geological Survey.

Appendix B

Definitions of ERSS from EflowStats [35]

- ma1 Mean of the daily mean flow values for the entire flow record
- ma2 Median of the daily mean flow values for the entire flow record
- ma3 Mean (or median - use preference option) of the coefficients of variation (standard deviation/mean) for each year. Compute the coefficient of variation for each year of daily flows. Compute the mean of the annual coefficients of variation
- ma4 Standard deviation of the percentiles of the logs of the entire flow record divided by the mean of percentiles of the logs. Compute the log(10) of the daily flows for the entire record. Compute the 5th, 10th, 15th, 20th, 25th, 30th, 35th, 40th, 45th, 50th, 55th, 60th, 65th, 70th, 75th, 80th, 85th, 90th and 95th percentiles for the logs of the entire flow record. Percentiles are computed by interpolating between the ordered (ascending) logs of the flow values. Compute the standard deviation and mean for the percentile values. Divide the standard deviation by the mean
- ma5 The skewness of the entire flow record is computed as the mean for the entire flow record (ma1) divided by the median (ma2) for the entire flow record
- ma6 Range in daily flows is the ratio of the 10-percent to 90-percent exceedence values for the entire flow record. Compute the 5-percent to 95-percent exceedence values for the entire flow record. Exceedence is computed by interpolating between the ordered (descending) flow values. Divide the 10-percent exceedence by the 90-percent value
- ma7 Range in daily flows is computed in the same way as ma6 except using the 20-percent and 80-percent exceedence values. Divide the 20-percent exceedence value by the 80-percent value

- ma8 Range in daily flows is computed in the same way as ma6 except using the 25-percent and 75-percent exceedence values. Divide the 25-percent exceedence value by the 75-percent value

- ma9 Spread in daily flows is the ratio of the difference between the 90th and 10th percentile of the logs of the flow data to the log of the median of the entire flow record. Compute the log(10) of the daily flows for the entire record. Compute the 5th, 10th, 15th, 20th, 25th, 30th, 35th, 40th, 45th, 50th, 55th, 60th, 65th, 70th, 75th, 80th, 85th, 90th and 95th percentiles for the logs of the entire flow record. Percentiles are computed by interpolating between the ordered (ascending) logs of the flow values. Compute ma9 as (90th-10th)/log10(ma2)

- ma10 Spread in daily flows is computed in the same way as ma9 except using the 20th and 80th percentiles

- ma11 Spread in daily flows is computed in the same way as ma9 except using the 25th and 75th percentiles.

- ma12-23 Requires pref argument to be either "mean" or "median" specifying monthly aggregation function. Default is "mean". Means (or medians - use preference option) of monthly flow values. Compute the means for each month over the entire flow record. For example, ma12 is the mean of all January flow values over the entire record.

- ma24-35 Variability (coefficient of variation) of monthly flow values. Compute the standard deviation for each month in each year over the entire flow record. Divide the standard deviation by the mean for each month. Take the mean (or median - use preference option) of these values for each month across all years.

- ma36-40 Variability and skewness across monthly flows. ma36 - compute the minimum, maximum and mean flows for each month in the entire flow record. ma36 is the maximum monthly flow minus the minimum monthly flow divided by the median monthly flow. ma37 - compute the first (25th percentile) and the third (75th percentile) quartiles. ma37 is the third quartile minus the first quartile divided by the median of the monthly means. ma38 - compute the 10th and 90th percentiles for the monthly means. ma38 is the 90th percentile minus the 10th percentile divided by the median of the monthly means. ma39 - compute the standard deviation for the monthly means. ma39 is the standard deviation times 100 divided by the mean of the monthly means. ma40 - skewness in the monthly flows. ma40 is the mean of the monthly flow means minus the median of the monthly means divided by the median of the monthly means.

- ma41-45 ma41 requires drainArea to be specified. Annual runoff and the variability and skewness across annual flows. ma41 - compute the annual mean daily flows. ma41 is the mean of the annual means divided by the drainage area. ma42 is the maximum annual flow minus the minimum annual flow divided by the median annual flow. ma43 - compute the first (25th percentile) and third (75th percentile) quartiles for the annual means. ma43 is the third quartile minus the first quartile divided by the median of the annual means. ma44 - compute the 10th and 90th percentiles for the annual means. ma44 is the 90th percentile minus the 10th percentile divided by the median of the annual means. ma45 - skewness in the annual flows. ma45 is the mean of the annual flow means minus the median of the annual means divided by the median of the annual means.

- mh1-12 Requires pref argument to be either "mean" or "median" specifying

monthly aggregation function. Default is "mean". Means (or medians - use preference option) of maximum daily flow values for each month. For example, mh1 is the mean of all January maximum flow values over the entire record.

- mh13 variability (coefficient of variation) across minimum monthly flow values. Compute the mean and standard deviation for the maximum monthly flows over the entire flow record. MH13 is the standard deviation times 100 divided by the mean maximum monthly flow for all years.

- ml14 Mean of annual minimum annual flows. ML14 is the mean of the ratios of minimum annual flows to the median flow for each year.

- ml15 Low flow index. ML15 is the mean (or median-Use Preference option) of the ratios of minimum annual flows to the mean flow for each year.

- ml16 Median of annual minimum flows. ML16 is the median of the ratios of minimum annual flows to the median flow for each year.

- ml17 Baseflow 1. Compute the mean annual flows. Compute the minimum of a 7-day moving average flow for each year and divide them by the mean annual flow for that year. ML17 is the mean (or median-Use Preference option) of those ratios.

- ml18 Variability in baseflow 1. Compute the standard deviation for the ratios of minimum 7-day moving average flows to mean annual flows for each year. ML18 is the standard deviation times 100 divided by the mean of the ratios.

- ml19 Baseflow 2. Compute the ratios of the minimum annual flow to mean annual flow for each year. ML19 is the mean (or median-Use Preference option) of these ratios times 100.

- ml20 Baseflow 3. Divide the daily flow record into 5-day blocks. Find the minimum flow for each block. Assign the minimum flow as a base flow for that block if 90 percent of that minimum flow is less than the minimum flows for the blocks on either side. Otherwise, set it to zero. Fill in the zero values using linear interpolation. Compute the total flow for the entire record and the total base flow for the entire record. ML20 is the ratio of total base flow to total flow.

- ml21 Variability across annual minimum flows. Compute the mean and standard deviation for the annual minimum flows. ML21 is the standard deviation times 100 divided by the mean.

- ml22 Specific mean annual minimum flow. ML22 is the mean (or median-Use Preference option) of the annual minimum flows divided by the drainage area.

- mh1-12 Requires pref argument to be either "mean" or "median" specifying monthly aggregation function. Default is "mean". Means (or medians - use preference option) of maximum daily flow values for each month. For example, mh1 is the mean of all January maximum flow values over the entire record.

- mh13 variability (coefficient of variation) across maximum monthly flow values. Compute the mean and standard deviation for the maximum monthly flows over the entire flow record. MH13 is the standard deviation times 100 divided by the mean maximum monthly flow for all years.

- mh14 median of annual maximum flows. Compute the annual maximum flows from monthly maximum flows. Compute the ratio of annual maximum flow to median annual flow for each year. MH14 is the median of these ratios.

- mh15-17 MH15; High flow discharge index. Compute the 1-percent exceedence value for the entire data record. MH15 is the 1-percent exceedence value divided

by the median flow for the entire record. MH16; Compute the 10-percent exceedence value for the entire data record. MH16 is the 10-percent exceedence value divided by the median flow for the entire record. MH17; Compute the 25-percent exceedence value for the entire data record. MH17 is the 25-percent exceedence value divided by the median flow for the entire record.

- mh18 variability across annual maximum flows. Compute the logs (log10) of the maximum annual flows. Find the standard deviation and mean for these values. MH18 is the standard deviation times 100 divided by the mean.

- mh19 the skewness in annual maximum flows (dimensionless-spatial). Use the equation: MH19 numerator = N2 ? sum(qm3)-3N ? sum(qm) ? sum(qm2) + 2 ? (sum(qm))3 denominator = N ? (N-1) ? (N-2) ? stddev3 Where: N = Number of years qm = Log10 (annual maximum flows) stddev = Standard deviation of the annual maximum flows

- mh20 specific mean annual maximum flow. MH20 is the mean (or median-Use Preference option) of the annual maximum flows divided by the drainage area (cubic feet per second/square mile-temporal).

- mh21-27 high flow volume indices. Compute the average volume for flow events above a threshold. Thresholds are equal to the median flow for the entire record for mh21, 3 times the median flow for the entire record for mh22,and 7 times the median flow for the entire record for mh23. Thresholds are equal to the median flow for the entire record for mh24, 3 times the median flow for the entire record for mh25, 7 times the median flow for the entire record for mh26, and the 75th percentile for the entire record for mh27. MH21 through 23 are the average volumes divided by the median flow for the entire record. MH24

through 27 are the average peak flows divided by the median flow for the entire record.

- FL1; Low flood pulse count. Compute the average number of flow events with flows below a threshold equal to the 25th percentile value for the entire flow record. FL1 is the average (or median-Use Preference option) number of events.

- FL2; Variability in low pulse count. Compute the standard deviation in the annual pulse counts for FL1. FL2 is 100 times the standard deviation divided by the mean pulse count.

- FL3; Frequency of low pulse spells. Compute the average number of flow events with flows below a threshold equal to 5 percent of the mean flow value for the entire flow record. FL3 is the average (or median-Use Preference option) number of events.

- fh1 High flood pulse count. Compute the average number of flow events with flows above a threshold equal to the 75th percentile value for the entire flow record. FH1 is the average (or median-Use Preference option) number of events.

- fh2 Variability in high pulse count. Compute the standard deviation in the annual pulse counts for FH1. FH2 is 100 times the standard deviation divided by the mean pulse count (number of events/year-spatial).

- fh3 High flood pulse count. Compute the average number of days per year that the flow is above a threshold equal to three times the median flow for the entire record. FH3 is the mean (or median-Use Preference option) of the annual number of days for all years.

- fh4 High flood pulse count. Compute the average number of days per year that

the flow is above a threshold equal to seven times the median flow for the entire record. FH4 is the mean (or median - Use Preference option) of the annual number of days for all years.

- fh5 Flood frequency. Compute the average number of flow events with flows above a threshold equal to the median flow value for the entire flow record. FH5 is the average (or median - Use Preference option) number of events.

- fh6 Flood frequency. Compute the average number of flow events with flows above a threshold equal to three times the median flow value for the entire flow record. FH6 is the average (or median-Use Preference option) number of events.

- fh7 Flood frequency. Compute the average number of flow events with flows above a threshold equal to seven times the median flow value for the entire flow record. FH7 is the average (or median-Use Preference option) number of events.

- fh8 Flood frequency. Compute the average number of flow events with flows above a threshold equal to 25-percent exceedence value for the entire flow record. FH8 is the average (or median-Use Preference option) number of events.

- fh9 Flood frequency. Compute the average number of flow events with flows above a threshold equal to 75-percent exceedence value for the entire flow record. FH9 is the average (or median-Use Preference option) number of events.

- fh10 Flood frequency. Compute the average number of flow events with flows above a threshold equal to median of the annual minima for the entire flow record. FH10 is the average (or median-Use Preference option) number of events.

- fh11 Flood frequency. Compute the average number of flow events with flows

above a threshold equal to flow corresponding to a 1.67-year recurrence interval. FH11 is the average (or median-Use Preference option) number of events.

- dl1 Annual minimum daily flow. Compute the minimum 1-day average flow for each year. DL1 is the mean (or median-Use Preference option) of these values.

- dl2 Annual minimum of 3-day moving average flow. Compute the minimum of a 3-day moving average flow for each year. DL2 is the mean (or median-Use Preference option) of these values.

- dl3 Annual minimum of 7-day moving average flows. Compute the minimum of a 7-day moving average flow for each year. DL3 is the mean (or median-Use Preference option) of these values.

- dl4 Annual minimum of 30-day moving average flows. Compute the minimum of a 30-day moving average flow for each year. DH4 is the mean (or median-Use Preference option) of these values.

- dl5 Annual minimum of 90-day moving average flows. Compute the minimum of a 90-day moving average flow for each year. DH5 is the mean (or median-Use Preference option) of these values.

- dl6 Variability of annual minimum daily average flow. Compute the standard deviation for the minimum daily average flow. DL6 is 100 times the standard deviation divided by the mean.

- dl7 Variability of annual minimum of 3-day moving average flows. Compute the standard deviation for the minimum 3-day moving averages. DL7 is 100 times the standard deviation divided by the mean.

- dl8 Variability of annual minimum of 7-day moving average flows. Compute the standard deviation for the minimum 7-day moving averages. DL8 is 100 times the standard deviation divided by the mean.

- dl9 Variability of annual minimum of 30-day moving average flows. Compute the standard deviation for the minimum 30-day moving averages. DL9 is 100 times the standard deviation divided by the mean.

- dl10 Variability of annual minimum of 90-day moving average flows. Compute the standard deviation for the minimum 90-day moving averages. DH10 is 100 times the standard deviation divided by the mean.

- dl11 Annual minimum daily flow divided by the median for the entire record. Compute the minimum daily flow for each year. DL11 is the mean of these values divided by the median for the entire record.

- dl12 Annual minimum of 7-day moving average flows divided by the median for the entire record. Compute the minimum of a 7-day moving average flow for each year. DL12 is the mean of these values divided by the median for the entire record.

- dl13 Annual minimum of 30-day moving average flows divided by the median for the entire record. Compute the minimum of a 30-day moving average flow for each year. DL13 is the mean of these values divided by the median for the entire record.

- dl14 Low exceedence flows. Compute the 75-percent exceedence value for the entire flow record. DL14 is the exceedence value divided by the median for the entire record.

- dl15 Low exceedence flows. Compute the 90-percent exceedence value for the entire flow record. DL15 is the exceedence value divided by the median for the entire record.

- dl16 Low flow pulse duration. Compute the average pulse duration for each year for flow events below a threshold equal to the 25th percentile value for the entire flow record. DL16 is the median of the yearly average durations.

- dl17 Variability in low pulse duration. Compute the standard deviation for the yearly average low pulse durations. DL17 is 100 times the standard deviation divided by the mean of the yearly average low pulse durations.

- dl18 Number of zero-flow days. Count the number of zero-flow days for the entire flow record. DL18 is the mean (or median-Use Preference option) annual number of zero flow days.

- dl19 Variability in the number of zero-flow days. Compute the standard deviation for the annual number of zero-flow days. DL19 is 100 times the standard deviation divided by the mean annual number of zero-flow days.

- dl20 Number of zero-flow months. While computing the mean monthly flow values, count the number of months in which there was no flow over the entire flow record.

- dh1 Annual maximum daily flow. Compute the maximum of a 1-day moving average flow for each year. dh1 is the mean (or median-Use Preference option) of these values.

- dh2 Annual maximum of 3-day moving average flows. Compute the maximum of a 3-day moving average flow for each year. dh2 is the mean (or median-Use

Preference option) of these values;

- dh3 Annual maximum of 7-day moving average flows. Compute the maximum of a 7-day moving average flow for each year. dh3 is the mean (or median-Use Preference option) of these values.

- dh4 Annual maximum of 30-day moving average flows. Compute the maximum of a 30-day moving average flow for each year. dh4 is the mean (or median-Use Preference option) of these values.

- dh5 Annual maximum of 90-day moving average flows. Compute the maximum of a 90-day moving average flow for each year. dh5 is the mean (or median-Use Preference option) of these values.

- dh6 Variability of annual maximum daily flows. Compute the standard deviation for the maximum 1-day moving averages. dh6 is 100 times the standard deviation divided by the mean.

- dh7 Variability of annual maximum of 3-day moving average flows. Compute the standard deviation for the maximum 3-day moving averages. dh7 is 100 times the standard deviation divided by the mean.

- dh8 Variability of annual maximum of 7-day moving average flows. Compute the standard deviation for the maximum 7-day moving averages. dh8 is 100 times the standard deviation divided by the mean.

- dh9 Variability of annual maximum of 30-day moving average flows. Compute the standard deviation for the maximum 30-day moving averages. dh9 is 100 times the standard deviation divided by the mean.

- dh10 Variability of annual maximum of 90-day moving average flows. Compute the standard deviation for the maximum 90-day moving averages. dh10 is 100 times the standard deviation divided by the mean.

- dh11 Annual maximum of 1-day moving average flows divided by the median for the entire record. Compute the maximum of a 1-day moving average flow for each year. dh11 is the mean of these values divided by the median for the entire record.

- dh12 Annual maximum of 7-day moving average flows divided by the median for the entire record. Compute the maximum of a 7-day moving average flow for each year. dh12 is the mean of these values divided by the median for the entire record.

- dh13 Annual maximum of 30-day moving average flows divided by the median for the entire record. Compute the maximum of a 30-day moving average flow for each year. dh13 is the mean of these values divided by the median for the entire record.

- dh14 Flood duration. Compute the mean of the mean monthly flow values. Find the 95th percentile for the mean monthly flows. dh14 is the 95th percentile value divided by the mean of the monthly means.

- dh15 High flow pulse duration. Compute the average duration for flow events with flows above a threshold equal to the 75th percentile value for each year in the flow record. dh15 is the median of the yearly average durations.

- dh16 Variability in high flow pulse duration. Compute the standard deviation for the yearly average high pulse durations. dh16 is 100 times the standard deviation divided by the mean of the yearly average high pulse durations.

- dh17 High flow duration. Compute the average duration of flow events with flows above a threshold equal to the median flow value for the entire flow record. dh17 is the mean duration of the events.

- dh18 High flow duration. Compute the average duration of flow events with flows above a threshold equal to three times the median flow value for the entire flow record. dh18 is the mean duration of the events.

- dh19 High flow duration. Compute the average duration of flow events with flows above a threshold equal to seven times the median flow value for the entire flow record. dh19 is the mean duration of the events .

- dh20 High flow duration. Compute the 75th percentile value for the entire flow record. Compute the average duration of flow events with flows above a threshold equal to the 75th percentile value for the median annual flows. dh20 is the average duration of the events.

- dh21 High flow duration. Compute the 25th percentile value for the entire flow record. Compute the average duration of flow events with flows above a threshold equal to the 25th percentile value for the entire set of flows. dh21 is the average duration of the events.

- dh22 Flood interval. Compute the flood threshold as the flow equivalent for a flood recurrence of 1.67 years. Determine the median number of days between flood events for each year. dh22 is the mean (or median-Use Preference option) of the yearly median number of days between flood events.

- dh23 Flood duration. Compute the flood threshold as the flow equivalent for a flood recurrence of 1.67 years. Determine the number of days each year that

the flow remains above the flood threshold. DH23 is the mean (or median-Use Preference option) of the number of flood days for years in which floods occur.

- dh24 Flood-free days. Compute the flood threshold as the flow equivalent for a flood recurrence of 1.67 years. Compute the maximum number of days that the flow is below the threshold for each year. DH24 is the mean (or median-Use Preference option) of the maximum yearly no-flood days.

- ta1; Constancy. Constancy is computed via the formulation of Colwell (see example in Colwell, 1974). A matrix of values is compiled where the columns are 11 flow categories and the rows are 365 days of the year (no leap years) defined as either calendar or water year. February 29th is removed on leap years. The cell values are the number of times that a flow falls into a category on each day. The categories are listed below. The row totals, column totals, and grand total are computed. Using the equations for Shannon information theory parameters, constancy is computed as 1-(uncertainty with respect to state)/log10(number of state)

  log(flow) < .1 x log(mean flow)

  .1 x log(mean flow) <= log(flow) < .25 x log(mean flow)

  .25 x log(mean flow) <= log(flow) < .5 x log(mean flow)

  .5 x log(mean flow) <= log(flow) < .75 x log(mean flow)

  .75 x log(mean flow) <= log(flow) < 1.0 x log(mean flow)

  1.0 x log(mean flow) <= log(flow) < 1.25 x log(mean flow)

  1.25 x log(mean flow) <= log(flow) < 1.5 x log(mean flow)

  1.5 x log(mean flow) <= log(flow) < 1.75 x log(mean flow)

1.75 x log(mean flow) <= log(flow) < 2.0 x log(mean flow)

2.0 x log(mean flow) <= log(flow) < 2.25 x log(mean flow)

log(flow) >= 2.25 x log(mean flow)

- ta2; Predictability. Predictability is computed from the same matrix as constancy (see example in Colwell, 1974). It is computed as: 1- (uncertainty with respect to interaction of time and state - uncertainty with respect to time)/log10(number of state).

- ta3; Seasonal predictability of flooding. Divide years up into 2-month periods (that is, Oct-Nov, Dec-Jan, and so forth). Count the number of flood days (flow events with flows > 1.67-year flood) in each period over the entire flow record. TA3 is the maximum number of flood days in any one period divided by the total number of flood days.

- tl1; Julian date of annual minimum. Determine the Julian date that the minimum flow occurs for each water year. Transform the dates to relative values on a circular scale (radians or degrees). Compute the x and y components for each year and average them across all years. Compute the mean angle as the arc tangent of y-mean divided by x-mean. Transform the resultant angle back to Julian date.

- tl2 Variability in Julian date of annual minima. Compute the coefficient of variation for the mean x and y components and convert to a date.

- tl3 Seasonal predictability of low flow. Divide years up into 2-month periods (that is, Oct-Nov, Dec-Jan, and so forth). Count the number of low flow events (flow events with flows <= 5 year flood threshold) in each period over the entire

flow record. TL3 is the maximum number of low flow events in any one period divided by the total number of low flow events.

- tl4 Seasonal predictability of non-low flow. Compute the number of days that flow is above the 5-year flood threshold as the ratio of number of days to 365 or 366 (leap year) for each year. TL4 is the maximum of the yearly ratios.

- th1 Julian date of annual maximum. Determine the Julian date that the maximum flow occurs for each year. Transform the dates to relative values on a circular scale (radians or degrees). Compute the x and y components for each year and average them across all years. Compute the mean angle as the arc tangent of y-mean divided by x-mean. Transform the resultant angle back to Julian date.

- th2 Variability in Julian date of annual maxima. Compute the coefficient of variation for the mean x and y components and convert to a date.

- th3 Seasonal predictability of nonflooding. Computed as the maximum proportion of a 365-day year that the flow is less than the 1.67-year flood threshold and also occurs in all years. Accumulate nonflood days that span all years. TH3 is maximum length of those flood-free periods divided by 365.

- ra1; Rise rate. Compute the change in flow for days in which the change is positive for the entire flow record. RA1 is the mean (or median-Use Preference option) of these values.

- ra2; Variability in rise rate. Compute the standard deviation for the positive flow changes. RA2 is 100 times the standard deviation divided by the mean.

- ra3; Fall rate. Compute the change in flow for days in which the change is

negative for the entire flow record. RA3 is the mean (or median-Use Preference option) of these values.

- ra4; Variability in fall rate. Compute the standard deviation for the negative flow changes. RA4 is 100 times the standard deviation divided by the mean.

- ra5; Number of day rises. Compute the number of days in which the flow is greater than the previous day. RA5 is the number of positive gain days divided by the total number of days in the flow record.

- ra6; Change of flow. Compute the log of the flows for the entire flow record. Compute the change in log of flow for days in which the change is positive for the entire flow record. RA6 is the median of these values.

- ra7; Change of flow. Compute the log of the flows for the entire flow record. Compute the change in log of flow for days in which the change is negative for the entire flow record. RA7 is the median of these log values.

- ra8; Number of reversals. Compute the number of days in each year when the change in flow from one day to the next changes direction. RA8 is the average (or median - Use Preference option) of the yearly values.

- ra9; Variability in reversals. Compute the standard deviation for the yearly reversal values. RA9 is 100 times the standard deviation divided by the mean.

Appendix C

Value, Standardized Data Ranges and Medians of Selected ERSS in Phase 2

Table 1: ERSS for all regional sites

	ma1	**ma2**	**ma3**	**ma4**	**ma5**	**ma6**	**ma7**	**ma8**	**ma9**
Batsto	117.66	98.70	56.95	9.82	1.19	3.70	2.31	1.93	0.29
Maurice	158.89	138.00	49.50	10.31	1.15	4.24	2.65	2.23	0.29
GreatEgg	85.99	74.00	54.99	11.45	1.16	4.11	2.53	2.10	0.33
Tuckahoe	41.80	31.00	69.54	16.86	1.35	5.33	3.22	2.55	0.49
Mullica	104.91	84.00	68.03	14.55	1.25	6.45	3.47	2.71	0.42
Oswego	84.80	69.00	60.91	11.86	1.23	4.25	2.52	2.10	0.34
Median	95.45	79.00	58.93	11.65	1.21	4.24	2.59	2.17	0.34
Data Range	1.23	1.35	0.34	0.60	0.16	0.65	0.45	0.36	0.60
	ma10	**ma11**	**ma12**	**ma13**	**ma14**	**ma15**	**ma16**	**ma17**	**ma18**
Batsto	0.18	0.14	137.89	142.84	166.36	155.75	127.85	94.33	89.74
Maurice	0.20	0.16	181.23	192.50	223.52	224.20	184.20	145.54	122.98
GreatEgg	0.22	0.17	102.54	105.79	122.96	118.06	95.11	71.62	63.74
Tuckahoe	0.34	0.27	48.99	52.73	67.80	66.95	52.45	38.01	26.45
Mullica	0.28	0.23	135.76	139.95	161.86	151.85	118.86	78.22	68.42
Oswego	0.22	0.18	97.48	100.45	117.67	113.25	96.94	71.58	67.11
Median	0.22	0.17	119.15	122.87	142.41	134.96	107.90	74.92	67.77
Data Range	0.73	0.75	1.11	1.14	1.09	1.17	1.22	1.44	1.42
	ma19	**ma20**	**ma21**	**ma22**	**ma23**	**ma24**	**ma25**	**ma26**	**ma27**
Batsto	96.29	83.96	86.42	104.85	126.91	29.53	28.51	28.98	28.18
Maurice	116.58	107.04	112.45	132.91	165.62	21.71	21.20	20.68	19.34
GreatEgg	60.66	56.62	63.10	76.76	95.95	29.26	28.30	29.26	26.78
Tuckahoe	27.00	22.39	25.51	33.05	41.07	33.72	32.78	38.45	36.00

Mullica	71.12	61.03	67.19	87.53	118.90	31.73	32.13	32.36	33.18
Oswego	72.33	58.76	63.21	78.03	81.62	30.08	28.65	31.02	31.54
Median	71.73	59.89	65.20	82.78	107.42	29.81	28.58	30.14	29.86
Data Range	1.25	1.41	1.33	1.21	1.16	0.40	0.41	0.59	0.56
	ma28	**ma29**	**ma30**	**ma31**	**ma32**	**ma33**	**ma34**	**ma35**	**ma36**
Batsto	27.30	23.11	31.40	35.18	30.76	25.29	22.15	25.82	2.88
Maurice	22.52	25.90	29.70	33.22	32.37	24.87	19.64	21.15	2.80
GreatEgg	26.95	29.03	34.08	34.60	35.64	30.73	23.81	27.80	2.68
Tuckahoe	32.88	37.84	35.18	51.96	42.10	38.07	28.80	30.95	4.85
Mullica	31.83	31.09	40.03	39.83	39.06	33.99	29.81	30.97	3.66
Oswego	33.51	34.92	39.25	43.63	38.37	32.07	28.42	28.41	3.10
Median	29.56	30.06	34.63	37.50	37.00	31.40	26.12	28.10	2.99
Data Range	0.37	0.49	0.30	0.50	0.31	0.42	0.39	0.35	0.72
	ma37	**ma38**	**ma39**	**ma40**	**ma41**	**ma42**	**ma43**	**ma44**	**ma45**
Batsto	0.65	1.17	47.15	0.09	1.74	1.13	0.29	0.59	-0.03
Maurice	0.77	1.37	49.29	0.10	1.42	1.14	0.39	0.82	-0.03
GreatEgg	0.69	1.28	46.93	0.08	1.51	1.06	0.29	0.61	-0.02
Tuckahoe	0.98	1.78	63.41	0.22	1.36	1.18	0.46	0.96	0.03
Mullica	0.89	1.64	59.77	0.13	2.25	1.15	0.34	0.81	-0.02
Oswego	0.71	1.30	50.58	0.11	1.17	1.23	0.35	0.84	0.03
Median	0.74	1.33	49.93	0.10	1.46	1.15	0.34	0.81	-0.02
Data Range	0.45	0.46	0.33	1.35	0.74	0.14	0.49	0.45	-2.77
	ml1	**ml2**	**ml3**	**ml4**	**ml5**	**ml6**	**ml7**	**ml8**	**ml9**
Batsto	90.35	96.84	105.84	103.16	84.47	66.11	57.44	56.47	55.14

Maurice	129.14	141.62	157.20	161.55	124.04	94.22	76.90	69.44	65.87
GreatEgg	66.80	72.45	79.88	80.18	63.37	46.51	38.57	36.15	35.32
Tuckahoe	30.42	34.17	38.78	41.67	31.60	22.22	16.52	14.13	13.89
Mullica	78.88	86.82	92.95	86.64	69.10	46.62	36.34	35.83	32.59
Oswego	60.85	67.03	70.67	69.32	56.51	43.55	37.52	38.16	34.57
Median	72.84	79.63	86.41	83.41	66.24	46.56	38.05	37.16	34.95
Data Range	1.36	1.35	1.37	1.44	1.40	1.55	1.59	1.49	1.49
	ml10	**ml11**	**ml12**	**ml13**	**ml14**	**ml15**	**ml16**	**ml17**	**ml18**
Batsto	59.61	71.39	83.67	36.15	0.43	0.37	0.43	0.42	20.57
Maurice	77.41	94.21	114.39	48.66	0.34	0.32	0.34	0.36	24.64
GreatEgg	42.02	52.00	62.04	40.70	0.38	0.33	0.37	0.35	22.76
Tuckahoe	15.82	22.05	26.21	55.82	0.34	0.28	0.33	0.30	32.27
Mullica	38.92	49.38	67.67	55.09	0.27	0.22	0.27	0.25	29.91
Oswego	39.39	49.14	50.97	41.78	0.38	0.32	0.37	0.36	22.73
Median	40.70	50.69	64.85	45.22	0.36	0.32	0.35	0.36	23.70
Data Range	1.51	1.42	1.36	0.43	0.45	0.46	0.45	0.48	0.49
	ml19	**ml20**	**ml21**	**ml22**	**mh1**	**mh2**	**mh3**	**mh4**	**mh5**
Batsto	37.00	0.75	29.11	0.62	262.67	258.18	302.91	290.35	243.34
Maurice	31.66	0.78	31.56	0.44	282.89	295.74	330.56	330.48	286.08
GreatEgg	33.19	0.74	26.71	0.49	186.25	185.33	214.05	204.48	166.08
Tuckahoe	28.08	0.70	30.35	0.36	100.90	105.16	146.75	133.40	112.76
Mullica	22.26	0.69	35.97	0.49	246.80	262.65	290.79	286.30	228.50
Oswego	32.00	0.70	29.85	0.36	184.65	183.84	214.73	214.65	192.54
Median	31.83	0.72	30.10	0.46	216.52	221.75	252.76	250.48	210.52

Data Range	0.46	0.13	0.31	0.57	0.84	0.86	0.73	0.79	0.82
	mh6	**mh7**	**mh8**	**mh9**	**mh10**	**mh11**	**mh12**	**mh13**	**mh14**
Batsto	160.14	201.22	232.28	191.19	160.98	173.80	219.91	78.57	5.20
Maurice	244.51	233.80	252.95	224.99	184.36	189.55	249.34	68.68	3.20
GreatEgg	130.40	132.32	129.93	126.01	121.24	124.05	169.99	64.06	4.19
Tuckahoe	92.31	60.41	93.58	57.80	59.79	63.59	81.88	88.10	5.59
Mullica	143.38	160.40	163.89	148.50	132.68	151.39	214.00	81.74	4.90
Oswego	152.98	165.28	195.61	142.52	124.25	139.42	149.13	75.76	4.88
Median	148.18	162.84	179.75	145.51	128.46	145.40	192.00	77.16	4.89
Data Range	1.03	1.06	0.89	1.15	0.97	0.87	0.87	0.31	0.49
	mh15	**mh16**	**mh17**	**mh18**	**mh19**	**mh20**	**mh21**	**mh22**	**mh23**
Batsto	4.57	1.97	1.39	8.56	-0.67	8.22	14.05	5.06	3.76
Maurice	3.51	1.99	1.47	8.18	0.01	5.02	15.39	3.49	4.21
GreatEgg	3.95	2.00	1.42	7.04	-0.62	5.90	12.36	3.34	2.48
Tuckahoe	5.71	2.58	1.65	10.00	0.39	7.65	17.39	5.69	6.77
Mullica	4.88	2.38	1.60	8.19	0.09	10.56	18.50	6.10	5.82
Oswego	4.76	2.13	1.46	8.65	-0.35	5.54	11.20	4.91	3.89
Median	4.66	2.06	1.47	8.38	-0.17	6.77	14.72	4.98	4.05
Data Range	0.47	0.30	0.18	0.35	-6.22	0.82	0.50	0.55	1.06
	mh24	**mh25**	**mh26**	**mh27**	**fl1**	**fl2**	**fl3**	**fh1**	**fh2**
Batsto	2.18	4.82	9.19	2.68	5.94	46.93	1.00	9.26	40.16
Maurice	1.79	4.24	9.30	2.32	6.98	49.59	-	7.54	53.34
GreatEgg	1.96	4.19	8.35	2.48	6.56	47.83	-	9.34	38.43
Tuckahoe	2.33	4.80	10.37	3.20	8.43	52.30	3.00	10.94	37.41

Mullica	2.26	4.65	9.80	2.93	5.56	47.19	1.00	8.90	43.09
Oswego	2.02	4.60	8.96	2.66	9.60	48.77	1.00	11.56	42.71
Median	2.10	4.63	9.25	2.67	6.77	48.30	1.00	9.30	41.43
Data Range	0.26	0.14	0.22	0.33	0.60	0.11	3.00	0.43	0.38
	fh3	**fh4**	**fh5**	**fh6**	**fh7**	**fh8**	**fh9**	**fh10**	**fh11**
Batsto	12.08	0.60	9.04	3.18	0.28	9.26	6.04	3.10	0.70
Maurice	7.60	0.26	7.92	1.84	0.10	7.54	7.04	2.72	0.86
GreatEgg	10.48	0.16	9.90	2.86	0.08	9.34	6.62	2.32	0.60
Tuckahoe	25.51	1.57	11.14	6.54	0.71	10.94	8.77	2.46	0.63
Mullica	18.71	0.79	9.06	3.81	0.33	8.90	5.54	2.63	1.02
Oswego	15.28	0.92	12.84	4.10	0.42	11.56	9.98	3.08	0.72
Median	13.68	0.70	9.48	3.50	0.31	9.30	6.83	2.67	0.71
Data Range	1.31	2.03	0.52	1.35	2.07	0.43	0.65	0.29	0.59
	dl1	**dl2**	**dl3**	**dl4**	**dl5**	**dl6**	**dl7**	**dl8**	**dl9**
Batsto	42.14	45.68	47.82	52.84	62.11	29.11	20.06	17.83	20.38
Maurice	48.90	51.92	55.08	64.90	75.93	31.56	30.95	30.00	30.06
GreatEgg	28.04	28.30	29.43	34.69	42.20	26.71	26.65	26.51	27.64
Tuckahoe	10.98	11.32	11.86	13.86	17.50	30.35	31.10	30.41	25.76
Mullica	22.83	24.22	25.67	30.95	40.80	35.97	36.34	35.37	36.23
Oswego	26.22	27.63	29.33	35.00	44.50	29.85	25.90	26.08	26.97
Median	27.13	27.96	29.38	34.85	43.35	30.10	28.80	28.25	27.30
Data Range	1.40	1.45	1.47	1.46	1.35	0.31	0.57	0.62	0.58
	dl10	**dl11**	**dl12**	**dl13**	**dl14**	**dl15**	**dl16**	**dl17**	**dl18**
Batsto	25.27	0.43	0.49	0.54	0.72	0.53	12.73	70.22	-

Maurice	26.48	0.35	0.40	0.47	0.66	0.47	10.85	62.85	-
GreatEgg	25.38	0.38	0.40	0.47	0.68	0.49	12.28	62.46	-
Tuckahoe	21.80	0.35	0.38	0.45	0.65	0.48	9.58	45.32	-
Mullica	38.59	0.27	0.31	0.37	0.59	0.37	17.06	54.60	-
Oswego	27.91	0.38	0.43	0.51	0.70	0.50	7.80	58.69	-
Median	25.93	0.37	0.40	0.47	0.67	0.48	11.56	60.57	-
Data Range	0.65	0.42	0.45	0.36	0.19	0.33	0.80	0.41	NA

	dl19	**dl20**	**dh1**	**dh2**	**dh3**	**dh4**	**dh5**	**dh6**	**dh7**
Batsto	NA	-	557.32	487.77	369.97	227.72	174.57	46.79	44.92
Maurice	NA	-	562.56	515.77	427.41	293.17	236.91	53.21	50.38
GreatEgg	NA	-	336.66	307.51	243.45	162.17	127.77	37.64	36.14
Tuckahoe	NA	-	235.60	195.55	140.47	88.94	69.27	65.09	62.09
Mullica	NA	-	493.08	447.54	359.06	228.03	172.16	56.08	52.69
Oswego	NA	-	401.74	363.21	274.54	166.45	126.58	47.87	47.33
Median	NA	-	447.41	405.37	316.80	197.09	149.97	50.54	48.86
Data Range	NA	NA	0.73	0.79	0.91	1.04	1.12	0.54	0.53

	dh8	**dh9**	**dh10**	**dh11**	**dh12**	**dh13**	**dh14**	**dh15**	**dh16**
Batsto	40.62	31.99	29.06	5.65	3.75	2.31	1.97	8.53	56.96
Maurice	40.07	31.94	30.43	4.08	3.10	2.12	1.95	9.65	99.93
GreatEgg	32.24	28.47	26.49	4.55	3.29	2.19	1.89	8.54	55.65
Tuckahoe	51.52	44.76	42.36	7.60	4.53	2.87	2.30	7.67	65.57
Mullica	42.61	35.38	31.93	5.87	4.28	2.72	2.21	8.74	52.86
Oswego	42.09	34.28	32.60	5.82	3.98	2.41	1.92	6.59	62.53
Median	41.35	33.13	31.18	5.73	3.86	2.36	1.96	8.53	59.75

Data Range	0.47	0.49	0.51	0.61	0.37	0.32	0.21	0.36	0.79
	dh17	**dh18**	**dh19**	**dh20**	**dh21**	**dh22**	**dh23**	**dh24**	**ta1**
Batsto	20.75	3.85	2.14	10.00	49.13	272.17	0.94	319.00	0.69
Maurice	23.75	4.13	2.60	12.26	41.73	257.27	1.26	307.50	0.67
GreatEgg	18.70	3.69	2.00	9.70	44.12	276.38	0.88	316.92	0.63
Tuckahoe	16.47	3.90	2.20	8.31	32.09	284.70	0.91	316.51	0.51
Mullica	20.58	4.96	2.38	10.25	54.11	247.28	1.52	295.44	0.56
Oswego	14.44	3.75	2.19	7.93	28.56	271.96	1.28	317.74	0.64
Median	19.64	3.87	2.20	9.85	42.93	272.06	1.10	316.72	0.63
Data Range	0.47	0.33	0.27	0.44	0.60	0.14	0.58	0.07	0.28
	ta2	**ta3**	**tl1**	**tl2**	**tl3**	**tl4**	**th1**	**th2**	**th3**
Batsto	74.04	0.12	245.00	41.25	0.01	0.03	88.31	73.63	0.11
Maurice	72.45	0.09	250.00	31.62	0.01	0.04	80.62	68.85	0.20
GreatEgg	69.57	0.12	247.00	32.35	0.01	0.03	65.67	71.58	0.13
Tuckahoe	61.01	0.15	247.00	30.12	0.01	0.04	103.43	67.18	0.31
Mullica	64.12	0.08	256.00	34.81	0.01	0.04	86.52	69.29	0.12
Oswego	68.16	0.11	246.00	38.83	0.01	0.04	121.30	73.37	0.11
Median	68.87	0.11	247.00	33.58	0.01	0.04	87.42	70.44	0.12
Data Range	0.19	0.69	0.04	0.33	1.00	0.43	0.64	0.09	1.64
	ra1	**ra2**	**ra3**	**ra4**	**ra5**	**ra6**	**ra7**	**ra8**	**ra9**
Batsto	18.53	215.85	10.37	191.09	0.32	0.07	0.05	90.08	13.67
Maurice	19.15	181.65	10.41	179.02	0.32	0.06	0.04	90.64	11.37
GreatEgg	13.77	153.31	7.18	149.64	0.30	0.09	0.05	75.58	10.60
Tuckahoe	12.10	213.09	5.54	199.66	0.27	0.13	0.07	97.23	7.62

Mullica	17.49	198.65	10.09	182.02	0.34	0.08	0.05	98.04	11.73
Oswego	17.40	184.45	9.10	160.84	0.31	0.10	0.07	109.32	11.07
Median	17.44	191.55	9.59	180.52	0.32	0.09	0.05	93.93	11.22
Data Range	0.40	0.33	0.51	0.28	0.22	0.82	0.65	0.36	0.54

Table 2: ERSS for Batsto SIM, SIM-BC, SIM-BCS, SIM-BCM

	ma7	**ma26**	**ml7**	**ml21**	**mh16**	**mh21**	**fl1**	**fl3**	**fh1**	**fh3**	**dl1**	**dl15**	**dh11**
SIM UC	2.035	19.391	76.755	24.16	1.724	7.854	8.18	0	10.02	3.26	50.47	0.585	3.845
SIM BC	2.479	25.082	68.841	30.782	2.005	11.163	8.18	0	10.02	9.4	39.96	0.504	5.842
SIM BCS	2.403	18.84	57.522	32.487	1.905	10.36	7.82	0	9.84	5.42	37.254	0.501	4.436
SIM BCM	2.416	20.928	55.737	27.406	1.899	10.326	7.56	0	9.64	5.98	36.576	0.487	4.109
OBS Value	2.308	28.984	57.436	29.111	1.966	14.052	5.94	1	9.26	12.08	42.138	0.531	5.647

	dh24	**ta2**	**ta3**	**tl1**	**tl3**	**th1**	**th2**	**ra5**	**ra7**
SIM UC	324.3	71.173	0.141	253	0.008	303.173	73.889	0.291	0.031
SIM BC	324.3	67.542	0.141	253	0.008	303.173	73.889	0.291	0.04
SIM BCS	317.92	70.32	0.161	249	0.006	140.474	75.736	0.294	0.036
SIM BCM	312.36	70.46	0.231	248	0.006	81.755	73.494	0.299	0.035
OBS Value	319	74.04	0.118	245	0.006	88.314	73.63	0.322	0.045

Table 3: ERSS for Maurice SIM, SIM-BC, SIM-BCS, SIM-BCM

	ma7	**ma26**	**ml7**	**ml21**	**mh16**	**mh21**	**fl1**	**fl3**	**fh1**	**fh3**	**dl1**	**dl15**	**dh11**
SIM UC	2.402	27.27	88.307	28.857	1.88	6.14	12.12	0	15.46	3.68	52.288	0.524	4.131
SIM BC	2.572	29.585	89.527	31.08	1.976	6.828	12.12	0	15.46	5.96	50.73	0.498	4.653
SIM BCS	2.693	25.097	75.18	31.525	1.977	7.48	12.16	0	14.34	4.8	45.245	0.471	4.252
SIM BCM	2.708	26.241	72.907	30.948	1.981	7.654	11.74	0	14.14	4.78	46.065	0.46	4.187
OBS Value	2.651	20.684	76.9	31.562	1.986	15.392	6.98	0	7.54	7.6	48.904	0.469	4.077

	dh24	**ta2**	**ta3**	**tl1**	**tl3**	**th1**	**th2**	**ra5**	**ra7**
SIM UC	319.18	70.67	0.115	287	0.008	53.654	81.124	0.261	0.039
SIM BC	319.18	69.675	0.115	287	0.008	53.654	81.124	0.261	0.042
SIM BCS	314.8	71.32	0.102	255	0.006	98.17	69.799	0.265	0.041
SIM BCM	315.9	71.556	0.095	250	0.008	93.517	65.656	0.267	0.041
OBS Value	307.5	72.45	0.09	250	0.006	80.622	68.854	0.318	0.04

Table 4: Batsto Watershed MODEL-BC ERSS compared to Observed

	ma3	**ma14**	**ma25**	**ml2**	**ml3**	**ml17**	**mh12**	**mh18**	**mh27**	**fl1**	**fl2**	**fh1**	**fh4**
MODEL-BC Median	41.98	131.38	21.96	94.51	93.39	0.45	204.15	8.14	1.88	9.98	50.16	10.98	0.16
MODEL-BC Data Range	0.27	0.15	0.27	0.12	0.17	0.16	0.48	0.63	0.19	0.29	0.52	0.26	2.88
OBS Value	56.95	166.36	28.51	96.84	105.84	0.42	219.91	8.56	2.68	5.94	46.93	9.26	0.60
OBS Median Value	58.93	142.41	28.58	79.63	86.41	0.36	192.00	8.38	2.67	6.77	48.30	9.30	0.70
OBS Data Range	0.34	1.09	0.41	1.35	1.37	0.48	0.87	0.35	0.33	0.60	0.11	0.43	2.03
	fh6	**dl8**	**dl11**	**dl15**	**dh5**	**dh7**	**dh14**	**ta2**	**ta3**	**tl1**	**tl2**	**th2**	**ra1**
MODEL-BC Median	1.25	24.44	0.47	0.60	161.14	51.33	1.83	71.91	0.17	283.00	60.88	73.62	14.62
MODEL-BC Data Range	0.69	0.53	0.15	0.14	0.22	1.26	0.16	0.03	1.19	0.18	0.32	0.24	0.19
OBS Value	3.18	17.83	0.43	0.53	174.57	44.92	1.97	74.04	0.12	245.00	41.25	73.63	18.53
OBS Median Value	3.50	28.25	0.37	0.48	149.97	48.86	1.96	68.87	0.11	247.00	33.58	70.44	17.44
OBS Data Range	1.35	0.62	0.42	0.33	1.12	0.53	0.21	0.19	0.69	0.04	0.33	0.09	0.40
	ra2	**ra8**											
MODEL-BC Median	163.60	98.55											
MODEL-BC Data Range	0.87	0.11											
OBS Value	215.85	90.08											
OBS Median Value	191.55	93.93											
OBS Data Range	0.33	0.36											

Table 5: Batsto Watershed MODEL-BCS ERSS Compared to Observed

	ma2	**ma6**	**ma14**	**ma40**	**ml3**	**ml13**	**ml16**	**ml19**	**mh16**	**mh18**	**mh24**	**fl1**	**fl2**
MODEL-BCS Median	101.00	3.13	150.72	0.09	116.90	44.25	0.39	36.74	1.77	6.85	1.46	9.21	43.03
MODEL-BCS Data Range	0.08	0.19	0.11	0.80	0.13	0.18	0.24	0.17	0.10	0.73	0.12	0.29	0.42
OBS Value	98.70	3.70	166.36	0.09	105.84	36.15	0.43	37.00	1.97	8.56	2.18	5.94	46.93
OBS Median Value	79.00	4.24	142.41	0.10	86.41	45.22	0.35	31.83	2.06	8.38	2.10	6.77	48.30
OBS Data Range	1.35	0.65	1.09	1.35	1.37	0.43	0.45	0.46	0.30	0.35	0.26	0.60	0.11
	fh1	**fh5**	**fh7**	**dl5**	**dl8**	**dl13**	**dl15**	**dh3**	**dh8**	**dh14**	**dh23**	**ta2**	**ta3**
MODEL-BCS Median	9.81	11.94	0.04	63.96	26.09	0.52	0.56	241.90	34.91	1.80	1.59	75.33	0.18
MODEL-BCS Data Range	0.23	0.26	3.00	0.12	0.74	0.20	0.14	0.28	1.24	0.14	1.30	0.05	1.26
OBS Value	9.26	9.04	0.28	62.11	17.83	0.54	0.53	369.97	40.62	1.97	0.94	74.04	0.12
OBS Median Value	9.30	9.48	0.31	43.35	28.25	0.47	0.48	316.80	41.35	1.96	1.10	68.87	0.11
OBS Data Range	0.43	0.52	2.07	1.35	0.62	0.36	0.33	0.91	0.47	0.21	0.58	0.19	0.69
	tl2	**th1**	**th2**	**th3**	**ra1**	**ra2**	**ra4**	**ra9**					
MODEL-BCS Median	34.56	52.72	66.66	0.15	12.73	140.24	150.15	7.44					
MODEL-BCS Data Range	0.47	1.39	0.46	1.21	0.15	0.62	0.84	0.36					
OBS Value	41.25	88.31	73.63	0.11	18.53	215.85	191.09	13.67					
OBS Median Value	33.58	87.42	70.44	0.12	17.44	191.55	180.52	11.22					
OBS Data Range	0.33	0.64	0.09	1.64	0.40	0.33	0.28	0.54					

Table 6: Batsto Watershed MODEL-BCM ERSS Compared to Observed

	ma3	**ma5**	**ma14**	**ma20**	**ma36**	**ml2**	**ml3**	**ml10**	**ml13**	**ml15**	**mh2**	**mh16**
MODEL-BCM Median	41.89	1.11	166.94	72.53	3.13	116.16	125.76	53.01	44.87	0.37	202.12	1.79
MODEL-BCM Data Range	0.17	0.05	0.12	0.18	0.52	0.09	0.14	0.18	0.18	0.16	0.19	0.11
OBS Value	56.95	1.19	166.36	83.96	2.88	96.84	105.84	59.61	36.15	0.37	258.18	1.97
OBS Median Value	58.93	1.21	142.41	59.89	2.99	79.63	86.41	40.70	45.22	0.32	221.75	2.06
OBS Data Range	0.34	0.16	1.09	1.41	0.72	1.35	1.37	1.51	0.43	0.46	0.86	0.30
	mh17	**mh22**	**mh24**	**fl1**	**fh1**	**fh4**	**fh5**	**fh6**	**fh9**	**dl5**	**dl8**	**dl11**
MODEL-BCM Median	1.36	2.26	1.45	8.77	9.12	0.04	11.04	0.84	8.65	61.64	24.86	0.40
MODEL-BCM Data Range	0.08	1.93	0.12	0.30	0.31	5.00	0.28	1.05	0.33	0.13	0.64	0.17
OBS Value	1.39	5.06	2.18	5.94	9.26	0.60	9.04	3.18	6.04	62.11	17.83	0.43
OBS Median Value	1.47	4.98	2.10	6.77	9.30	0.70	9.48	3.50	6.83	43.35	28.25	0.37
OBS Data Range	0.18	0.55	0.26	0.60	0.43	2.03	0.52	1.35	0.65	1.35	0.62	0.42
	dl14	**dh3**	**dh8**	**dh18**	**dh20**	**dh23**	**ta2**	**ta3**	**tl1**	**tl2**	**th1**	**th2**
MODEL-BCM Median	0.73	244.57	33.11	3.24	10.03	1.62	76.33	0.21	261.00	37.73	66.95	62.37
MODEL-BCM Data Range	0.07	0.25	0.70	1.21	0.33	1.28	0.06	1.00	0.07	0.43	0.81	0.38
OBS Value	0.72	369.97	40.62	3.85	10.00	0.94	74.04	0.12	245.00	41.25	88.31	73.63
OBS Median Value	0.67	316.80	41.35	3.87	9.85	1.10	68.87	0.11	247.00	33.58	87.42	70.44
OBS Data Range	0.19	0.91	0.47	0.33	0.44	0.58	0.19	0.69	0.04	0.33	0.64	0.09
	ra3	**ra4**	**ra8**	**ra9**								
MODEL-BCM Median	6.24	140.37	101.96	7.49								
MODEL-BCM Data Range	0.11	0.74	0.10	0.36								
OBS Value	10.37	191.09	90.08	13.67								
OBS Median Value	9.59	180.52	93.93	11.22								
OBS Data Range	0.51	0.28	0.36	0.54								

Table 7: Batsto Watershed RCM-BC ERSS Compared to Observed

	ma3	**ma4**	**ma38**	**ma39**	**ml1**	**ml9**	**ml15**	**ml21**	**mh13**	**mh15**	**mh20**	**mh21**
RCM-BC Median	53.87	10.30	1.31	55.00	89.02	65.29	0.33	29.23	83.59	4.14	7.49	9.67
RCM-BC Data Range	0.19	0.19	0.28	0.16	0.22	0.22	0.28	0.50	0.77	0.25	0.40	0.38
OBS Value	56.95	9.82	1.17	47.15	90.35	55.14	0.37	29.11	78.57	4.57	8.22	14.05
OBS Median Value	58.93	11.65	1.33	49.93	72.84	34.95	0.32	30.10	77.16	4.66	6.77	14.72
OBS Data Range	0.34	0.60	0.46	0.33	1.36	1.49	0.46	0.31	0.31	0.47	0.82	0.50
	fl1	**fl2**	**fh1**	**fh3**	**fh4**	**fh6**	**dl1**	**dl7**	**dl9**	**dl16**	**dh6**	**dh11**
RCM-BC Median	9.97	50.37	10.98	11.39	0.60	2.32	38.01	29.34	28.87	8.27	73.36	5.29
RCM-BC Data Range	0.28	0.53	0.25	0.65	1.23	0.67	0.21	0.52	0.45	0.41	1.38	0.43
OBS Value	5.94	46.93	9.26	12.08	0.60	3.18	42.14	20.06	20.38	12.73	46.79	5.65
OBS Median Value	6.77	48.30	9.30	13.68	0.70	3.50	27.13	28.80	27.30	11.56	50.54	5.73
OBS Data Range	0.60	0.11	0.43	1.31	2.03	1.35	1.40	0.57	0.58	0.80	0.54	0.61
	dh18	**dh20**	**ta2**	**ta3**	**tl1**	**tl2**	**th1**	**th2**	**th3**	**ra1**	**ra4**	**ra8**
RCM-BC Median	4.72	8.42	69.21	0.17	283.00	60.80	315.69	73.62	0.21	19.07	224.49	98.46
RCM-BC Data Range	0.64	0.25	0.05	1.19	0.18	0.33	1.14	0.24	1.11	0.29	1.18	0.11
OBS Value	3.85	10.00	74.04	0.12	245.00	41.25	88.31	73.63	0.11	18.53	191.09	90.08
OBS Median Value	3.87	9.85	68.87	0.11	247.00	33.58	87.42	70.44	0.12	17.44	180.52	93.93
OBS Data Range	0.33	0.44	0.19	0.69	0.04	0.33	0.64	0.09	1.64	0.40	0.28	0.36

Table 8: Batsto Watershed RCM-BCS ERSS Compared to Observed

	ma3	**ma16**	**ma31**	**ma38**	**ma42**	**ml5**	**ml13**	**ml19**	**ml21**	**mh6**	**mh9**	**mh13**
RCM-BCS Median	48.99	109.35	32.68	1.26	1.11	74.83	50.76	30.18	31.52	173.90	170.69	67.93
RCM-BCS Data Range	0.14	0.10	0.37	0.19	0.90	0.15	0.15	0.20	0.60	0.27	0.55	0.82
OBS Value	56.95	127.85	35.18	1.17	1.13	84.47	36.15	37.00	29.11	160.14	191.19	78.57
OBS Median Value	58.93	107.90	37.50	1.33	1.15	66.24	45.22	31.83	30.10	148.18	145.51	77.16
OBS Data Range	0.34	1.22	0.50	0.46	0.14	1.40	0.43	0.46	0.31	1.03	1.15	0.31
	mh15	**mh21**	**fl1**	**fl2**	**fh1**	**fh3**	**fh4**	**fh9**	**fh11**	**dl5**	**dl8**	**dl11**
RCM-BCS Median	3.42	8.62	9.67	44.87	10.51	6.53	0.22	9.55	0.71	62.65	31.70	0.34
RCM-BCS Data Range	0.29	0.41	0.35	0.39	0.27	0.81	1.82	0.35	0.68	0.13	0.54	0.20
OBS Value	4.57	14.05	5.94	46.93	9.26	12.08	0.60	6.04	0.70	62.11	17.83	0.43
OBS Median Value	4.66	14.72	6.77	48.30	9.30	13.68	0.70	6.83	0.71	43.35	28.25	0.37
OBS Data Range	0.47	0.50	0.60	0.11	0.43	1.31	2.03	0.65	0.59	1.35	0.62	0.42
	dl13	**dh7**	**dh10**	**dh16**	**dh20**	**dh21**	**ta2**	**ta3**	**tl1**	**tl2**	**tl4**	**th2**
RCM-BCS Median	0.48	55.59	30.96	71.45	8.72	29.68	70.70	0.18	257.50	38.97	0.06	75.10
RCM-BCS Data Range	0.17	1.29	0.50	1.25	0.29	0.40	0.04	1.10	0.09	0.54	3.14	0.19
OBS Value	0.54	44.92	29.06	56.96	10.00	49.13	74.04	0.12	245.00	41.25	0.03	73.63
OBS Median Value	0.47	48.86	31.18	59.75	9.85	42.93	68.87	0.11	247.00	33.58	0.04	70.44
OBS Data Range	0.36	0.53	0.51	0.79	0.44	0.60	0.19	0.69	0.04	0.33	0.43	0.09
	th3	**ra1**	**ra4**	**ra8**	**ra9**							
RCM-BCS Median	0.15	16.89	183.50	100.53	7.46							
RCM-BCS Data Range	1.25	0.24	1.23	0.10	0.35							
OBS Value	0.11	18.53	191.09	90.08	13.67							
OBS Median Value	0.12	17.44	180.52	93.93	11.22							
OBS Data Range	1.64	0.40	0.28	0.36	0.54							

Table 9: Batsto Watershed RCM-BCM ERSS Compared to Observed

	ma3	**ma4**	**ma24**	**ma33**	**ma40**	**ml1**	**ml9**	**ml12**	**ml13**	**ml14**	**mh9**	**mh13**
RCM-BCM Median	49.31	10.15	20.85	29.12	0.12	98.66	51.72	86.08	50.43	0.35	153.77	62.97
RCM-BCM Data Range	0.12	0.07	0.31	0.42	0.82	0.13	0.18	0.16	0.13	0.16	0.27	0.43
OBS Value	56.95	9.82	29.53	25.29	0.09	90.35	55.14	83.67	36.15	0.43	191.19	78.57
OBS Median Value	58.93	11.65	29.81	31.40	0.10	72.84	34.95	64.85	45.22	0.36	145.51	77.16
OBS Data Range	0.34	0.60	0.40	0.42	1.35	1.36	1.49	1.36	0.43	0.45	1.15	0.31
	mh16	**mh21**	**mh27**	**fl1**	**fl2**	**fh1**	**fh4**	**fh6**	**fh9**	**dl8**	**dl10**	**dl11**
RCM-BCM Median	1.96	9.12	2.06	9.31	44.82	10.19	0.18	1.85	9.45	29.32	26.24	0.35
RCM-BCM Data Range	0.09	0.39	0.10	0.33	0.50	0.34	1.89	0.39	0.31	0.46	0.47	0.18
OBS Value	1.97	14.05	2.68	5.94	46.93	9.26	0.60	3.18	6.04	17.83	25.27	0.43
OBS Median Value	2.06	14.72	2.67	6.77	48.30	9.30	0.70	3.50	6.83	28.25	25.93	0.37
OBS Data Range	0.30	0.50	0.33	0.60	0.11	0.43	2.03	1.35	0.65	0.62	0.65	0.42
	dl15	**dl16**	**dh7**	**dh10**	**dh11**	**dh20**	**dh21**	**ta2**	**ta3**	**tl1**	**tl2**	**th1**
RCM-BCM Median	0.51	9.08	48.42	30.35	4.11	9.02	30.50	71.25	0.20	251.00	41.27	74.10
RCM-BCM Data Range	0.10	0.36	0.95	0.42	0.30	0.37	0.34	0.03	1.29	0.11	0.38	1.34
OBS Value	0.53	12.73	44.92	29.06	5.65	10.00	49.13	74.04	0.12	245.00	41.25	88.31
OBS Median Value	0.48	11.56	48.86	31.18	5.73	9.85	42.93	68.87	0.11	247.00	33.58	87.42
OBS Data Range	0.33	0.80	0.53	0.51	0.61	0.44	0.60	0.19	0.69	0.04	0.33	0.64
	th2	**th3**	**ra1**	**ra4**	**ra8**							
RCM-BCM Median	71.98	0.12	16.73	162.74	101.70							
RCM-BCM Data Range	0.18	1.25	0.20	0.65	0.10							
OBS Value	73.63	0.11	18.53	191.09	90.08							
OBS Median Value	70.44	0.12	17.44	180.52	93.93							
OBS Data Range	0.09	1.64	0.40	0.28	0.36							

Table 10: Maurice Watershed MODEL-BC ERSS Compared to Observed

	ma2	**ma3**	**ma40**	**ma44**	**ml5**	**ml6**	**ml17**	**ml21**	**mh3**	**mh7**	**mh9**	**mh21**
MODEL-BC Median	135.44	40.63	0.06	0.47	113.74	102.02	0.44	23.39	322.75	232.18	256.13	4.11
MODEL-BC Data Range	0.35	0.14	1.24	0.53	0.42	0.36	0.17	0.54	0.50	0.46	0.53	0.68
OBS Value	138.00	49.50	0.10	0.82	124.04	94.22	0.36	31.56	330.56	233.80	224.99	15.39
OBS Median Value	79.00	58.93	0.10	0.81	66.24	46.56	0.36	30.10	252.76	162.84	145.51	14.72
OBS Data Range	1.35	0.34	1.35	0.45	1.40	1.55	0.48	0.31	0.73	1.06	1.15	0.50
	fl1	**fl2**	**fh1**	**fh4**	**fh5**	**fh9**	**dl1**	**dl10**	**dl11**	**dl16**	**dh9**	**dh10**
MODEL-BC Median	14.90	47.62	18.61	-	21.48	15.24	58.33	20.41	0.43	5.79	24.90	23.10
MODEL-BC Data Range	0.46	0.48	0.49	Inf	0.44	0.44	0.27	0.58	0.21	0.47	0.67	0.58
OBS Value	6.98	49.59	7.54	0.26	7.92	7.04	48.90	26.48	0.35	10.85	31.94	30.43
OBS Median Value	6.77	48.30	9.30	0.70	9.48	6.83	27.13	25.93	0.37	11.56	33.13	31.18
OBS Data Range	0.60	0.11	0.43	2.03	0.52	0.65	1.40	0.65	0.42	0.80	0.49	0.51
	dh12	**dh20**	**ta2**	**tl1**	**tl2**	**th2**	**th3**	**ra1**	**ra3**	**ra4**	**ra8**	
MODEL-BC Median	2.29	4.93	73.72	291.50	49.45	71.86	0.18	31.99	15.02	125.95	132.97	
MODEL-BC Data Range	0.21	0.66	0.03	0.12	0.54	0.26	1.41	0.67	0.59	0.22	0.32	
OBS Value	3.10	12.26	72.45	250.00	31.62	68.85	0.20	19.15	10.41	179.02	90.64	
OBS Median Value	3.86	9.85	68.87	247.00	33.58	70.44	0.12	17.44	9.59	180.52	93.93	
OBS Data Range	0.37	0.44	0.19	0.04	0.33	0.09	1.64	0.40	0.51	0.28	0.36	

Table 11: Maurice Watershed MODEL-BCS ERSS Compared to Observed

	ma3	**ma5**	**ma14**	**ma44**	**ml5**	**ml10**	**ml19**	**ml21**	**mh3**	**mh16**	**mh20**	**fl1**
MODEL-BCS Median	42.84	1.11	225.78	0.44	118.43	74.39	34.74	23.94	339.66	1.81	3.85	13.48
MODEL-BCS Data Range	0.11	0.05	0.11	0.53	0.11	0.13	0.16	0.72	0.14	0.11	0.30	0.27
OBS Value	49.50	1.15	223.52	0.82	124.04	77.41	31.66	31.56	330.56	1.99	5.02	6.98
OBS Median Value	58.93	1.21	142.41	0.81	66.24	40.70	31.83	30.10	252.76	2.06	6.77	6.77
OBS Data Range	0.34	0.16	1.09	0.45	1.40	1.51	0.46	0.31	0.73	0.30	0.82	0.60
	fl2	**fh1**	**fh3**	**fh5**	**dl7**	**dl8**	**dl12**	**dl15**	**dh2**	**dh5**	**dh9**	**dh24**
MODEL-BCS Median	42.14	16.06	1.86	18.46	24.27	24.90	0.42	0.54	370.27	223.23	22.86	308.12
MODEL-BCS Data Range	0.43	0.28	1.05	0.26	0.69	0.66	0.16	0.14	0.25	0.12	0.42	0.05
OBS Value	49.59	7.54	7.60	7.92	30.95	30.00	0.40	0.47	515.77	236.91	31.94	307.50
OBS Median Value	48.30	9.30	13.68	9.48	28.80	28.25	0.40	0.48	405.37	149.97	33.13	316.72
OBS Data Range	0.11	0.43	1.31	0.52	0.57	0.62	0.45	0.33	0.79	1.12	0.49	0.07
	ta2	**tl2**	**th2**	**th3**	**ra1**	**ra4**						
MODEL-BCS Median	76.78	32.68	59.98	0.21	30.04	121.11						
MODEL-BCS Data Range	0.04	0.58	0.40	1.25	0.15	0.19						
OBS Value	72.45	31.62	68.85	0.20	19.15	179.02						
OBS Median Value	68.87	33.58	70.44	0.12	17.44	180.52						
OBS Data Range	0.19	0.33	0.09	1.64	0.40	0.28						

Table 12: Maurice Watershed MODEL-BCM ERSS Compared to Observed

	ma3	**ma5**	**ma41**	**ma45**	**ml5**	**ml8**	**ml15**	**ml21**	**mh3**	**mh16**	**mh20**	**fl1**
MODEL-BCM Median	43.57	1.10	1.37	0.01	130.79	68.81	0.35	22.82	349.07	1.82	3.82	13.20
MODEL-BCM Data Range	0.11	0.05	0.10	7.70	0.11	0.14	0.15	0.61	0.15	0.10	0.30	0.27
OBS Value	49.50	1.15	1.42	- 0.03	124.04	69.44	0.32	31.56	330.56	1.99	5.02	6.98
OBS Median Value	58.93	1.21	1.46	- 0.02	66.24	37.16	0.32	30.10	252.76	2.06	6.77	6.77
OBS Data Range	0.34	0.16	0.74	- 2.77	1.40	1.49	0.46	0.31	0.73	0.30	0.82	0.60
	fl2	**fh1**	**fh3**	**fh5**	**fh6**	**dl5**	**dl8**	**dl11**	**dl12**	**dh5**	**dh7**	**dh13**
MODEL-BCM Median	39.69	15.42	1.70	17.32	0.94	82.83	23.18	0.38	0.42	227.22	26.62	1.91
MODEL-BCM Data Range	0.50	0.29	1.25	0.23	1.02	0.13	0.61	0.16	0.17	0.12	0.89	0.13
OBS Value	49.59	7.54	7.60	7.92	1.84	75.93	30.00	0.35	0.40	236.91	50.38	2.12
OBS Median Value	48.30	9.30	13.68	9.48	3.50	43.35	28.25	0.37	0.40	149.97	48.86	2.36
OBS Data Range	0.11	0.43	1.31	0.52	1.35	1.35	0.62	0.42	0.45	1.12	0.53	0.32
	dh20	**ta2**	**tl1**	**tl2**	**th1**	**th2**	**th3**	**ra2**	**ra3**	**ra8**		
MODEL-BCM Median	5.95	78.00	260.00	35.81	68.89	56.91	0.21	125.03	13.96	134.42		
MODEL-BCM Data Range	0.32	0.05	0.08	0.44	0.69	0.40	1.10	0.17	0.07	0.11		
OBS Value	12.26	72.45	250.00	31.62	80.62	68.85	0.20	181.65	10.41	90.64		
OBS Median Value	9.85	68.87	247.00	33.58	87.42	70.44	0.12	191.55	9.59	93.93		
OBS Data Range	0.44	0.19	0.04	0.33	0.64	0.09	1.64	0.33	0.51	0.36		

Table 13: Maurice Watershed RCM-BC ERSS Compared to Observed

	ma1	**ma2**	**ma20**	**ma39**	**ma43**	**ml13**	**ml15**	**ml17**	**ml21**	**mh15**	**mh18**	**mh20**	**mh21**
RCM-BC Median	158.81	134.55	131.02	46.90	0.32	50.48	0.29	0.33	30.50	3.66	5.41	5.69	5.93
RCM-BC Data Range	0.27	0.29	0.30	0.22	0.65	0.22	0.26	0.24	0.66	0.22	0.73	0.30	0.77
OBS Value	158.89	138.00	107.04	49.29	0.39	48.66	0.32	0.36	31.56	3.51	8.18	5.02	15.39
OBS Median Value	95.45	79.00	59.89	49.93	0.34	45.22	0.32	0.36	30.10	4.66	8.38	6.77	14.72
OBS Data Range	1.23	1.35	1.41	0.33	0.49	0.43	0.46	0.48	0.31	0.47	0.35	0.82	0.50
	fl1	**fl2**	**fh3**	**fh6**	**fh7**	**fh9**	**dl9**	**dl10**	**dl11**	**dl13**	**dl14**	**dh1**	**dh6**
RCM-BC Median	14.89	47.65	9.01	4.57	0.14	15.22	29.73	26.03	0.34	0.50	0.69	637.55	39.49
RCM-BC Data Range	0.46	0.47	0.78	0.68	1.71	0.45	0.58	0.55	0.24	0.24	0.08	0.30	1.51
OBS Value	6.98	49.59	7.60	1.84	0.10	7.04	30.06	26.48	0.35	0.47	0.66	562.56	53.21
OBS Median Value	6.77	48.30	13.68	3.50	0.31	6.83	27.30	25.93	0.37	0.47	0.67	447.41	50.54
OBS Data Range	0.60	0.11	1.31	1.35	2.07	0.65	0.58	0.65	0.42	0.36	0.19	0.73	0.54
	dh10	**dh13**	**dh21**	**ta2**	**tl1**	**tl2**	**th2**	**ra2**	**ra3**	**ra6**	**ra8**		
RCM-BC Median	29.08	2.23	18.60	70.72	291.50	49.44	71.86	142.50	21.22	0.16	133.05		
RCM-BC Data Range	0.55	0.18	0.60	0.06	0.12	0.54	0.26	0.29	0.60	0.45	0.32		
OBS Value	30.43	2.12	41.73	72.45	250.00	31.62	68.85	181.65	10.41	0.06	90.64		
OBS Median Value	31.18	2.36	42.93	68.87	247.00	33.58	70.44	191.55	9.59	0.09	93.93		
OBS Data Range	0.51	0.32	0.60	0.19	0.04	0.33	0.09	0.33	0.51	0.82	0.36		

Table 14: Maurice Watershed RCM-BCS ERSS Compared to Observed

	ma1	**ma3**	**ma8**	**ma14**	**ma25**	**ma39**	**ml2**	**ml13**	**ml19**	**ml21**	**ml22**	**mh1**
RCM-BCS Median	158.27	52.93	2.17	222.97	27.68	46.52	135.76	52.31	26.39	32.09	0.37	327.42
RCM-BCS Data Range	0.01	0.09	0.07	0.09	0.26	0.10	0.16	0.11	0.17	0.65	0.16	0.23
OBS Value	158.89	49.50	2.23	223.52	21.20	49.29	141.62	48.66	31.66	31.56	0.44	282.89
OBS Median Value	95.45	58.93	2.17	142.41	28.58	49.93	79.63	45.22	31.83	30.10	0.46	216.52
OBS Data Range	1.23	0.34	0.36	1.09	0.41	0.33	1.35	0.43	0.46	0.31	0.57	0.84
	mh15	**mh17**	**mh20**	**mh21**	**mh27**	**fl1**	**fl2**	**fh1**	**fh3**	**fh5**	**fh7**	**fh9**
RCM-BCS Median	3.40	1.47	5.41	5.88	2.17	14.26	44.60	18.04	6.72	20.22	0.08	14.16
RCM-BCS Data Range	0.14	0.06	0.20	0.39	0.06	0.35	0.36	0.32	0.65	0.30	1.75	0.36
OBS Value	3.51	1.47	5.02	15.39	2.32	6.98	49.59	7.54	7.60	7.92	0.10	7.04
OBS Median Value	4.66	1.47	6.77	14.72	2.67	6.77	48.30	9.30	13.68	9.48	0.31	6.83
OBS Data Range	0.47	0.18	0.82	0.50	0.33	0.60	0.11	0.43	1.31	0.52	2.07	0.65
	fh11	**dl1**	**dl6**	**dl9**	**dl13**	**dl16**	**dh10**	**dh11**	**dh17**	**dh23**	**dh24**	**ta2**
RCM-BCS Median	0.72	41.42	32.09	29.94	0.46	6.15	27.39	4.41	9.09	0.72	315.44	71.76
RCM-BCS Data Range	0.69	0.16	0.65	0.53	0.19	0.33	0.42	0.22	0.35	0.92	0.07	0.03
OBS Value	0.86	48.90	31.56	30.06	0.47	10.85	30.43	4.08	23.75	1.26	307.50	72.45
OBS Median Value	0.71	27.13	30.10	27.30	0.47	11.56	31.18	5.73	19.64	1.10	316.72	68.87
OBS Data Range	0.59	1.40	0.31	0.58	0.36	0.80	0.51	0.61	0.47	0.58	0.07	0.19
	tl1	**tl2**	**th2**	**th3**	**ra1**	**ra2**	**ra3**	**ra4**	**ra8**			
RCM-BCS Median	260.00	35.77	70.97	0.19	42.05	139.84	20.14	140.04	134.54			
RCM-BCS Data Range	0.06	0.60	0.32	1.43	0.22	0.35	0.24	0.35	0.11			
OBS Value	250.00	31.62	68.85	0.20	19.15	181.65	10.41	179.02	90.64			
OBS Median Value	247.00	33.58	70.44	0.12	17.44	191.55	9.59	180.52	93.93			
OBS Data Range	0.04	0.33	0.09	1.64	0.40	0.33	0.51	0.28	0.36			

Table 15: Maurice Watershed RCM-BCM ERSS Compared to Observed

	ma1	**ma3**	**ma8**	**ma36**	**ma39**	**ma45**	**ml1**	**ml10**	**ml13**	**ml19**	**ml21**	**mh2**
RCM-BCM Median	158.59	52.74	2.20	3.01	46.01	0.02	120.37	71.63	51.89	26.89	30.97	328.62
RCM-BCM Data Range	0.01	0.08	0.06	0.64	0.10	5.60	0.15	0.17	0.11	0.13	0.38	0.19
OBS Value	158.89	49.50	2.23	2.80	49.29	- 0.03	129.14	77.41	48.66	31.66	31.56	295.74
OBS Median Value	95.45	58.93	2.17	2.99	49.93	- 0.02	72.84	40.70	45.22	31.83	30.10	221.75
OBS Data Range	1.23	0.34	0.36	0.72	0.33	- 2.77	1.36	1.51	0.43	0.46	0.31	0.86
	mh8	**mh16**	**mh19**	**mh20**	**mh21**	**fl1**	**fl2**	**fh3**	**fh5**	**fh7**	**fh10**	**fh11**
RCM-BCM Median	310.25	2.00	0.84	5.30	5.93	14.04	42.58	6.00	19.56	0.08	2.62	0.70
RCM-BCM Data Range	0.39	0.06	2.25	0.17	0.35	0.33	0.48	0.52	0.31	1.75	0.36	0.69
OBS Value	252.95	1.99	0.01	5.02	15.39	6.98	49.59	7.60	7.92	0.10	2.72	0.86
OBS Median Value	179.75	2.06	- 0.17	6.77	14.72	6.77	48.30	13.68	9.48	0.31	2.67	0.71
OBS Data Range	0.89	0.30	- 6.22	0.82	0.50	0.60	0.11	1.31	0.52	2.07	0.29	0.59
	dl3	**dl4**	**dl6**	**dl13**	**dl16**	**dh10**	**dh11**	**dh14**	**dh17**	**dh23**	**dh24**	**ta2**
RCM-BCM Median	48.49	62.97	30.97	0.46	6.26	25.67	4.30	1.87	9.45	0.68	319.30	71.93
RCM-BCM Data Range	0.11	0.14	0.38	0.17	0.31	0.44	0.18	0.09	0.33	0.71	0.08	0.02
OBS Value	55.08	64.90	31.56	0.47	10.85	30.43	4.08	1.95	23.75	1.26	307.50	72.45
OBS Median Value	29.38	34.85	30.10	0.47	11.56	31.18	5.73	1.96	19.64	1.10	316.72	68.87
OBS Data Range	1.47	1.46	0.31	0.36	0.80	0.51	0.61	0.21	0.47	0.58	0.07	0.19
	tl1	**tl2**	**th2**	**ra2**	**ra3**	**ra4**	**ra8**	**ra9**				
RCM-BCM Median	251.00	39.42	72.16	141.84	19.87	140.55	134.44	6.28				
RCM-BCM Data Range	0.08	0.39	0.26	0.22	0.23	0.23	0.10	0.51				
OBS Value	250.00	31.62	68.85	181.65	10.41	179.02	90.64	11.37				
OBS Median Value	247.00	33.58	70.44	191.55	9.59	180.52	93.93	11.22				
OBS Data Range	0.04	0.33	0.09	0.33	0.51	0.28	0.36	0.54				